Fall 12-16-2016

Biloxi Marsh Platform Response due to Meteorological Forcing

Rachelle Thomason
University of New Orleans, rthomaso@uno.edu

Biloxi Marsh Platform Response due to Meteorological Forcing

A Thesis

Submitted to the Graduate Faculty of the
University of New Orleans
in partial fulfillment of the
requirements for the degree of

Master of Science
in
Earth and Environmental Sciences

by

Rachelle Faye Lyon Thomason

B.S. Mississippi State University 2014

December 2016

Acknowledgement

There are many people who are responsible for making this thesis possible. First, I would like to thank Dr. Mark Kulp for acting as my faculty advisor, mentor, friend, and teacher during this process. This would not have been possible if he had not decided to take a chance on, and provide funding to, a student whose background was in geosciences but not traditional geology. Mark was willing to sit down with me on numerous occasions to help me think more comprehensively and work through many dead ends that were found during this research. I have been blessed to be able to have an advisor who allowed me to pursue other opportunities that were related to my research, as well as some that were not. These opportunities have increased my knowledge and skill set in many facets of coastal processes. Finally, I thank him for to reining me and keeping me grounded when some of my ideas were outside the scope of my research hypotheses and my work appetite was larger than the time that I had.

Thank you to my committee members Dr. Ioannis Georgiou and Dr. Duncan Fitzgerald and for their time, patience, guidance, and advice while preparing this document. Also, thanks to Dr. Mike Miner who provided guidance and advice during my prospectus defense when Dr. Georgiou could not attend. I would also like to thank Mike Brown, Tara Yocum, David Cross, Andrew Courtois, and Rachael Gaspard for assisting me in the collection of data, even though it was not the most glamorous task. Thank you to Geoff Udoff for enduring a few hours of teaching me how to use R, Benjamin Sanderson for giving me lengthy, but necessary, statistics lessons, and thank you again to Tara Yocum for having intellectual conversations about my research that lead to new conclusions. Also, thank you to everyone at UNO who was involved in the fieldwork effort for the Barrier Island Comprehensive Monitoring

Table of Contents

List of Figures

List of Tables

Abstract

The Biloxi Marsh of the eastern Mississippi River delta plain is exposed to meteorological forces ranging from large-scale, mid-latitude cyclones to smaller scale storms and squalls. Each time that these marsh platforms are exposed to a storm event, the potential exists for either deposition or erosion to take place. This study examines the connection between wind speeds, stratigraphic composition, marsh edge morphology, and marsh edge erosion at 4 sites in the Biloxi Marsh. As much as 2.17 m of erosion were measured during the 9-month study with a maximum, averaged erosion rate of 0.03 m day^{-1}. Shell berm transgression was also documented as the result of winds from a low-pressure system near the site that resulted large waves. Shell berm movement occurred as a result of high wind speeds on shore but there was no connection between wind speeds and erosion for the duration of this study across all sites.

Keywords: Marsh Edge Erosion; Meteorology

CHAPTER 1. INTRODUCTION

Wetlands in Louisiana account for approximately 40 percent of the wetlands found within the contiguous United Sates and Louisiana alone accounts for 80 percent of the total wetland loss in the U.S. (Williams, 1995; Couvillion et al., 2011). Since the early 1930's, Louisiana has lost approximately 4,662 km^2 (1,800 mi^2) of land and is projected to lose another 1,750 square miles by 2060 under the current conditions (CPRA, 2012). These rates of land loss have been attributed to a variety of natural and anthropogenic factors (Stedman and Dahl, 2008; Couvillion et al., 2011; CPRA, 2012), including subsidence, erosion, submergence, and the direct removal of sediments (Boesch et al., 1994; Penland et al., 2002; CPRA, 2012). The majority of coastal wetland loss is attributed to submergence as a result of the dewatering of subsurface sediments and a lack of sediment supply that limits marsh elevation increases, which coupled with sea level rise and subsidence, can cause eventual drowning of the marsh (Boesch et al., 1994; White and Tremblay, 1995; Conservation, 1998; Day et al., 2000; Penland et al., 2002). Subsidence rates, largely thought to be driven by compaction of water-saturated, deltaic sediments, vary spatially from approximately 2 mm yr^{-1}to 35 mm yr^{-1}at the current Mississippi River Delta (CPRA, 2012). Anthropogenic factors such as the direct removal of sediment and the dewatering of sediments through the extraction of oil and gas are believed to attribute for a portion of wetland loss as well (Conservation, 1998; Day et al., 2000; Penland et al., 2002).

Coastal Louisiana wetlands are economically significant for ecotourism, fisheries, the petroleum industry, and recreational fishing and hunting (Conservation, 1998; CPRA, 2012). Another important service of wetlands is that they act as a barrier between the open ocean and the more landward populated onshore areas (GCERTF, 2011; CPRA, 2012) and act to attenuate

waves and dampen storm surge thereby reducing damages caused by storms (Wamsley et al., 2007; Costanza et al., 2008; Barbier et al., 2013; Boutwell and Westra, 2015). The marsh acts as a buffer by diminishing wave energy from storms and protects coastal communities (Möller, 2006; Wamsley et al., 2007; Wamsley et al., 2010). The Biloxi Marsh consists of saline and brackish marsh environments (Sasser et al., 2014). In the absence of the Biloxi Marsh, areas that were once farther inland would be subjected to higher salinity and would experience a transition in marsh environment from freshwater or intermediate marsh to brackish or saline.

Due to subsidence and sea-level rise, coastal Louisiana is subject to high rates of wetland loss. The high rates of relative sea level rise causes marsh platform and bay-fronting sandy shorelines to transgress, creating relatively larger fetch for waves to develop within open water of the interior delta plain (Fitzgerald et al., 2003). As a result, a greater extent of marsh platform is now susceptible to wave action and erosion increase with an increase in fetch and tidal prism (Fitzgerald et al., 2003). With the disappearance of coastal marshes, marshes that are farther inland become more vulnerable to meteorological events due to an increase in wave energy.

The Northern Gulf of Mexico is impacted by a range of meteorological events ranging from small-scale storms to large-scale cyclonic systems. It is the combination of meteorological events and seasonal wind patterns that drives the overall wave climate of this north-central Gulf coastal zone (Moeller et al., 1993; Georgiou et al., 2005). The frequency of extratropical and tropical cyclones is somewhat dependent on the El Nino-Southern Oscillation (ENSO) (Saravanan and Chang, 2000). While it is known that extratropical cyclones occur more frequently than tropical cyclones, it is known that both contribute to coastal wetland loss in Louisiana (Conservation, 1998; Barras, 2006; Cahoon, 2006).

2

CHAPTER 2. BACKGROUND

2.1 Regional Setting and Processes Governing Erosion

The St. Bernard delta complex of the Holocene Mississippi River delta (MRD) system created brackish and fully marine wetlands that extend from Lake Pontchartrain to the Chandeleur Islands. This delta complex was active approximately 3,500 years BP and became inactive approximately 1,500 years BP as defined by the delta complex age revision proposed by Törnqvist et al. (1996). Prior studies have suggested different time frames during which the St. Bernard delta complex was active along the coast (Fisk, 1944; Frazier, 1967). During the occupation of the St. Bernard delta complex, overlapping sediments deposited by the shelf-phase delta created the subsurface stratigraphy that is unique to this delta complex (Roberts, 1997). After abandonment, marine processes reworked the prograded deltaic deposits to create the Chandeleur Islands (Penland et al., 1988) and the Biloxi marshlands as they appear today (Fig. 1).

The Biloxi Marsh extends eastward from Lake Borgne to Chandeleur Sound and consists of densely vegetated marsh platforms that are dominated by *Spartina alterniflora* and are locally bordered by sand and shell-rich shorelines and scarps that are attached to subaqueous terraces that protrude seaward (Frazier, 1967; Rogers et al., 2009; Ellison, 2011). The Biloxi Marsh is currently in a morphological state of deterioration due to interior ponding and edge erosion within the interior ponds as well as the edge of the entire marsh platform. Interior erosion of the Biloxi Marsh begins with ponding on the marsh surface and submergence of the interior marsh. Once ponding is initiated the disintegration of the marsh continues outwards in nearly circular patterns (Reed, 1989). Edge erosion along the Biloxi Marsh takes place as a result of wave action

3

and scour along the shoreline (Wilson and Allison, 2008). Biloxi Marsh is subjected to lower rates of relative sea-level rise compared to other MRD marshes (CPRA, 2012). In the 2012 State Master plan subsidence rates in southeastern Louisiana are indicated to be between 15 to 35 mm year^{-1} in the Plaquemine/Balize delta (Fig. 1), whereas rates of 1 to 15 mm yr^{-1} are common to the location of the St. Bernard Delta (e.g. Biloxi Marshes) (CPRA, 2012).
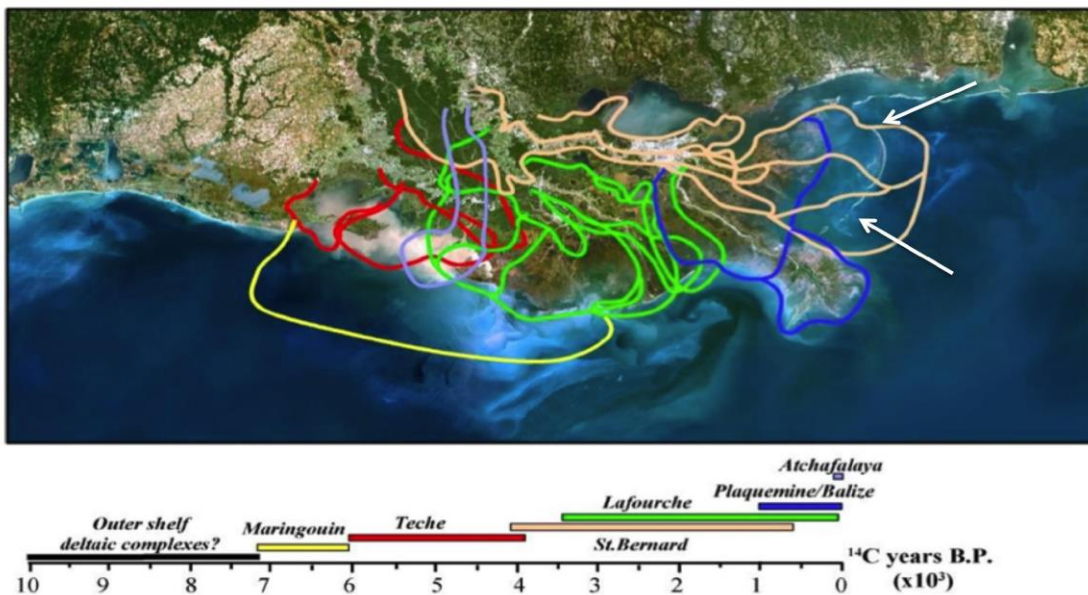
Figure 1. Map and timeline of the deltaic deposition of the Mississippi River Delta across Louisiana. The St. Bernard delta is shown in orange and the extent of the Chandeleur Islands is identified by the white arrow. Kulp (2005) modified from Frazier (1967).

Meteorological forcing such as tropical and extratropical (e.g. cold fronts, blizzards, Nor'easters) cyclones cause extensive morphological change to marshes by locally eroding and depositing sediments on them. While hurricanes are known to cause erosion they also

4

significantly contribute to a majority of sediments deposited on a marsh platform (Tweel and

Turner, 2014; Nyman et al., 1995; McKee and Cherry, 2009; Cahoon, 2006; Cahoon et al.,

1995). Cold fronts are also a key factor in salt marsh accretion in Louisiana (Reed 1989).

2.2 Background Research

2.2.1 Marsh Edge Erosion

Coastal wetlands evolve vertically and laterally through the duration of their existence.

The vertical evolution of wetlands is the result of the deposition and erosion of inorganic and

organic sediments that has been investigated with numerical modeling and field observations

(Cahoon, 2006; Kirwan and Murray, 2007; Mudd, 2011; Bianchette et al., 2015). While the

vertical evolution of marshes is fundamental to determining if the marsh will be able to keep

pace with rising sea level, or if it will drown, lateral evolution of the marsh is key to

understanding how the marsh edge evolves. Marsh edge erosion varies depending upon factors

such as substrate composition, rooting depth, organic content, marsh edge morphology, subaerial

composition, However, it has been recognized that waves impacting the marsh edge are the most

important factor determining the style of lateral evolution of a marsh edge (Schwimmer, 2001;

Watzke, 2004; Wilson and Allison, 2008; Trosclair, 2013; Karimpour et al., 2015).

Wilson and Allison (2008) proposed a conceptual long-term equilibrium model

describing the lateral shoreline retreat of a fringing marsh (Fig. 6). This model shows that as

subaerial marshes submerge due to relative sea-level rise (RSLR), an increase in water depth

results in an increase in wave power that impacts the marsh edge (Wilson and Allison, 2008; Fig.

2-A). The force exerted by the increased wave energy results in the retreat of the marsh edge and

the formation of a marsh scarp (Wilson and Allison, 2008; Fig. 2-B). As RSLR continues, the

submerging adjacent bay bottom becomes submerged to a depth where the wave base no longer

impacts the bay-bottom causing waves to break against the marsh edge rather than in open water

(Wilson and Allison, 2008; Fig. 2-C-D). As subsidence continues and creates accommodation

space on the bay-bottom, mud that has been liberated as a result of edge erosion and scouring is

also deposited, and the profile is maintained (Wilson and Allison, 2008; Fig. 2-C-D). Ellison

(2011) adjusted this model to include shell fragments that are found within the marsh substrate

and on the surface of the platform. The submergence of the platform results in the transgression

of the marsh shoreline. With the regression of the shoreline waves can impact areas that were

previously farther inland. As the shoreline submerges a larger fetch is also created, enhancing

wave attack (Fitzgerald et al., 2003; Fagherazzi et al., 2007; Fagherazzi and Wiberg, 2009;

Karimpour et al., 2015).
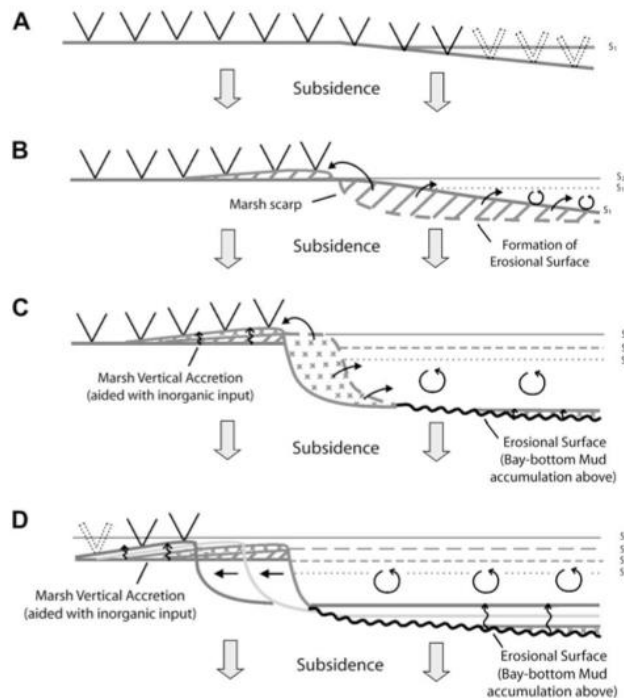
Figure 2. A conceptual equilibrium model of fringing marsh shorelines with RSLR in southeast Louisiana
(from Wilson and Allison, 2008).

While it has been demonstrated that waves are a factor that results in marsh edge erosion, the characteristics of the marsh platform still need to be addressed to adequately understand lateral erosion due to meteorological forcing. For example, vegetation on the marsh results in higher soil strength and acts as a sediment trap on marsh platforms and makes the marsh less vulnerable to erosion during meteorological events. Thus, a larger force must be exerted in order to strip the vegetation from the platform and cause large-scale erosion (Howes et al., 2010; Anderson et al., 2011). Vegetated marsh platforms also attenuate wave energy more effectively than non-vegetated marsh platforms (Möller and Spencer, 2002). Feagin et al. (2009) argue that soil characteristics are more important in determining lateral erosion and that plants do not significantly reduce marsh edge erosion. Leonard and Reed (2002) suggest that flow speeds on the marsh surface are reduced by vegetation and are reduced even more so if the flow occurs within the canopy of the marsh. Contrasting opinions are provided by Temmerman et al. (2007) and Fagherazzi et al. (2012) who argue that vegetation is a crucial factor in determining marsh edge erosion because it acts as a flow-topography feedback where higher flow concentrations are found between vegetation patches, thus leading to preferential erosion of channels. However, the ability for vegetation to laterally disperse and retain sediment may be dependent upon the morphology of the canopy (Leonard and Reed, 2002; Lightbody and Nepf, 2006). Similarly, unvegetated marsh terraces that are not submerged are more susceptible to edge erosion during meteorological events than those that are heavily colonized by vegetation (Trosclair, 2013; Currin et al., 2015).

2.2.2 Meteorological Forcing

Meteorological forcing along the coastline results in a transfer of energy in the form of winds, waves, and water levels (Pepper and Stone, 2004; Watzke, 2004). The resulting energy transfer can lead to vertical accretion and erosion, as well as lateral erosion of marshes (Baumann 1980; Reed 1989; Nyman et al., 1995; Moeller et al., 1993; Watzke, 2004; Cahoon, 2006; Turner et al., 2006; Fagherazzi et al., 2012; Schuerch et al., 2013; Tweel and Turner, 2014). In the upper 24 cm of soils in the Chenier plain of western Louisiana it is estimated that storm surge-induced deposition resulting from tropical cyclones accounts for at least 80% of inorganic sedimentation, and at least 65% in abandoned delta lobes (Tweel and Turner, 2014). As a result of Hurricane Katrina, two subsiding brackish marshes (located within the interior of the delta plain) gained 3 to 8 cm of sediment from storm surge, offsetting the local subsidence rate (McKee and Cherry, 2009). In 1992, Hurricane Andrew resulted in vertical accretion 4 to 11 times greater than the long-term marsh accretion rate in coastal Louisiana (Nyman et al., 1995). Schuerch et al. (2013) research shows that an increase in storminess, with an available amount of fine-grained sediment will lead to an increase in the vertical accretion of marshes. In the Biloxi Marsh, cold fronts occur during the winter months and have contributed to a large percentage of deposition on the marsh platform (Turner et al., 2006; Baumann 1980; Reed 1989; Moeller et al., 1993; Cahoon, 2006).

While it has been demonstrated through multiple studies that marshland vertically accretes after the passage of a hurricane or cold front due to the deposition of sediments onto the platform (Baumann 1980; Reed 1989; Dingler et al., 1993; Moeller et al., 1993; Nyman et al., 1995; Cahoon, 2006; Turner et al., 2006; Schuerch et al., 2013; Tweel and Turner, 2014), it is important to also understand the lateral morphological response of the marsh platform. Increased

wave forcing as a result of the passage of frontal systems facilitates edge erosion of marshes. This is because waves that approach the shoreline of a shallow bay are depth-limited, rather than fetch limited. Depth-limited waves are steeper and thus transfer more energy when they break on the shore (Fagherazzi, 2007; Trosclair, 2013). However, the overall morphology of the marsh platform and the water level at the time of storm-driven waves dictates which part of the platform will be subjected to wave energy (Tonelli et al., 2010; Bendoni et al., 2016).

Pre-frontal winds produced by an extratropical cyclone in southeast Louisiana lead to an elevation in water levels on marsh platforms. During this time, waves inundate subaerial marsh terraces. A decrease in the water level during post-front prevents waves from inundating higher terraces and focuses wave action at the lower scarp of the marsh edge (Trosclair, 2013). Marsh terraces can develop as a result of wave-induced erosion from energetic frontal conditions occur. Figure 3 shows how water levels control the vertical location that waves exert a shear or impact force along the marsh edge and thus the location of the scarp (Trosclair, 2013). Bottom shear stress enhances the removal of sediments from the lower scarp platform when water levels are low (Trosclair, 2013). When water levels are high, bottom shear stress impacts the marsh terrace. Wave forces exert discontinuous shear and normal stress on the platform, creating terraces, erosive scarps, and ultimately scarp failure (Trosclair, 2013). On the platform, the passage of multiple frontal systems leads to differential erosion and exposure of less resistant, unvegetated substrate (Trosclair, 2013). USGS station number 300722089150100 at Mississippi Sound near Grand Pass is a station that could have been utilized for water levels and wind speed data to relate to Trosclair (2013) and how water levels induce erosion but the station was recognized as

unreliable upon analyzing wind speed data.
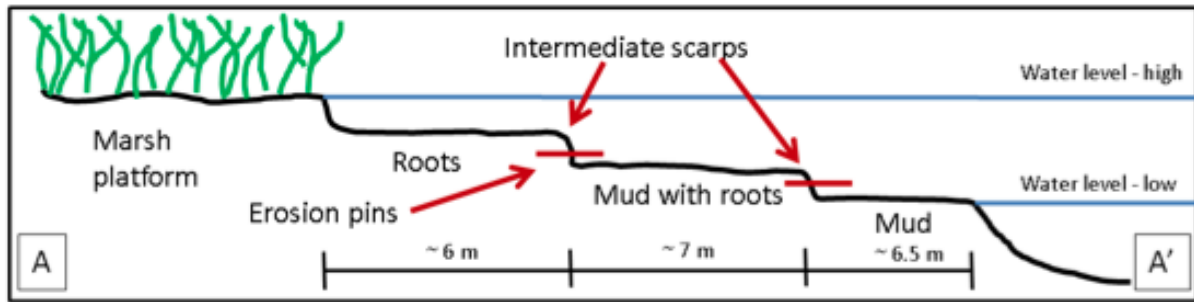
Figure 3. A cross-sectional view of a marsh platform with terraces (From Trosclair, 2013).

2.2.3 Location of Cyclogenesis

Current research does not address the depositional or erosional effects to a marsh platform locally based on the storm angle, strength, or speed at which a meteorological forcing takes place (Moeller et al., 1993; Turner et al., 2006). Storm approach angle, strength, and speed may strengthen or weaken storm surge and waves that impact an area (Zhang, 2012). There is also no literature that incorporates the erosional effects of warm, occluded and stationary fronts on a marsh platform. It is possible for a warm front to produce strong winds that generate strong waves that can have a large impact on a platform. For example, April 12, 2009 at 2100 Z a warm front approaching southeast Louisiana created a south-south easterly wind at 7.72 m s^{-1} and at 0000 Z on April 13, this wind increased to 10.29 m s^{-1} from the south. This example provides evidence that meteorological forcings, besides cold fronts and hurricanes, can result in high wind speeds. In order to create a holistic sense of marsh edge erosion, all meteorological events must be analyzed with respect to marsh edge erosion

Moreover, literature is currently lacking that unites marsh platform response to meteorological forcing on the basis of the location of cyclogenesis (the development of an extratropical system) for an extratropical cyclone (Fig. 4). The location of cyclogenesis changes

the accepted assumption is that prefrontal winds are southerly and that postfrontal winds are northerly (Baumann 1980; Reed 1989; Moeller et al., 2006). Pepper and Stone (2004) categorized two types of storms known as "arctic surges (AC)" and "migrating cyclones (MC)." AC storms are storms that have a weak pre-frontal phase followed by powerful post-frontal winds and MC storms are categorized as being dominated by a strong low-pressure system with strong pre-and post-frontal winds (Pepper and Stone, 2004). Stone et al. (2004) mentioned three distinct cold front types known as (1) the mid-latitude cyclone, (2) the Arctic surge, and (3) the Gulf cyclones. While these systems have been named, their particular attributes have not been described in terms of the location of their cyclogenesis and its relationship to edge erosion of marshes. On November 25, 2007, an extratropical cyclone began to form in the Gulf of Mexico. At 9Z the ASOS (Automated Surface Observing System) in Slidell Louisiana (20 km northeast of New Orleans) recorded easterly winds at 25 knots due to a warm front that was positioned to the south. Following the passage of the cold front that was associated with this system, the recorded post-frontal winds were out of the southwest at 10 knots. The prior is an example of how the location of cyclogenesis in the Gulf of Mexico changes the direction and strength of winds that are impacting the shoreline. A broad assumption of wind speed and direction that are typical to cold fronts cannot be made because of this. Cyclogenesis in the Gulf of Mexico can take place as many as 7 times per year (Hardy and Hsu, 1997). Recorded data shows that the typical wind response to what would be considered a "classic extratropical" cyclone pre-and post front is not always accurate.
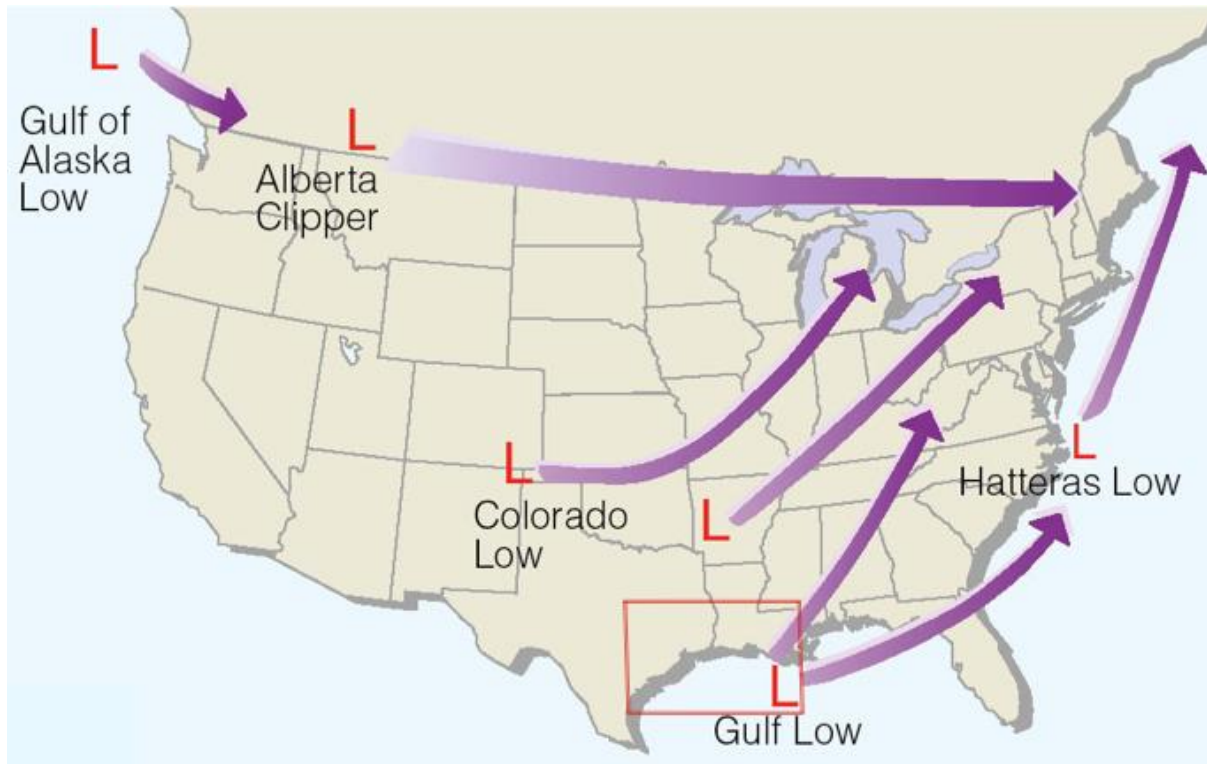
Figure 4. A map depicting the most common locations of cyclogenesis in the United States. The red box represents the area of cyclogenesis, described in the text, that occurs within the northwestern Gulf of Mexico. (modified from Ahrens, 2011).

2.2.4 Shell-rimmed Shorelines

Some, but not all, Marsh platforms within the Biloxi Marsh have deposits of shell hash due to the presence of oyster reefs that have existed since the early 1900's (Lopez, 2009). The presence of shells produced by current and paleo oyster reefs combined with wave run-up onto marsh platforms leads to a buildup of shells along many of the Biloxi marsh edges. Ellison (2010) created a conceptual model illustrating how marsh edge processes lead to shell-pocket beaches. The formation of a marsh scarp on a slowly subsiding marsh in combination with the liberation of shell-rich bottom bay sediments with energy provided from a high-energy event (cold fronts, warm fronts, tropical cyclones, etc.) deposits shell material on the marsh surface (Ellison, 2010). Shells can be sourced from either active reef accumulations or excavated from

12

the stratigraphy underlying bay bottoms and representing past accumulations of oyster shells. Locally these oyster shells armor marsh platform shorelines and may contribute to reduced rates of erosion, depending upon the shell abundance and consolidation of the marsh substrate (Piazza et al., 2005; Rodriguez et al., 2014). Modeling experiments with field validation show that once shells are deposited, it is more difficult for them to become reentrained in the water column due to the imbrication of the shells (Allen, 1984). Weill et al. (2010) concluded that the imbrication of shells also results in a protective covering on the shoreline, resisting entrainment and erosion. The shell-lined shorelines are also sediment traps for finer grained sediment due to their high porosity (Ellison, 2010).

The purpose of this research is to determine relationships between marsh edge erosion, meteorological events, scarp and terrace evolution, and stratigraphy. Each site has a set of unique characteristics based on shoreline orientation, seasonality, erosion, and subaerial and stratigraphic sedimentary composition. These characteristics range from frequency of exposure to meteorological events, erosion rates, total erosion, proximity to shell berms, presence of sand and organic content within stratigraphic columns, and scarp and terrace evolution. Researching the connections between these variables will give insight into marsh edge erosion occurring at the Biloxi Marsh.

2.3 Scientific Research Questions

The study area is within the Biloxi Marsh that extends eastward from Lake Borgne to Chandeleur Sound (Fig. 5). Marsh platforms at the study location have a series of scarps that are attached to terraces, are locally fringed by sand and shell-rich shorelines (Frazier, 1967; Rogers et al., 2009; Ellison, 2011) and are densely vegetated with *Spartina alterniflora*. As

a result of interior ponding and edge erosion within the interior ponds as well as the edge of the entire marsh platform the Biloxi Marsh is deteriorating. Because of the disappearance of wetlands in the Biloxi Marsh and the regional services they provide, the goal of this research is to determine the following:

1. What is the spatial and temporal variability of erosion patterns at several sites in the Biloxi marsh within the course of 9 months?

2. How does daily marsh edge erosion differ from erosion forced by meteorological events (e.g. cold fronts, warm fronts, tropical cyclones)?

3. What are the conditions under which shell berm movement occurs at this location and is it driven by meteorological events?

2.4 Scientific Hypothesis

H1 Wind waves will force a change of the marsh edge morphology and the characteristics of the winds (e.g. velocity, direction, and duration) can be used to approximate the style of marsh edge modification.

H2 Shell berm movement at this location is a function of water level controls and an acting meteorological force.

CHAPTER 3. METHODS

3.1 Geographic and Meteorological Site Description

Figure 5 shows the locations that were chosen as research sites in the Biloxi Marsh. These locations were initially selected from *Google Earth* on the basis of their size, proximity to open water, and the presence of shell deposits on their shorelines. Following the selection of sites on the basis of the imagery, a field reconnaissance was performed to make a final decision about the field sites.

Figure 5. The study location is located in southeastern Louisiana in the Biloxi Marsh. Red circles represent the locations of Sites 1-4 and yellow triangles represent the locations of two extensive shell berms.

The Biloxi Marsh is exposed to a variety of meteorological forces ranging from large-scale cyclones to macro scale in size. Examples of such events are squall lines, tropical cyclones, and extratropical cyclones. Between 1851 and 2015 a total of 11 tropical systems have made a direct landfall on the Biloxi Marsh (Fig. 6). Between 2006 and 2015 cold fronts directly impacted the Biloxi Marsh, ranging from 38 to 57 times a year within that time period (Fig. 7). During the passage of a cold front, prefrontal winds are southerly and postfrontal winds are northerly (Baumann 1980; Reed 1989; Moeller et al., 1993; Turner et al., 2006). Southerly winds allow for Gulf water to pile-up in the Biloxi Marsh creating an increase of the height at which waves will impact the platform. Postfrontal winds act to push the water back out to the open Gulf of Mexico, allowing the water level to drop, which results in the deposition of entrained sediments on the platform.

Occluded fronts, stationary fronts, and warm fronts occur infrequently and likely play an important role in the morphology of a marsh platform (Fig. 8). An occluded front occurs when dense air of a cold front becomes wedged underneath a slowly advancing warm front. A stationary front occurs when the airflow on either side of a front flows almost parallel to the front leading to moderate precipitation. A warm front takes place when a warm air mass advects into an area that was occupied by cooler air. Squall lines are a narrow band of thunderstorms that develop ahead of a cold front. These storms can persist for 10 hours or more and are capable of producing heavy downpours, isolated tornadoes, and strong winds. Because squall lines can produce high wind speeds, and thus wind waves, these events should also be taken into consideration when analyzing how marsh edge erosion occurs. When a meteorological forcinge impacts an area, it causes a change in wind speed and direction, thus leading to a change in the

16

direction and speed at which waves approach a shoreline. These changes in wind speed result in the creation of wind waves that will impact the shoreline.

Figure 6. Tracks of tropical cyclones that have made landfall within the Biloxi Marsh between 1851 and 2014 (obtained and modified by ESRI). Hurricane strength is indicated by the color of the line. A category 5 is shown by a maroon line, 4 by a crimson line, 3 by a red line, 2 is shown by an orange line, 1 is shown by a solid yellow line, a tropical storm is shown by a dotted yellow line, and a tropical depression is shown by a dotted yellow line with small spacing.
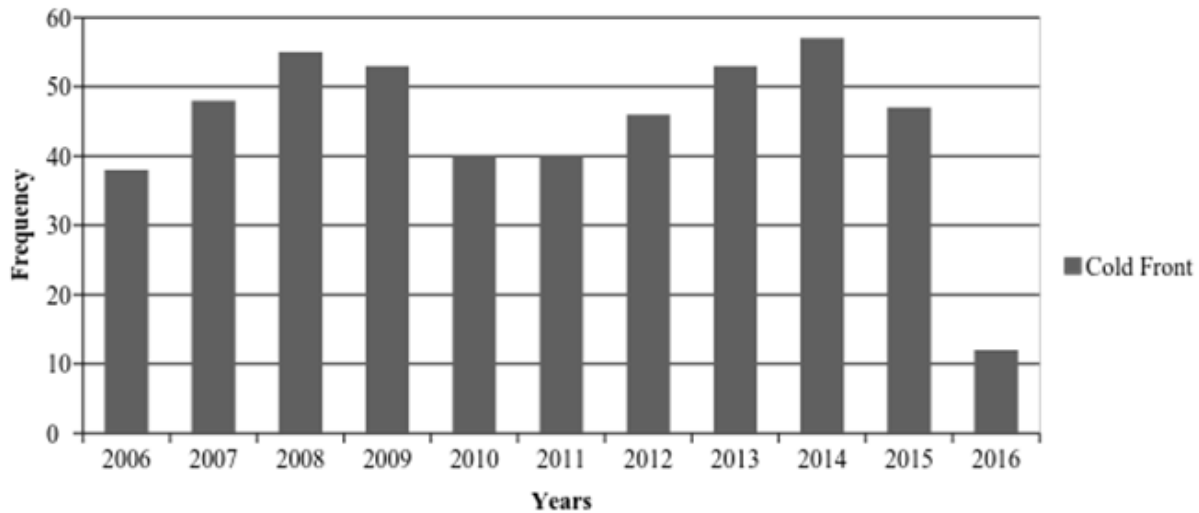
Figure 7. Plot of cold front frequency per year in southeastern Louisiana based. *Data for 2006 did not

start until 3/29 at 18Z and data for 2016 ended on March 4th, 2016 (WPC, 2016).
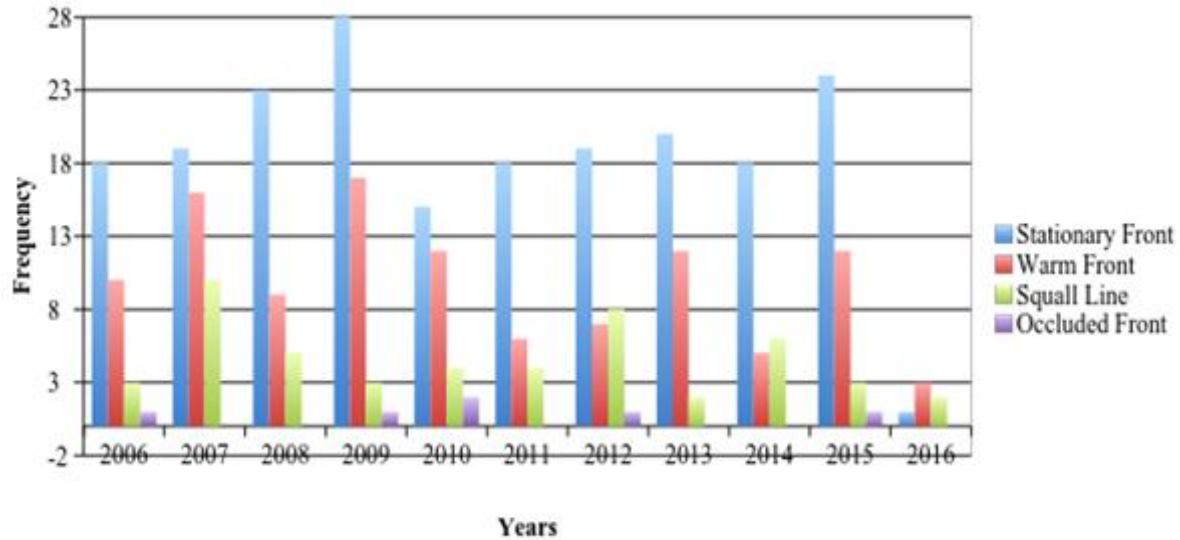
Figure 8. The frequency of stationary, warm, and occluded fronts based on the Weather Prediction Center's Surface Analysis Archive. Squall lines that have impacted the area are also recorded. *Data for 2006 did not start until 3/29 at 18Z and data for 2016 ended on March 4th, 2016 (WPC, 2016).

3.2 Research Timeline

The collection of field data effort began May 28th, 2015 and ended on March 4th, 2016. This nearly year-long duration of field work provided an opportunity to observe a range of meteorological events and to examine their contributions to morphologic evolution of the marsh edges of the study sites. Field sites were visited a total of 6 times, each time interval between successive site visits is herein referred to as epochs. A total of five Epochs (1 to 5) were established and are the intervals of time during which changes to marsh edge morphologies were observed and meteorological events examined (Table 1). Epoch 1 began on May 28th and ended on July 8th, 2015, Epoch 2 began on July 8th and ended on September 24th, 2015, Epoch 3 began on September 24th and ended on October 28th, 2015, Epoch 4 began on October 28th and ended on December 9th, 2015, and Epoch 5 began on December 9th, 2015 and ended on March 4th,

18

2016. Data collected during this project provides an opportunity to assess marsh platform

morphological change due to the weather conditions during the course the study.

Data collected during the study includes, erosion pin exposure measurements, station

marker heights, lateral marsh edge measurements, and front and back terrace measurements. The

front terrace is considered the seaward most terrace and the back terrace was the terrace directly

attached to the vegetated marsh platform.

Table 1. Dates of field site visits between May 28th, 2015 and March 4th, 2016. Epochs represent the time
period between two site visits.

Field Visit Dates	Purpose of Visit	Epoch Number	
May 28th, 2015	Field reconnaissance Insert erosion pins		
		Epoch 1	(40 days)
July 8th, 2015	Routine measurements		
		Epoch 2	(76 days)
September 24th, 2015	Routine measurements		
		Epoch 3	(34 days)
October 28th, 2015	Routine measurements		
		Epoch 4	(41 days)
December 9th, 2015	Routine measurements		
		Epoch 5	(85 days)
March 4th, 2016	Routine measurements		

3.3 Marsh Measurements

The first installment at each site was a station marker made of PVC pipe to serve as a

reference location for each site. Each station marker was pushed into the platform approximately

15 m inland from the marsh edge. This station marker was used as a reference position for all

measurements during the course of the study, labeled in Fig. 8 as the "Station Marker." In

addition to acting as reference points, the PVC pipe station markers also provided a method of quantifying vertical changes of elevation on the marsh platform at sites 1-4, which follows a methodology proposed by Ellison (2011). Measurements were taken during each site visit to document whether station marker heights show an increase or decrease in elevation.

To quantify marsh edge erosion meter-long steel erosion pins were pushed horizontally into the edge of the marsh platform, perpendicular to the marsh edge scarp. Each pin was approximately 15 to 20 cm below the top edge of the marsh scarp and 12 to 20 cm of each pin was left exposed to provide the first measurement of the distance between the exposed end of the pin and the edge of the marsh scarp. Each site had two pins that were placed in the marsh edge along equidistant bearings, approximately 15 m apart from one another, along the shoreline. During their initial installment, the exposed length of the pin from the tip of the pin to the marsh edge was measured with a cm-graduated tape measure (Fig. 9). The exposure of the pin was measured during each field visit to record the amount of erosion that had occurred during the time period between each visit. In addition to pin measurements, erosion along the marsh edge was also measured along a constant bearing from the station marker to the edge in order to

measure lateral changes to the marsh platform.
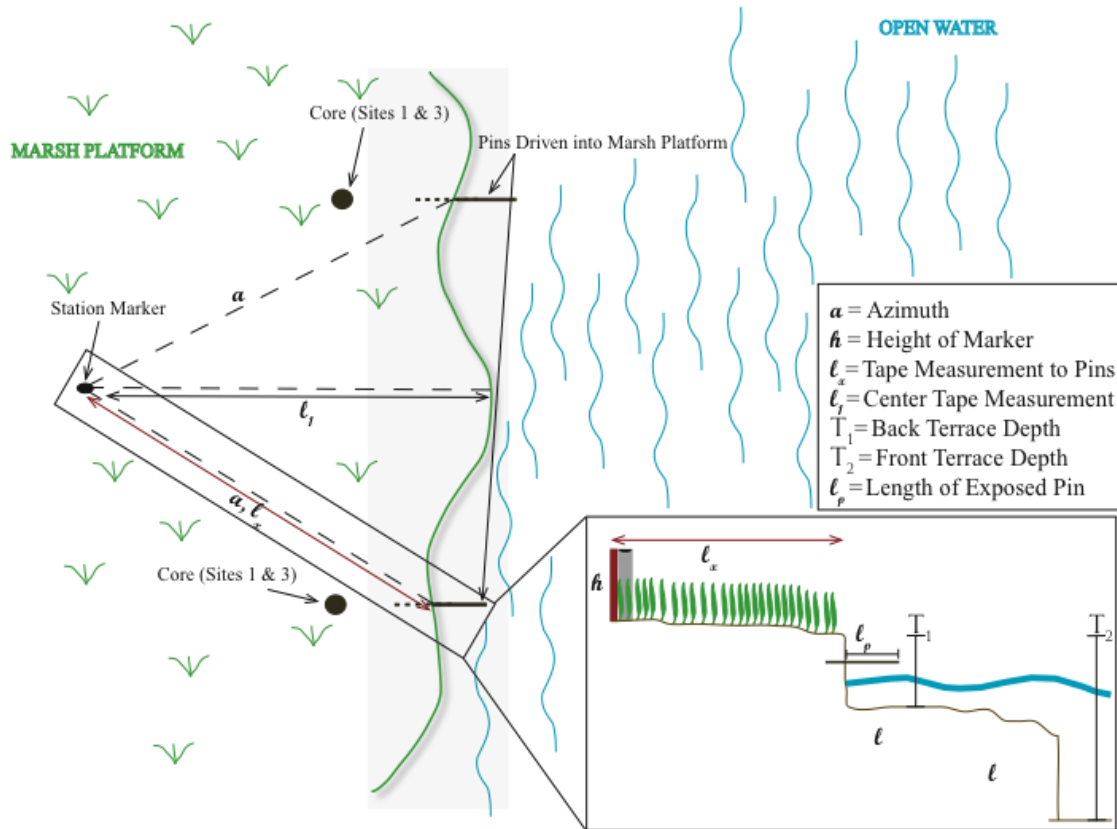
Figure 9. Conceptual diagram of the approach and methods that were used to measure pin exposure (l_p), station marker height (h), front and back terrace depths (T_1, T_2), center tape measurement along a consistent bearing to the marsh edge (l_1), and lateral measurements (l_x) from the station marker to the marsh edge along equidistant azimuths (a) from the center azimuth. Cores were only taken at Sites 1 and 3 and are labeled near the relative location at which they were taken at each site.

3.4 Terrace Measurements

As many as two different terraces were measured during a site visit but typically only one measurement was able to be accurately measured because of changes in water level. The two landward most terraces were measured and were labeled as the "front" and "back" terrace. The front terrace is considered the seaward most terrace, whereas the back terrace was the terrace directly attached to the vegetated marsh platform (Fig. 9). Back and front terrace

measurements were recorded at the location of each erosion pin using a cm-graduated measuring stick, a method from Trosclair (2013). The back terrace was measured from the subaerial vegetated marsh platform at the edge to the subsequent platform of a lesser elevation. Front terrace measurements were recorded at the erosional scarp from the edge of the back terrace platform to the scarp (Fig. 9). Front terrace measurements were not recorded during each visit at some sites because only one terrace was visible during elevated water levels.

3.5 Shell Berm Measurements

During the initial field visit, shell berms were marked with two PVC pipes, approximately 1-m in length, that were driven into the marsh platform as a land stake that was placed on the landward side of the berm and as a sea stake that was placed on the seaward side of the berm along a constant bearing (Fig. 10). During each site visit, the height of each stake was measured from the marsh platform to the top of the stake (Fig. 10). The height of the berm (H_B) was approximated with a tape measure from the surface of the marsh platform to the top of the berm (Fig. 10). Berm width (W_B) was also measured during each site visit prior to October 28th, 2015 along a consistent bearing of 142° for the East Shell Berm and 125° for the West Shell Berm from the landward side of the berm to the seaward side. Site visits thereafter consisted of recording measurements with the above methods. However, after September 24th, 2015 when the berm transgressed and covered the landward stake the berm width was no longer recorded and the berm height and stake height were measured relative to the landward stake rather than being approximated with a tape measure (Fig. 10). Calculation of the berm height was done by measuring the height of exposure of the landward stake above the berm. The height of exposure could then be subtracted from the height of the landward stake prior to the movement of the

berm to get an approximated height of the berm (H_B). After this date, the berm width (W_B) was no longer recorded and instead the berm migration (M_B) was measured instead. This was measured by measuring along the same respective bearing for each berm with a tape measure from the land stake to the furthest inland extent of the berm.
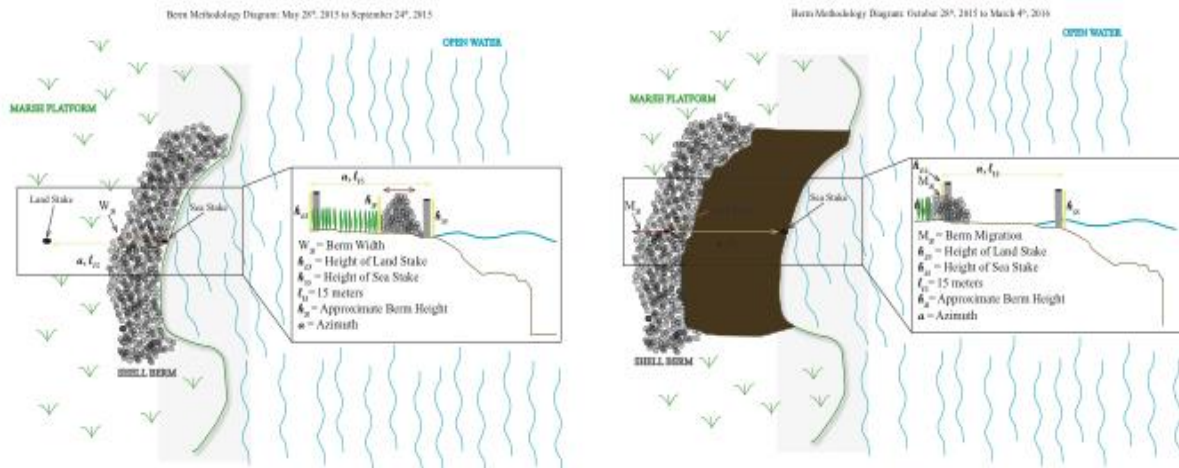
Figure 10. Diagram describing methods used to measure the physical characteristics of the east and west shell berms before transgression (left) and after transgression (right). The land stake height (h_{LS}), sea stake height (h_{SS}), berm height (H_B) and the 15-m distance between each stake (l_{15}) were all measured before and after the landward transgression of the berm. During the time period before transgression (May 28th, 2015 to September 24th, 2015), the berm width (W_B) was recorded. After the berm transgressed (October 28th, 2015 to March 4th, 2016) the berm width (W_B) was no longer recorded and the berm migration was recorded (M_B). The red circles on each diagram are to help indicate where the position of the stake is on the diagram against the darker background.

3.6 Core Analysis

Two marsh cores were collected using a half-m Russian sediment/peat borer at sites 1 and 3 on December 9th, 2015 at a distance of 1.5 m behind each erosion pin (Fig. 9). A core was obtained by pushing a hollow 5-cm inner diameter sharpened PVC tube into the marsh platform to a depth of 0.5 m. Once fully penetrated the PVC was rotated and a sharp edge along the barrel cut into the substrate and trapped the sample inside of the barrel with a cover plate. After the initial 0.5 m retrieval, a second attempt resulted in the retrieval of an additional 0.5 to 1.0 m of strata

depending upon substrate resistivity. Retrieved cores were placed into PVC half pipes, wrapped

in cling plastic, and secured with duct-tape to avoid disruption of strata during transport. In the

laboratory, each core was photographed and visually analyzed on the basis of stratigraphic,

sedimentary, and organic characteristics.

3.7 Photo Comparison and Marsh Edge Characteristics

Photographs of field sites were taken at the beginning and end of each epoch

during the May 2015 through March 2016 study period. The photographs were taken from each

pin looking along the marsh edge towards the opposing erosion pin. This method allowed for the

entirety of the marsh edge within the study area at each site to be photographed and documented

for comparative analyses of the morphological evolution of the marsh edge during the study.

Shorelines styles are characterized by (1) cleft and neck (Schwimmer, 2001), (2) linear,

and (3) bays and headlands. Clefts and are characterized by V-shaped notches created by erosion

and necks are the adjacent portion of marsh that protrudes outwards (Schwimmer, 2001). Linear

shoreline style is characterized by a shoreline that is mostly straight in nature and is close to a

state of equilibrium. Bays and headlands are somewhat parabolic in shape and gently roll from

protruding headlands to embayed bays that are smoother in shape than clefts and necks.

Examples of each of these shoreline styles will be referred to in the correlating results section.

3.8 Meteorological Data

A surface analysis map that is published by the Weather Prediction Center (WPC)

provides data of weather conditions such as temperature, wind speed, frontal position, barometric

pressure, sky conditions, and dew point over a geographical area based on information from

ground-based weather stations at specified time intervals throughout the day. Therefore, daily

surface analysis maps from WPC's Surface Analysis Archive were used to observe past and present weather conditions and meteorological anomalies such as extratropical cyclones. This data was also used to evaluate extratropical cyclone development as well as yearly to seasonal regional meteorological variability (Figs. 4&5). Local radar loops were analyzed also; these radar loops from the IEM (2016) provided insight on the intensity of storms that occurred based on wind speeds, approach angle, and reflectivity values at each study site. The sites fell within the warning jurisdiction of the National Weather Service office for Baton Rouge/New Orleans; therefore, this office issued all text products that were associated with warnings for the sites. By correlating warning text products with radar loop imagery and surface analysis maps for the same date and time, the meteorological conditions for the day at each site can be determined.

3.9 Wind Data Analysis

Wind data was collected from station WYCM6 – 8747437 at Bay Waveland Yacht Club, Mississippi (NDBC, 2016). This station records wind speed and direction at 6-minute increments and was used to document the frequency of wind direction and speed during the study period. This data was then applied to the marsh edge at each site where the platform meets open water. This will be referred to as the "Shoreline Azimuth" and it is the range of azimuth degrees where wind directly blows towards the marsh edge (Fig. 11). Each site has a specific shoreline azimuth that is a result of its location and orientation relative to open water. This was done in order to understand the azimuth degrees that were considered open water at each site. The specific direction (azimuth) at which wind was blowing from was extracted from the wind data for each site (Fig. 11). This data was then compiled to determine the percentage of each epoch when the wind was blowing towards the marsh edge, thus creating waves, which

could impact the marsh edge. The compiled wind data was also used to calculate the maximum

and average wind speeds for each site during each epoch.
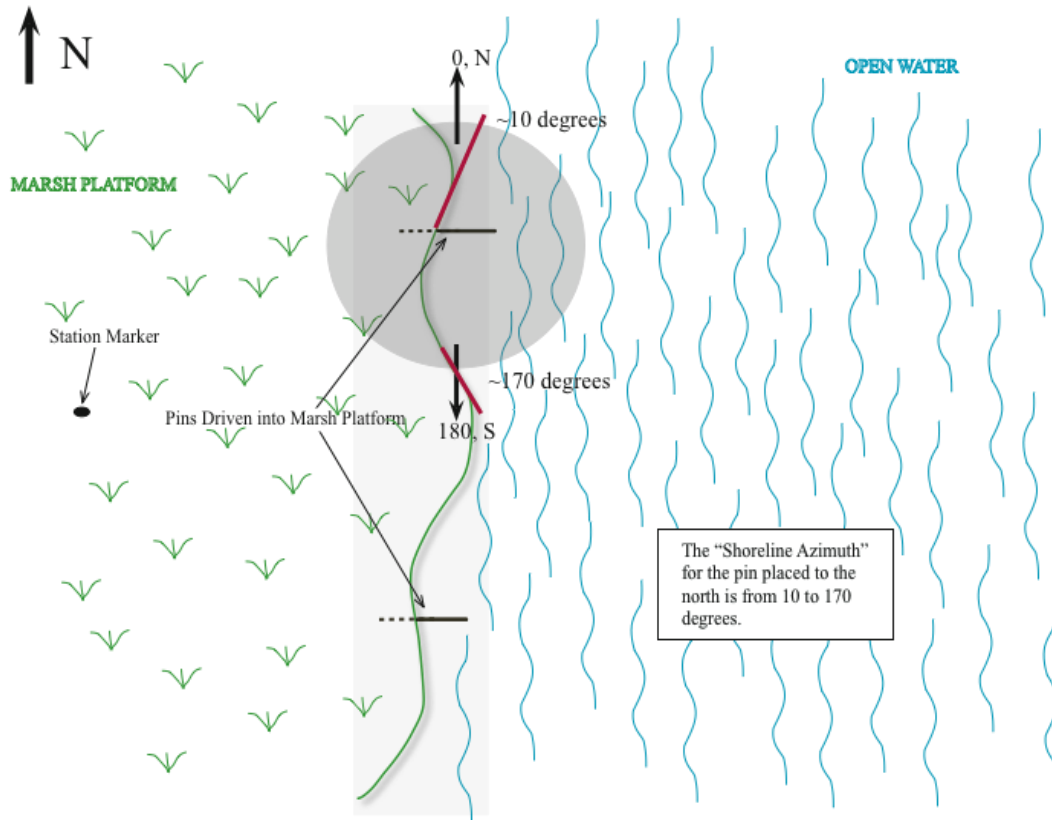
Figure 11.The "Shoreline Azimuth" for a particular pin is defined as the range of azimuth degrees where shoreline exists at each site. The figure illustrates how this is defined based on the placement of erosion pins at each site. The shaded circle represents the area in question that is proximal to the erosion pin. The area between the red lines within the circle represents the extent from which waves can travel to impact the erosion pin. Thus, for the example in the figure, the Shoreline Azimuth for the northernmost pin is from 10° to 170°. This means that wind that would create waves between these azimuth degrees was considered for the study.

CHAPTER 4. RESULTS

4.1 Site 1

Site 1 is located on a peninsula of the Biloxi Marsh and its marsh edge is exposed to the Mississippi Sound (Fig. 2). This site is situated the furthest north in comparison to all sites.

4.1.1 Station Marker and Erosion Pin Exposure Measurements

Station marker measurements and erosion pin measurements are shown in Table 2 and are referenced throughout the results section. Station marker measurements, with the exception of a slight increase in height on July 8th, 2015, at Site 1 consistently show a decrease in height of the station marker, suggesting that deposition occurred. Site 1 NE pin had the highest amount of recorded erosion from erosion pin exposure length with a value of 2.17 m during the study. With the exception of Site 4 pins, Site 1 SW pin had the smallest recorded amount of erosion at 1.09 m. Both the NE and SW pins recorded their highest amounts of erosion during Epoch 2. Site 1 NE pin recorded approximately 0.65 m of erosion during this epoch and Site 1 SW pin recorded approximately 0.64 m. An interesting observation to make is that during Epoch 3, Site 1 NE pin experienced 0.48 m of erosion and Site 1 SW pin experienced a dramatically lesser amount of erosion that was recorded to be 0.04 m (Table 2).

In comparison to erosion pin exposure measurements that occurred during epochs, the approximated daily erosion rate is shown on the left-hand side of Figure 12 for Site 1 NE pin and Figure 13 for Site 1 SW pin. While the highest amount of erosion was recorded during Epoch 2 for the NE and SW pin, the daily rate of 1.41 cm day^{-1} during Epoch 3 was higher than the daily rate of 0.85 cm day^{-1} during Epoch 2 for Site 1 NE pin. The smallest daily rate of erosion for Site 1 NE pin was calculated to be during Epoch 1 at a rate of 0.49 cm day^{-1}. The highest daily rate of

erosion at Site 1 SW corresponds with the highest erosion that was recorded during Epoch 2 at a rate of 0.84 cm day^{-1}. During Epoch 3 a rate of 0.12 cm day^{-1} was calculated and was the smallest value of daily erosion rate.

4.1.2 Terrace Measurements

Terrace and lateral marsh edge erosion measurements are labeled as Site 1 NE Pin and Site 1 SW Pin and are shown in Figure 12 and 13. Both locations have minimal terrace depth measurements in comparison to other sites. Site 1 NE Pin back terrace measurements were observed to be 40 cm on December 9th, 2015 and were observed as 11 cm on March 4th, 2016. There was only one recorded front terrace depth on March 4th, 2016 at a depth of 89 cm. The lack of front terrace measurements is a result of the fact that terraces were not observed at Site 1 until March 4th, 2016. Figure 12 illustrates the transgression of the marsh edge, with reference to the station marker, as a result of erosion from 16.94 m at the beginning of the study to 13.93 m at the end of the study. The greatest amount of erosion took place during Epoch 2 with a recorded amount of 1.65 m of erosion.
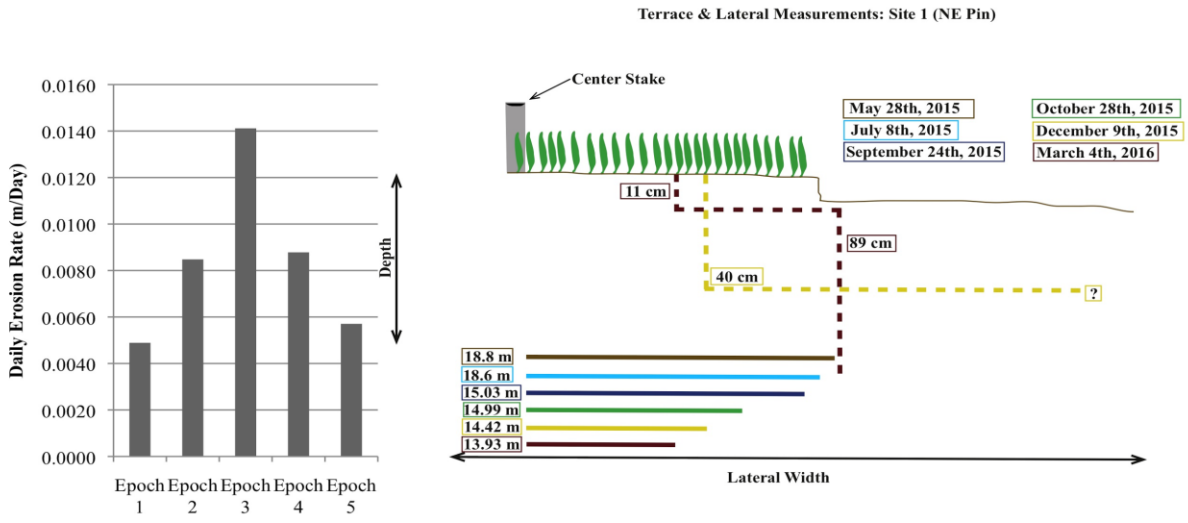
Figure 12. Left side of figure shows the calculated daily erosion rate for each epoch on the basis of Site 1 NE erosion pin measurements. The right side is a cross sectional depiction of the marsh edge and terrace systems, at Site 1 NE Pin.

Marsh edge erosion and terrace depth measurements are illustrated on Figure 13 for Site 1 SW Pin. Back terrace data at this site was collected on December 9th, 2015 and March 4th, 2016. During the site visit on December 9th, 2015, the back terrace was 42 cm deep and the depth reduced to 22 cm during the final visit. There is only a singular measurement of 73 cm on March 4th, 2016 for the front terrace at this location because front terraces were not apparent until this date. The initial distance from the station marker to the SW erosion pin at the marsh edge on May 28th, 2015 was recorded to be 18.8 m. Final marsh edge measurements from the station marker were recorded to be 14.74 m. During the study, the greatest change in erosion was recorded during Epoch 2 from July 8th, 2015 to September 24th, 2014 when 3.37 m of erosion

occurred.
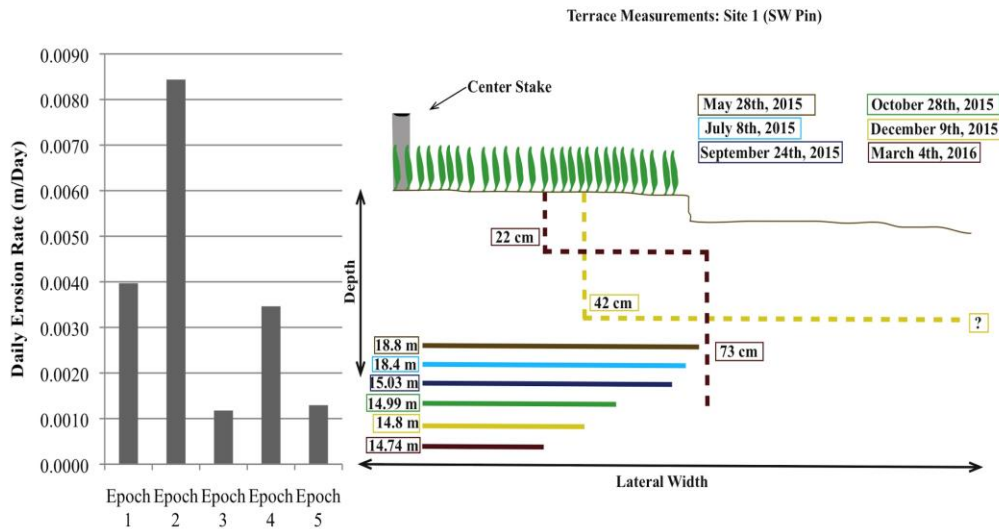
Figure 13. Left side of figure shows the calculated daily erosion rate for each epoch on the basis of Site 1 SW erosion pin measurements. The right side is a cross sectional depiction of the marsh edge and terrace systems, at Site 1 SW Pin.

4.1.3 Core Analysis

Two shallow sedimentary cores were taken from Site 1 on December 9th, 2015, labeled as "S1-NE-Core" and S1-SW-Core." The S1-NE-Core (Fig. 14) penetrated 1-m of marsh platform strata. Strata in the core fines from top to bottom and from clay to silt with inter-bedded sand stringers throughout the column. From the base of the 1-m long core strata showing a subtle fining upward textural trend of clay to silt with thin, less than 0.1 cm thick fine-grained quartz sand stringers throughout. Sand stringers were present at 0.15, 0.23 to 0.25, 0.36 to 0.41, and at 0.46 m the upper 0.5 m of the column contain "stiff" sediments that is underlain by "soft" sediments in the lower 0.5 m of the column. From the surface to 1-m below, organic content decreases from approximately 50% to less than 10%. From 0.23 to 0.25 m thick sand stringer

30

was present, replacing organic content that would have been present in this section of the core.
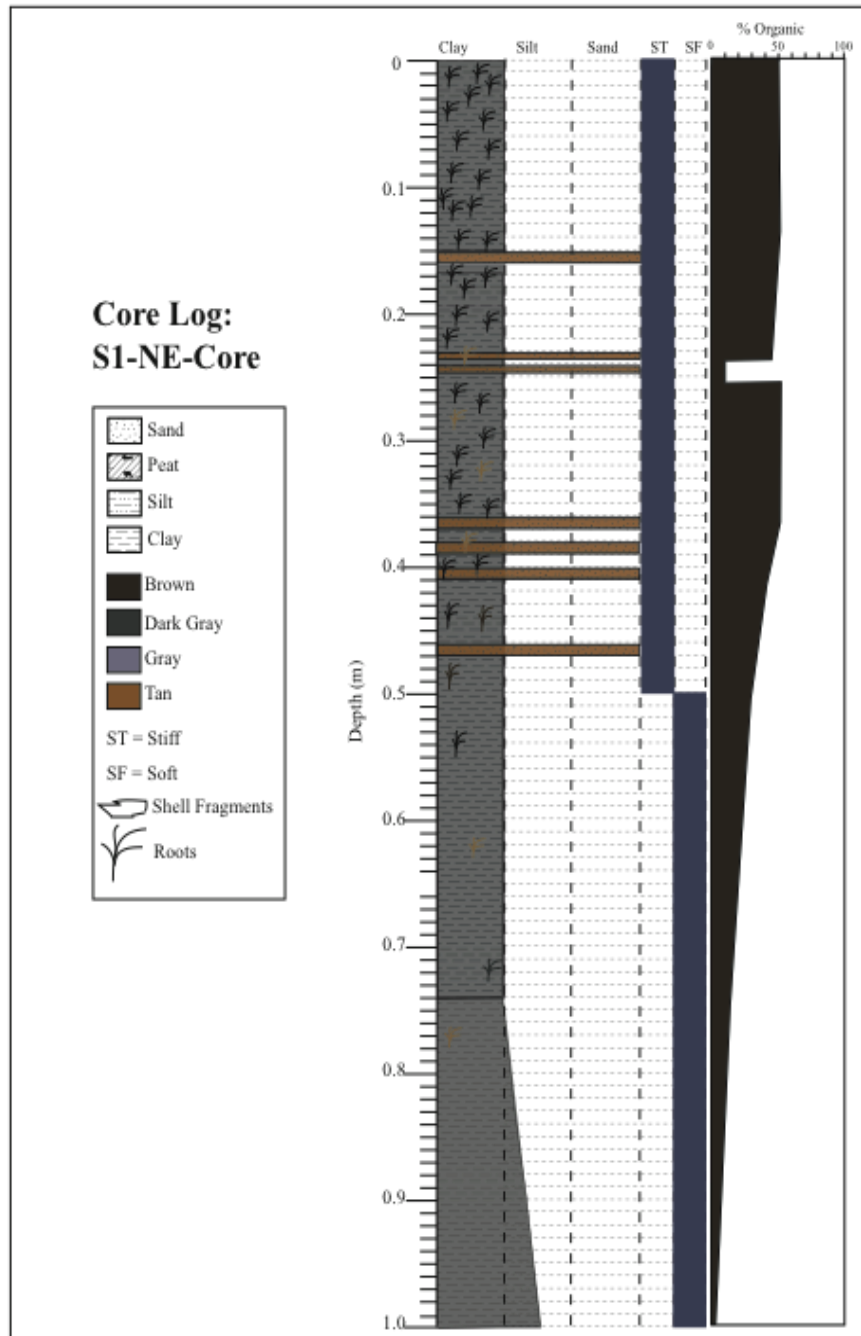
Figure 14. Core description log for the 1-m push core taken 1.5 m landward from the Site 1 NE erosion pin placement.

      The core labeled S1-SW-Core (Fig. 15) provides a record of the shallow marsh platform

strata proximal to the southwest erosion pin. Compared to the other cores the marsh platform

stratigraphy here contains the highest percentage of sand. From the surface to 1-mdepth, sediments are mostly clay with sand stringers that; grade into siltier units in the lower 0.5-m section of the core. There are approximately 60% more sand stringers from 0.08 to 0.12, 0.28 to 0.36, and 0.39 to 0.4 m with a thick sand stringer located from 0.2 to 0.22 m in comparison to S1-NE-Core. From 0-m to 0.22 m, the sediments are "stiff." From 0.22 to 0.8 m, sediments are "soft" but then are underlain by to "stiff" sediments for the last 0.2 m of the core. Upon visual analysis of the core, shell fragments were also observed at 0.26 and 0.38 m. The overall organic content of this stratigraphic column decreases from a maximum of approximately 60% at the surface and decrease to approximately 30% at 0.53 m where organic content increases slightly to 50% and then decreases again to less than 1% near 1-m depth.
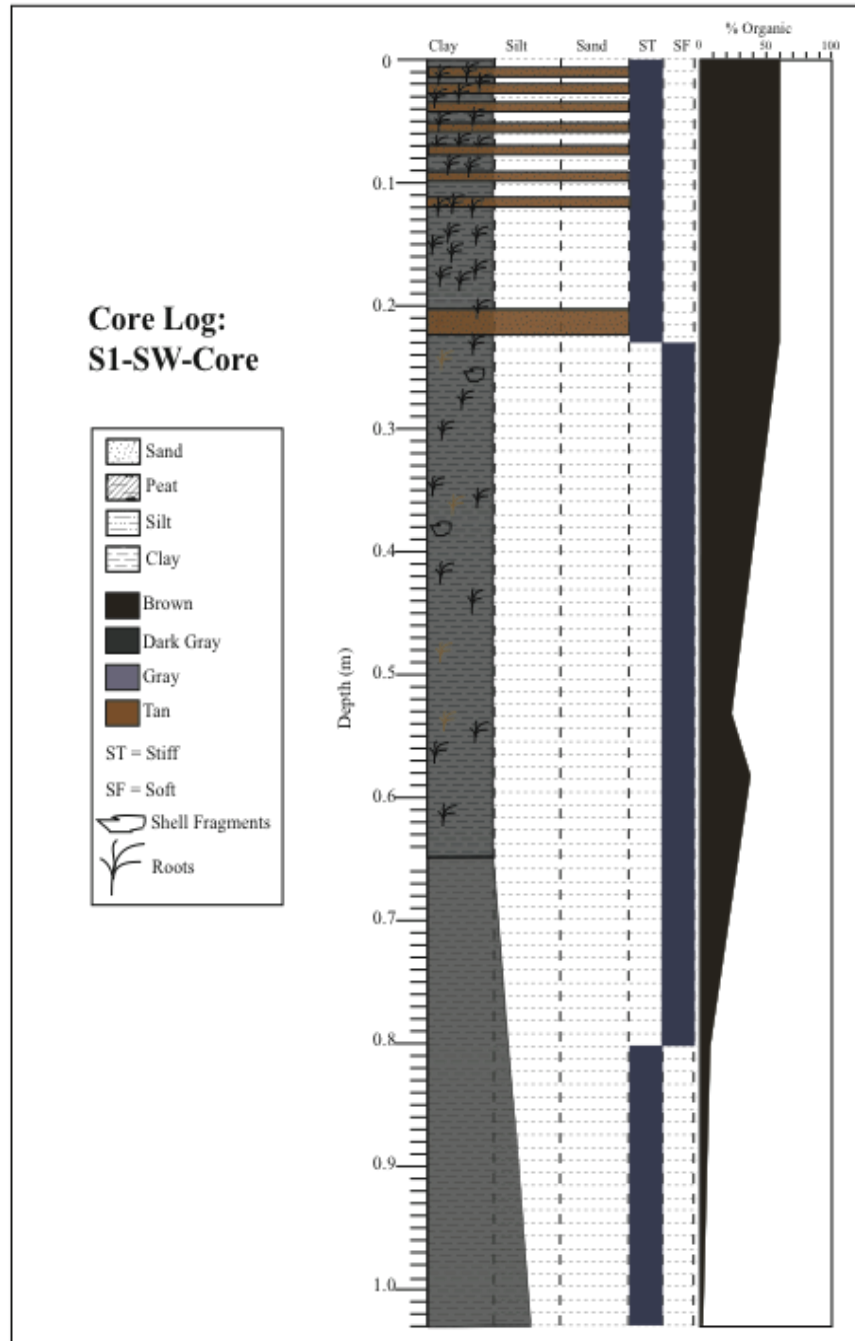
Figure 15. Core description log for the 1-m push core taken 1.5 m landward from the Site 1 SW erosion pin placement.

4.1.4 Photo Comparison and Marsh Edge Characteristics

Figure 16 is a chronology of marsh edge evolution at Site 1 and forms the basis for subsequent discussions of marsh edge evolution. During the initial site visit on May 28th, 2015, the edge at Site 1 was characterized by small neck and cleft (*sensu* Schwimmer, 2001*)* formations along the marsh edge. Visual observations from the second site visit on July 8th, 2015 indicated that the edge still had cleft and neck morphology but became more linear as the necks did not protrude as far into the water and the clefts were not embayed as far into the interior platform. On September 24th, 2015, the water was high as a result of a spring tide and the majority of marsh edge features were underwater. However, it was evident during this site visit that the edge was more linear to the northeast but the shoreline to the southwest transitioned to cleft and neck formations. Vegetation near the marsh edge also began to brown and there were indications of plant death.

On October 28th, 2015, the vegetation along the edge was mostly dead and vegetation that had been farther inland was entering senescence as a result of the changing seasons. The marsh edge at this point in time was characterized by cleft and neck formations once again. The marsh edge to the southwest appeared to have vertically and laterally incised cleft and necks than the shoreline to the northeast. During the site visit on December 9th, 2015 the lower marsh scarp was visible and the edge was characterized by smaller cleft and neck formations (Fig. 16). On December 9th, 2015, most of the *Spartina alterniflora* had died off at the edge and interior of the marsh. The marsh edge on March 4th, 2016 had an abundant amount of cleft and neck formations along the marsh edge that were tightly spaced together (Fig. 16). During this site visit, the lower scarp was also visible and *Spartina alterniflora* started to grow once again (Fig. 16). The marsh edge at this site evolved during the course of the study by transitioning from cleft and neck

34

formations to a more linear edge that transition back to more enhanced clefts and necks (Fig. 16).
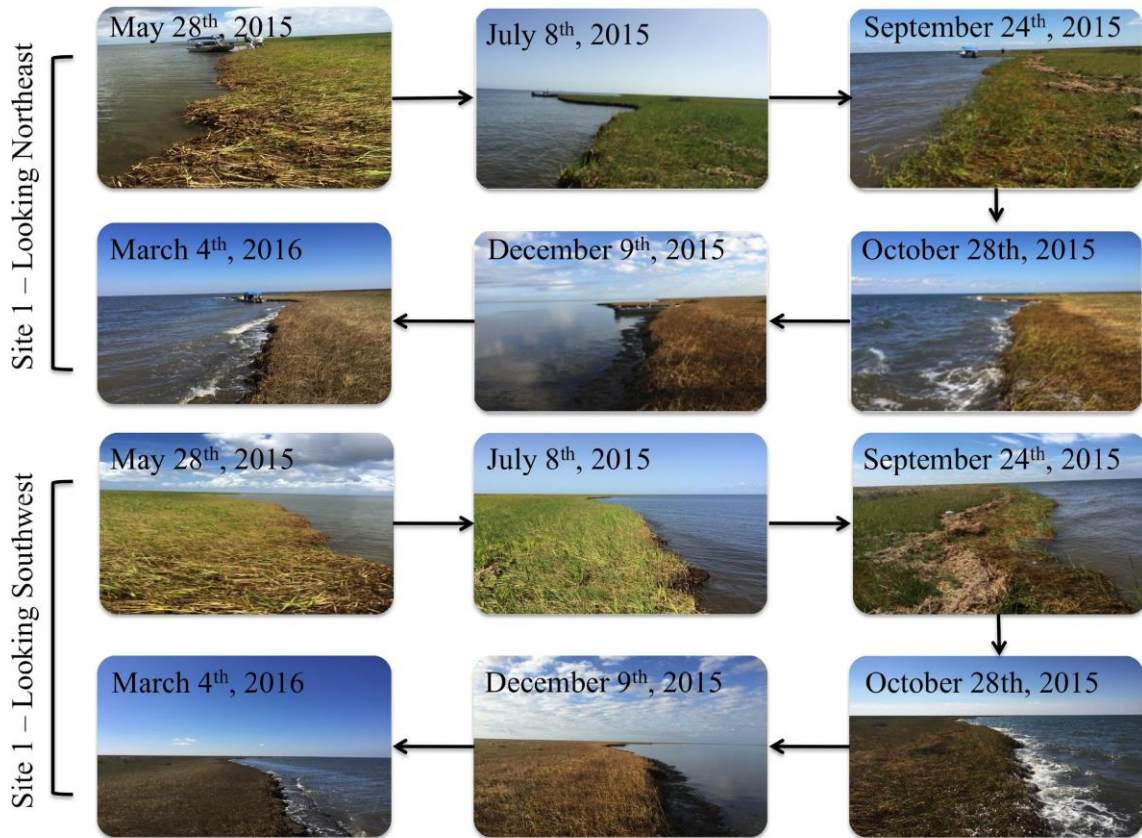
Figure 16. A timeline of photos that were taken during each site visit to Site 1 that were used to track marsh-edge characteristics. The photos in the upper-half of the figure are taken with the perspective along the marsh edge that is oriented to the east. Photos in the bottom-half of the figure represent the perspective along the marsh edge that is oriented westward. Photos from October 28th, 2015 are missing due to file corruptions.

4.2 Site 2

Site 2 is located on a peninsula of the Biloxi Marsh and its marsh edge is exposed to the Mississippi Sound (Fig. 2). This site is situated to the southwest of Site 1.

4.2.1 Station Marker and Erosion Pin Exposure Measurements

Station marker heights for Site 2 on Table 2 show an initial decrease in height from 0.65 m to 0.62 m from May 28th to July 8th, 2015. On September 24th, 2015, the height was

recorded to be 0.67 m. every measurement recorded after September 24th, 2015 decreases, suggesting that there is deposition occurring on the platform near the station marker. The two erosion pins at Site 2 are labeled as "Site 2 NE" and "Site 2 SW." Site 2 NE pin recorded the second highest cumulative erosion behind Site 1 NE with a value of 2.14 m. Site 2 SW pin recorded over a meter less erosion than the NE pin with a value of 1.3 m. The highest amount of erosion for both pins occurred during Epoch 2 when the NE pin experienced 0.59 m of erosion and the SW pin experienced 0.65 m. Similar to Site 1, it should be noted that during Epoch 4 the NE and SW recorded dramatically different erosion measurements with 0.61 m of recorded erosion at Site 2 NE and 0.01 m of recorded erosion at Site 2 SW (Table 2).

The approximated daily erosion rate is shown on the left-hand side of Figure 17 for Site 2 NE pin and Figure 18 for Site 2 SW pin. During epoch 2, the greatest amount of erosion pin exposure was recorded for both pins. However, the daily rate of 1.49 cm day^{-1} during Epoch 4 was higher than the daily rate of 0.79 cm day^{-1} during Epoch 2 for Site 2 NE pin. The smallest calculated rate of daily erosion for the duration of the study was 0.46 cm day^{-1} during Epoch 5. The maximum daily rate of erosion at Site 2 SW is similar to the rate at Site 1 SW pin with a rate of 0.85 cm day^{-1}. This maximum also corresponds with the highest erosion that was recorded during Epoch 2. During Epoch 3 a rate of 0.03 cm day^{-1} was calculated and was the smallest value of daily erosion rate for Site 2 SW.

4.2.2 Terrace Measurements

Lateral erosion measurements and terrace depth measurements taken at Site 2 NE Pin are shown in Figure 17 and Site 2 SW Pin measurements are shown in Figure 18. Site 2 NE Pin terrace measurements were not started until September 24th, 2015 and ended on March 4th,

2016. Back terrace measurements are initially deep with a measurement of 43 cm that decreased in depth to 16 cm on October 28th, 2015 and increased in depth again for the proceeding measurements. Front terrace measurements are not consistent due to the absence of a second terrace or inability to identify it. Measurements taken on December 9th, 2015 and March 4th, 2016 for the front terrace increased in depth from 13 cm to 35 cm. Lateral erosion measurements are based on the length of exposure of each erosion pin. Through the duration of the study, edge erosion occurred between each epoch. Overall erosion of the marsh edge was calculated to be 4.74 m for the entirety of the study. The greatest amount of erosion took place from July 8th, 2015 to September 24th, 2015 when approximately 3.2 m of erosion occurred.
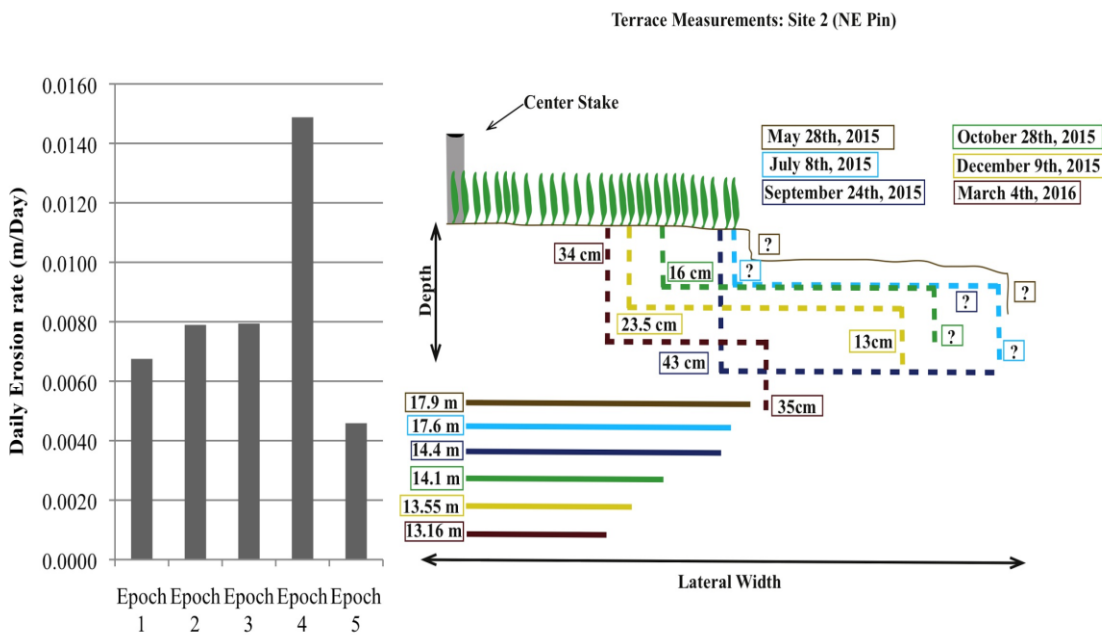
Figure 17. Left side of figure shows the calculated daily erosion rate for each epoch on the basis of Site 2 NE erosion pin measurements. The right side is a cross sectional depiction of the marsh edge and terrace systems, at Site 2 NE Pin.

Back terrace measurements at Site 2 SW Pin had an initial depth of 36 cm on September 24th, 2015 and decreased to a depth of 19 cm on March 4th, 2016. Front terrace measurements at

this location were scarce but the two measurements from December 9th, 2015 and March 4th, 2016 increased in depth from 17 cm to 41 cm. Lateral erosion of the marsh edge that is recorded by measuring the exposure of the SW erosion pin at Site 2, shows a landward transgression of the marsh edge through the duration of the study from 20 to 15.68 m. The greatest amount of erosion occurred during Epoch 2 from July 8th, 2015 to September 24th, 2015 and was approximated to be 3.67 m.
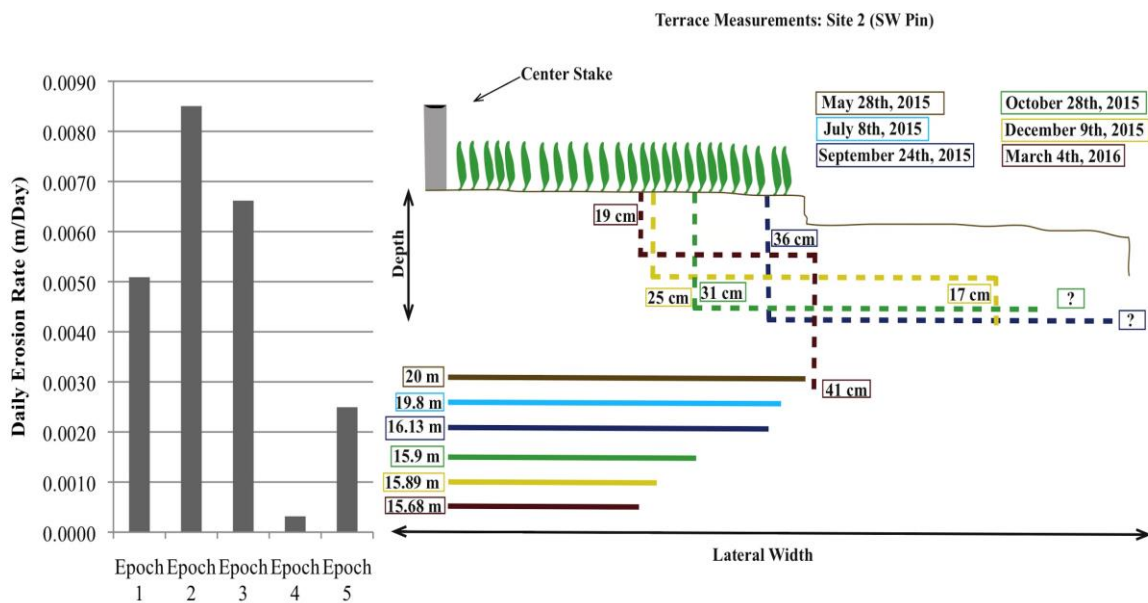
Figure 18. Left side of figure shows the calculated daily erosion rate for each epoch on the basis of Site 2 SW erosion pin measurements. The right side is a cross sectional depiction of the marsh edge and terrace systems, at Site 2 SW Pin.

4.2.3 Photo Comparison and Marsh Edge Characteristics

Figure 19 provides a timeline of photos taken during each visit to Site 2. These photos provide the basis for marsh edge characterization and evolution within the following results section. The initial site visit on May 28th, 2015 identified a linear marsh edge to the northeast that became, in the opposing direction to the southwest, dominated by incised cleft and

Neck formations. The predominant vegetation was *Spartina alterniflora.* On July 8th, 2015, the marsh edge to the northeast became less linear and was characterized by cleft and Neck formations. The edge to the southwest was still dominated by cleft and neck formations that are visible but the necks eroded closer to the edge while the clefts did not incise further. *Spartina alterniflora* during the September 24th, 2015 visit began to die off and turn brown near the marsh edge. The marsh edge was still characterized by clefts and necks although it is difficult to determine the extent as a result of the high water level.

Marsh edge characteristics that were observed during the site visit on October 28th, 2015 still represented a marsh edge with cleft and neck formations. However, most of the vegetation died off near the edge and began to die off towards the interior of the marsh. The lower scarp and terrace were visible on December 9th, 2015 and cleft and neck formations still characterized the marsh edge. At this point in time, vegetation on the marsh platform died off for the winter. On March 4th, 2016, the lower scarp at the marsh edge was visible and there was an abundant amount of terraces, approximately 2 to 3. The marsh edge was still characterized by cleft and neck formations but during this point in time, the formations appeared to be spaced closer together and more numerous. Cleft and neck formations dominated the marsh edge at this

site and continuously evolved from incised clefts to less incised clefts adjacent to necks.
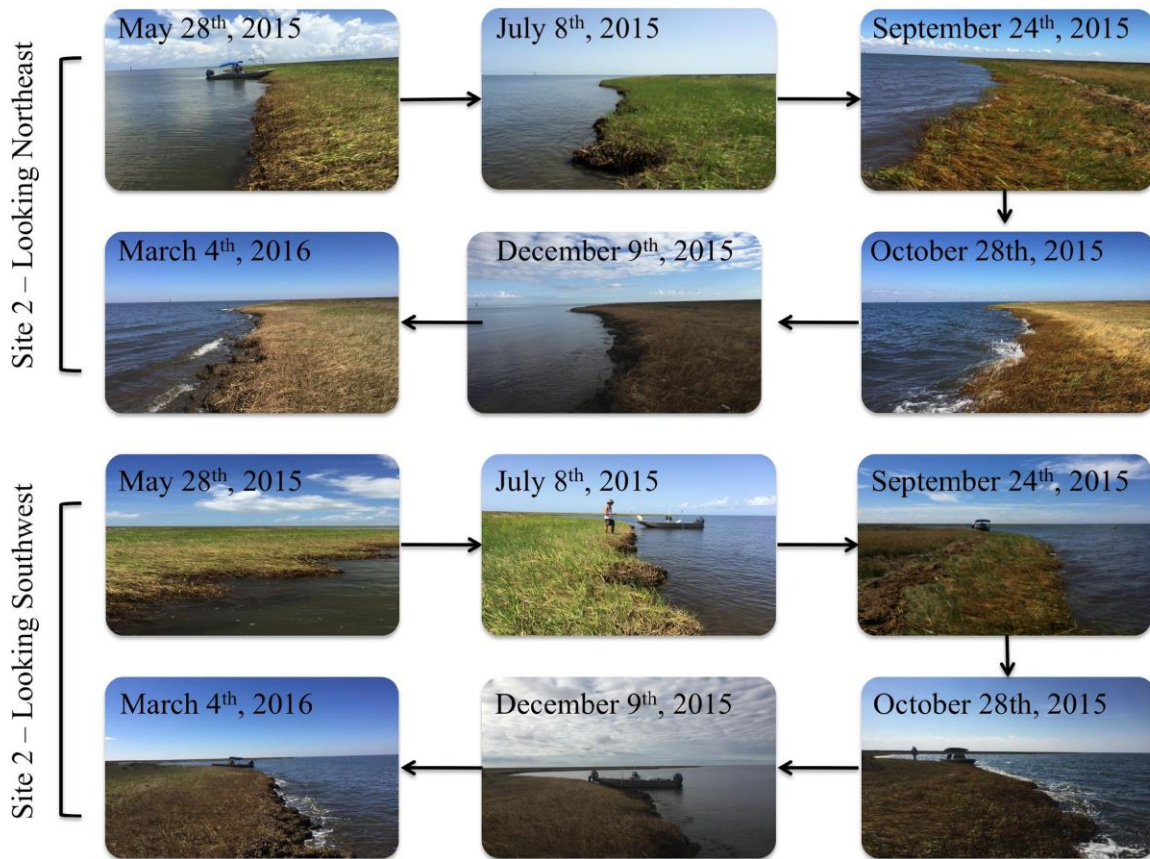

Figure 19. A timeline of photos that were taken during each site visit to Site 2 that were used to track marsh-edge characteristics. The photos in the upper-half of the figure are taken with the perspective along the marsh edge that is oriented to the east. Photos in the bottom-half of the figure represent the perspective along the marsh edge that is oriented westward. Photos from October 28th, 2015 are missing due to file corruptions.

4.3 Site 3

Site 3 is located on a peninsula of the Biloxi Marsh and its marsh edge is exposed to Grand Pass and the Gulf of Mexico (Fig. 2). This site is situated on the eastern part of the peninsula and is located to the southeast of Site 1.

4.3.1 Station Marker and Erosion Pin Exposure Measurements

Site 3's station marker measurements shown on Table 2 are similar to measurements recorded at Site 1 and 2 in that the measurements decrease from the beginning of the study to the end of the study. The initial station marker height was observed to be 0.55 m and decreased to 0.37 m on March 4th, 2016. Although the original height that was observed is lesser than sites 1 and 2, the overall change recorded was a decrease in height of 0.18 m, which is the maximum decrease in height when comparing to sites 1 and 2. The two erosion pins at Site 3 are labeled as "Site 3 N" and "Site 3 S." Site 3 N pin did not record the highest amount of erosion but still recorded a cumulative erosion of 2.13 m for the study. However, this pin recorded the maximum amount of erosion that occurred during any epoch across all of the sites with a value of 0.88 m during Epoch 3. Site 3 S pin recorded a cumulative erosion total of 1.668 m for the study and recorded its peak erosion during Epoch 2 with a value of 0.5682 m. During Epoch 3, a similar observation was made to that of Site 2's pins where Site 3 N pin measured 0.88 m of erosion and Site 3 S pin recorded 0.1 m, a significantly less amount of erosion (Table 2).

In comparison to erosion pin exposure measurements, the approximated daily erosion rate is shown on the left-hand side of Figure 20 for Site 3 N pin and Figure 21 for Site 3 S pin. For Site 3 N pin the highest daily erosion rate was calculated to be 2.59 cm day^{-1} during Epoch 3, the same epoch during which the highest amount of erosion pin length exposure was recorded. The maximum daily rate at Site 3 N pin is also the highest daily rate recorded across all pins for the duration of the study. The smallest daily erosion rate for Site 3 N pin was 0.29 cm day^{-1} during Epoch 5. The maximum daily rate of erosion at Site 3 S occurred during Epoch 4 at a rate of 1.29 cm day^{-1}. This maximum does not correspond with the highest erosion pin exposure

measurement that was recorded during Epoch 2. The minimum daily erosion rate during the study occurred during Epoch 4 at a rate of 0.24 cm day^{-1}.

4.3.2 Terrace Measurements

Terrace depth and marsh edge measurements for Site 3 are labeled as "Site 3 N Pin" and "Site 3 S Pin" and are shown in Figure 20 and Figure 21. There are abundant measurements at Site 3 for front and back terraces due to the coastal geomorphology at this particular site. Back terrace measurements at Site 3 N Pin show a pattern of decreasing, to increasing, to decreasing in depth again throughout the duration of the study. Front terrace measurements do not appear to have a similar pattern as the back terrace measurements. Instead, the front terrace is measured at a depth of 20 cm on May 28th, 2015 and slightly increased in depth on July 8th, 2015. Data collected on October 28th, 2015 suggests that the terrace decreased in depth by approximately 2 cm. However, the terrace began to increase in depth significantly and was recorded to be 32 cm on December 9th, 2015 and increased in depth again to 48 cm on March 4th, 2016 (Fig. 20). The initial marsh edge measurement from the station marker was 16.9 m on May 28th, 2015. Final marsh edge measurement taken on March 4th, 2016 was 13.1 m, showing that a total of 3.8 m of the marsh edge was eroded during the course of the study. The greatest amount of erosion at this site occurred during Epoch 1 from May 28th, 2015 to July 8th, 2015 when 1.75 m of marsh edge eroded.
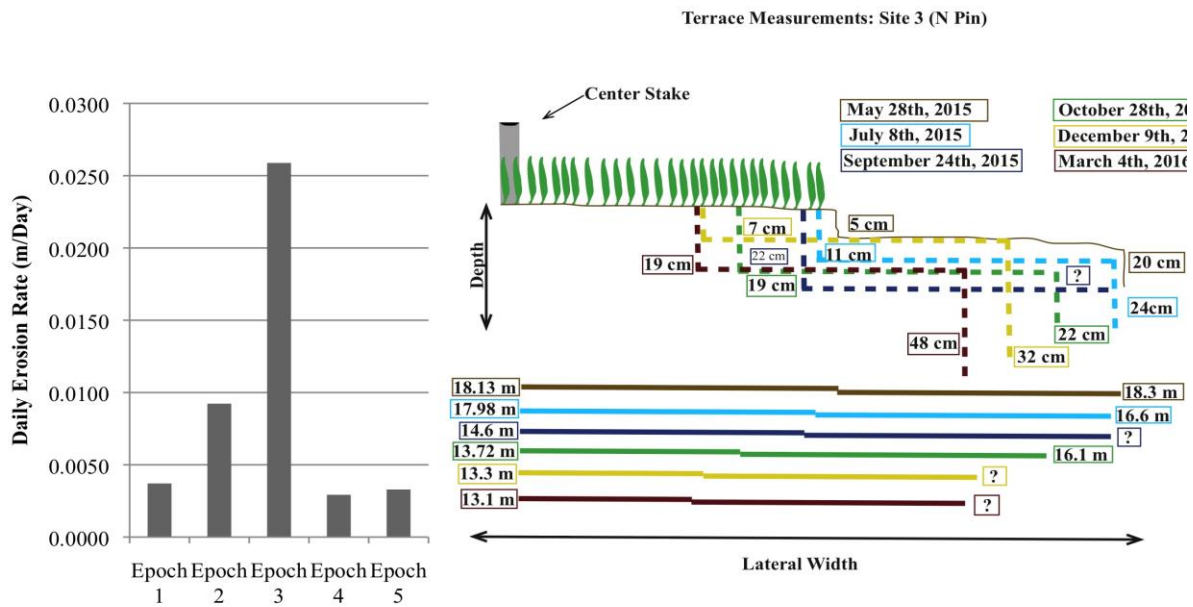
Figure 20. Left side of figure shows the calculated daily erosion rate for each epoch on the basis of Site 3 N erosion pin measurements. The right side is a cross sectional depiction of the marsh edge and terrace systems, at Site 3 N Pin.

Site 3 S Pin has similar front and back terrace measurements to those measured at

Site 3 N Pin and is described in Figure 21. Back terrace measurements at Site 3 S Pin

consistently decreased in depth throughout the duration of the study from 25 cm, on May 28th,

2015 to 8 cm on March 4th, 2016. However, it should be noted that back terrace depths for this

site were not recorded on December 9th, 2015. Front terrace measurements do not follow the

same pattern as the back terrace measurements and instead remained nearly constant at

approximately 65 cm from May 28th to July 8th, 2015, then decreased in depth to 33 cm on

October 28th, and finally the terrace increased in depth once again to 49 cm on March 4th, 2016.

The initial marsh edge measurement from the station marker to the south erosion pin was

measured to be 20.04 m. During the last site visit, the marsh edge was measured to be 16.41 m

from the station marker giving a total erosion of 3.63 m for the study. The greatest amount of erosion at this site occurred during Epoch 2 when 2.47 m of erosion occurred at this site.
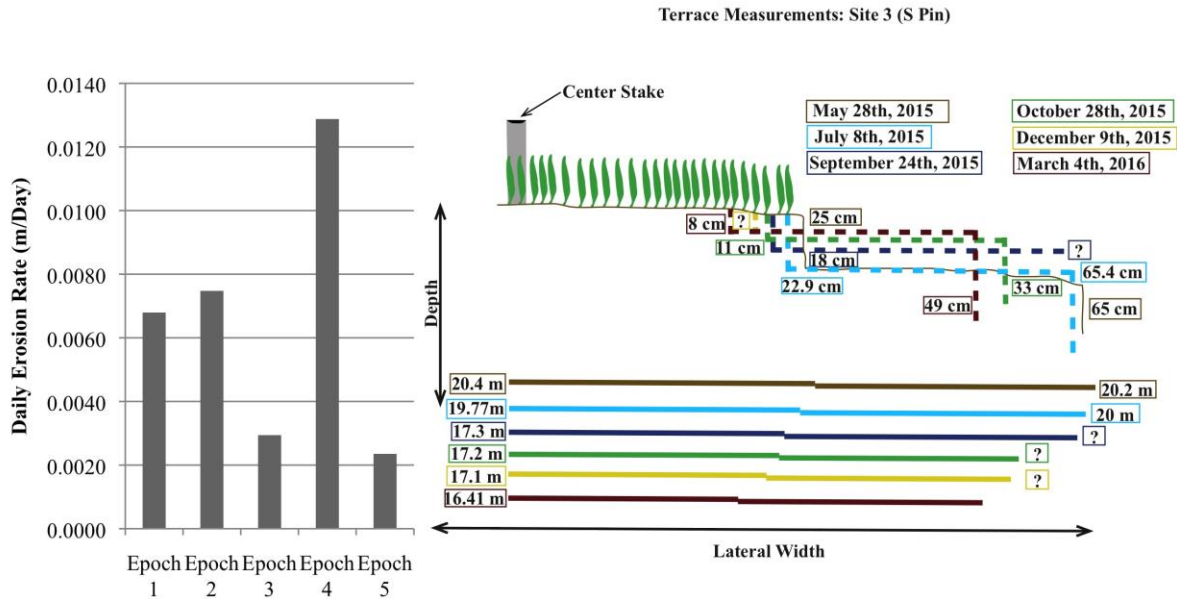
Figure 21. Left side of figure shows the calculated daily erosion rate for each epoch on the basis of Site 3 S erosion pin measurements. The right side is a cross sectional depiction of the marsh edge and terrace systems, at Site 3 S Pin.

4.3.3 Core Analysis

   Two cores labeled as "S3-N-Core" and "S3-S-Core" designates the visual core analysis at Site 3 and is illustrated in Figures 22 and 23. Both cores show different stratigraphic and sedimentary features than those at Site 1. S3-N-Core core represents the 1-m stratigraphic column that was sampled 1.5 m landward from the north erosion pin. Visual analysis of this core from the surface to 1-m below the surface shows mostly clay-sized sediments with few sand stringers, in comparison to other cores, throughout the stratigraphic column that are underlain by siltier sediments starting at approximately 0.65 m depth. This core has the least amount of sand (~5%) and the highest organic content (~60%) in comparison to all of the sampled cores. Near

44

the surface, the column contains an abundance of organic material that is underlain by siltier sediments as a depth of half a meter is reached. There are few shell fragments present within the column (~2%) that are mostly focused below a shallow layer of peat from 0.27 to 0.3 m. There is a transition from "stiff" sediments in the upper 0.5 to 0.6 m that is underlain by "soft" sediments in the lower half of the core as well (Fig. 22).
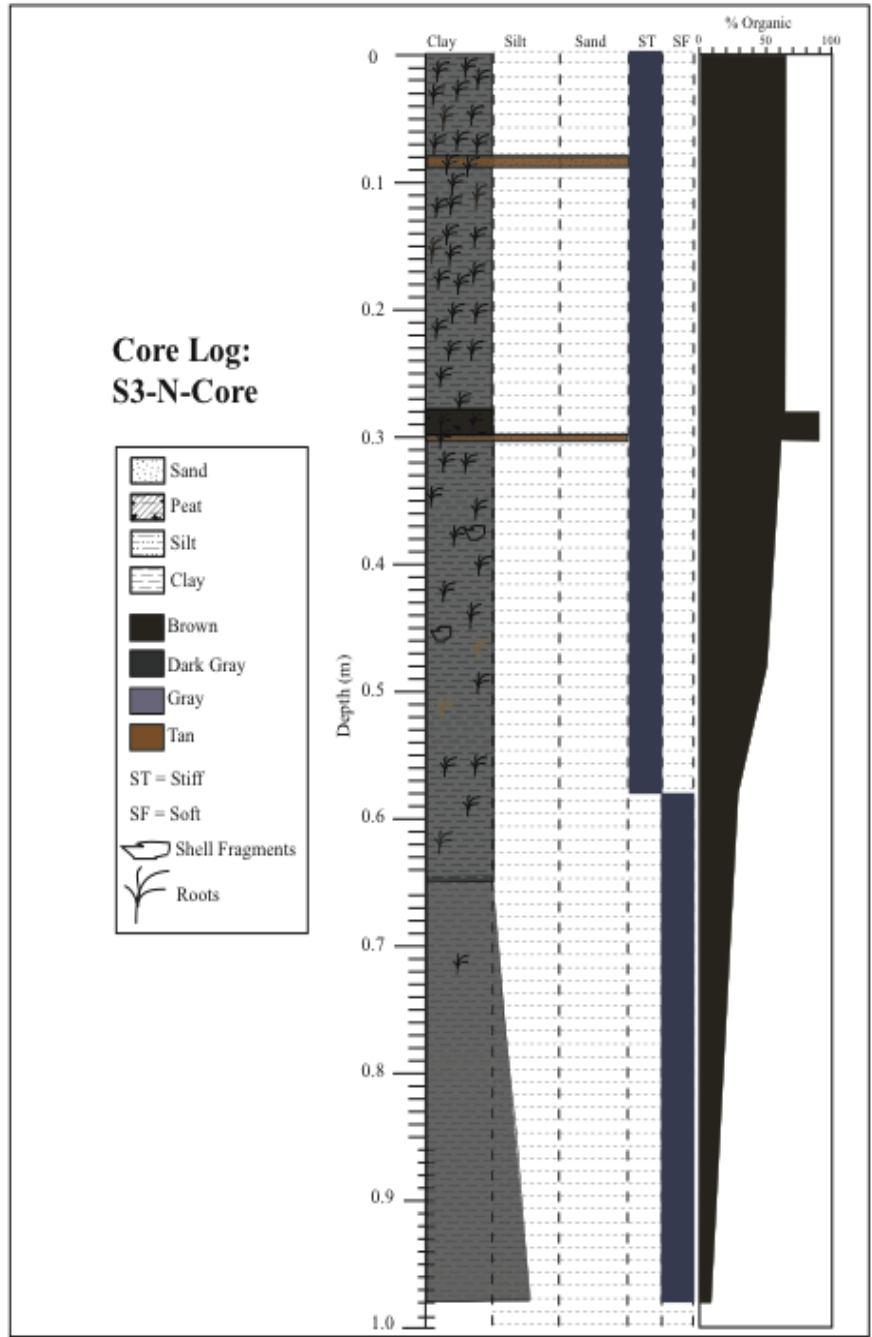
Figure 22. Core description log for the 1-m push core taken 1.5 m landward from the Site 3 N erosion pin placement.

S3-S-Core is illustrated in Figure 23 and represents the stratigraphic column that was

sampled 1.5 m directly behind the south erosion pin at Site 3. The strata of this core is dissimilar

from S3-N-Core. From the surface to 1-m depth, organic content decreases from approximately 60% to less than 5%. This stratigraphic column does not have shell fragments or peat present in it, unlike the core taken near the north pin. However, it does have more abundant amounts of sand in the form of multiple stringers throughout the column. From the surface to 1-m depth the characteristic of the sediment changes from soft clays (0 to 0.2 m) to stiffer clays. The soft clay is underlain by sand stringers and stiffer sediments until 0.5 m. Soft sediments in the latter half of the core underlie this layer as the composition transitions from clay to silt (Fig. 23).
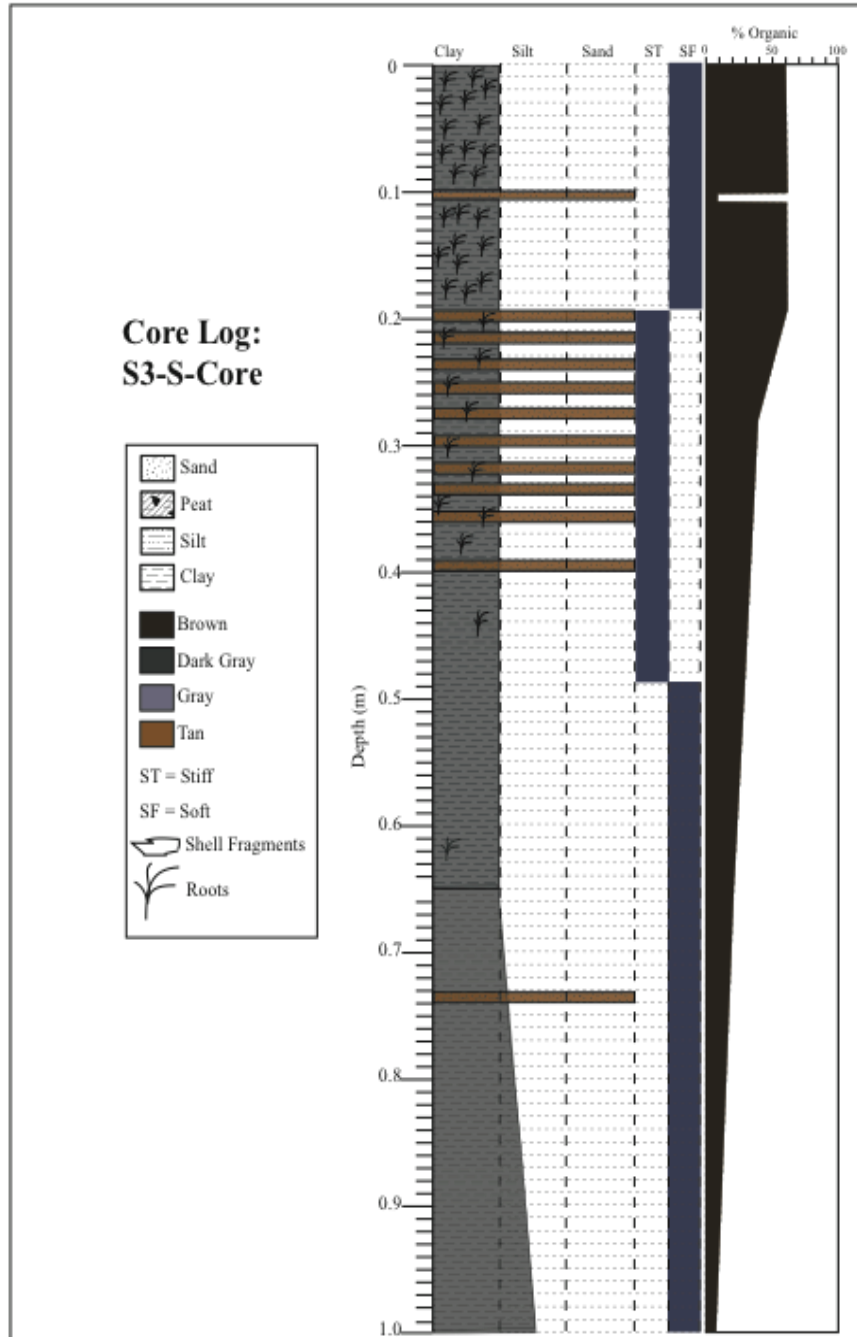
Figure 23. Core description log for the 1-m push core taken 1.5 m landward from the Site 3 S erosion pin placement.

4.3.4 Photo Comparison and Marsh Edge Characteristics

Figure 24 shows a timeline of photos that were taken during each site visit to Site 3 and will be used to identify marsh edge characteristics in the following results section. On May 28th, 2015, a submerged lower terrace was visible near the marsh edge and the edge was characterized by cleft and neck formations. The scarp that was attached to the platform was relatively shallow and vegetation near the edge began to die off. The marsh edge on July 8th, 2015 was characterized by incised cleft and neck formations with a subaerial terrace that had been stripped of vegetation and vegetation on the upper terrace appeared to be dying off near the edge. During the site visit on September 24th, 2015 the marsh edge appeared to be more linear with a gently rolling parabolic shape more similar to bays and headlands rather than clefts and necks.

A lower terrace that had been stripped of vegetation was visible and appeared to have been recently inundated. *Spartina alterniflora* at this site on this date had died off along the entire marsh edge and further into the interior marsh in comparison to other sites. On December 9th, 2015, the exposed lower terrace had algae growing on it and the vegetation was dead from the edge of the marsh towards the interior. The edge had small cleft and neck formations present but they were not as well formed as those observed on July 8th, 2015. During the final site visit on March 4th, 2016 *Spartina alterniflora* had begun to grow back from the interior towards the marsh edge, although the vegetation proximal to the edge was still dead. A lower terrace that had been stripped of vegetation was visible and looked similar to previous terraces that were observed during previous site visits. The marsh edge was characterized by a minimal amount of cleft and neck formations to the north that gently transitioned to a more linear shoreline towards the south. However, further south cleft and neck formations were observed adjacent to the bay.

49

This site was dominated by cleft and neck formations along the edge with a developing subaerial terrace that had been stripped of vegetation. These formations transitioned into bays and headlands through time and transitioned back to cleft and neck formations.
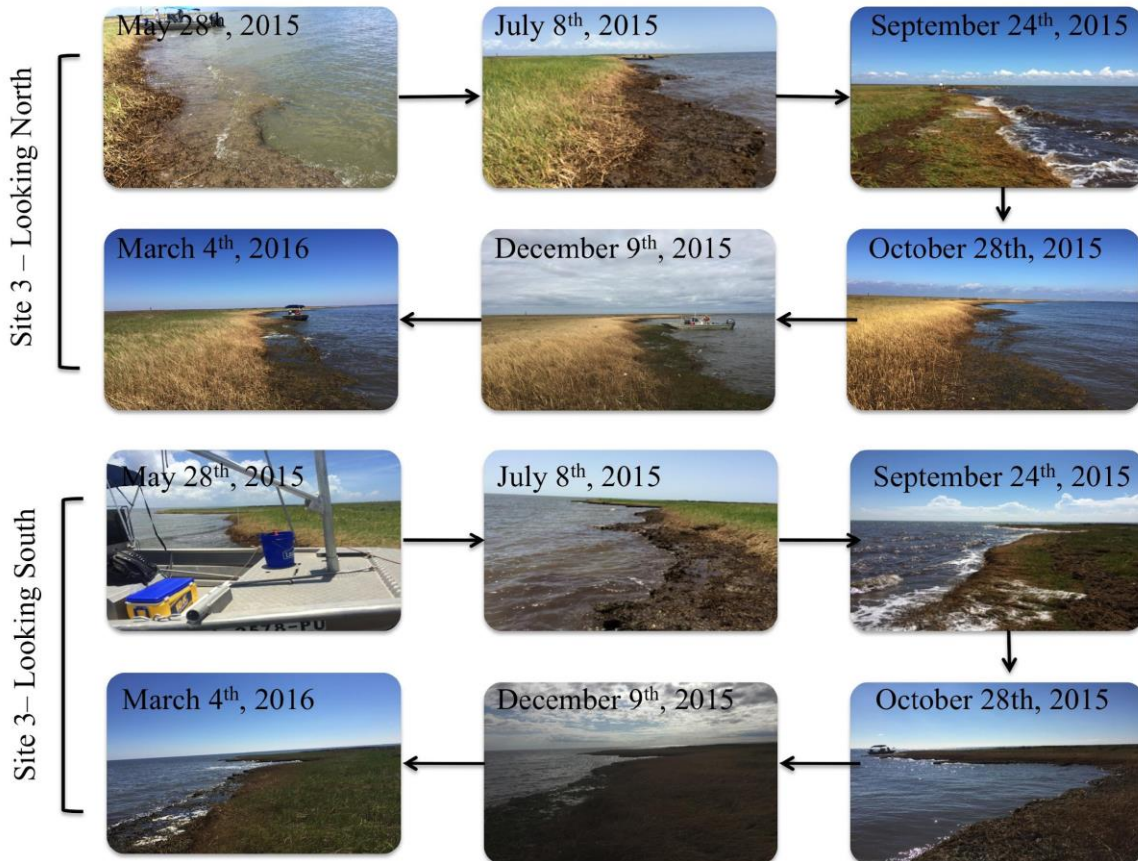
Figure 24. A timeline of photos that were taken during each site visit to Site 3 that were used to track marsh-edge characteristics. The photos in the upper-half of the figure are taken with the perspective along the marsh edge that is oriented to the east. Photos in the bottom-half of the figure represent the perspective along the marsh edge that is oriented westward. Photos from October 28th, 2015 are missing due to file corruptions.

4.4 Site 4

Site 4 is located on a northeast island of the Biloxi Marsh and its marsh edge is exposed to the Gulf of Mexico (Fig. 2). This site is situated the furthest east in comparison to all sites and is adjacent to shell berms and a tidal channel that splits the island.

50

4.4.1 Station Marker and Erosion Pin Exposure Measurements

               Station marker and erosion pin exposure measurements for Site 4 are shown on Table 2. The initial measurement taken on May 28th, 2015 is 0.37 m. The Next recorded measurement on July 8th, 2015 is 0.67 m, suggesting that 0.30 m of height had been added to the station marker. Measurements following these show a slight decrease in height to 0.63 m on September 24th, 2015 followed by a small increase in height on October 28th, 2015 with a measurement of 0.64 m. The first of the two final measurements observe another increase in station marker height to 0.62 m on December 9th, 2015 that decreases once again by March 4th, 2016 to 0.64 m. Erosion pins at Site 4 are labeled as "Site 4 E Pin," "Site 4 E* Pin," and "Site 4 W Pin." Site 4 E* pin is the replacement pin that was installed on September 24th, 2015 when Site 4 E Pin was believed to have fallen out of the substrate. Overall, Site 4 recorded the least amount of erosion in comparison to all other sites. Site 4 E pin recorded the least amount of cumulative erosion with a total of 0.97 m in comparison to all other pins that were installed at the same time. Site 4 E* pin recorded 0.67 m of erosion and Site 4 W pin recorded 0.42 m of erosion from September 24, 2015, the installment date, to March 4th, 2016. Site 4 E pin recorded its greatest amount of erosion during Epoch 1 with a recorded erosion value of 0.27 m. Site 4 E* pin recorded a maximum of 0.49 m of observed erosion during Epoch 5, which is the highest amount of erosion recorded between any of the pins for this epoch. The greatest amount of erosion at Site 4 W pin was observed to be 0.27 m during Epoch 3.

          Approximated daily erosion rates are shown on the left-hand side of figure 25 for Site 4 E pin, figure 26 for Site 4 E* pin, and figure 27 for Site 4 W pin. The maximum daily erosion rate at Site 4 E pin is 0.7 cm day^{-1} during Epoch 1, the same epoch during which the highest amount

of erosion pin length exposure was recorded. At this pin the minimum daily recorded erosion rate was 0 m day^{-1} during Epoch 5 when the pin exposure length remained constant. The additional pin, Site 4 E*, that was installed on September 24th, 2015 recorded a maximum daily erosion rate of 0.58 cm day^{-1} during Epoch 5. The minimum daily erosion rate of 0.17 cm day^{-1} for this pin occurred during Epoch 4. The maximum daily erosion rate corresponds to the same epoch as when the highest erosion pin length exposure measurement was made. At Site 4 W the maximum daily rate occurred during Epoch 3 with a daily rate of 0.79 cm day^{-1}. Similarly, to Site 4 E*, Site 4 W minimum daily erosion rate of 0.07 cm day^{-1} occurred during Epoch 4.

4.4.2 Terrace Measurements

Terrace depths and lateral transgression of the shoreline is depicted in figures 25-27 and are labeled as Site 4 E Pin, Site 4 E* Pin, and Site 4 W Pin. Site 4 E* Pin served as the replacement pin when the original Site 4 E Pin was not found as a result of high water on September 24th, 2015.Measurements at Site 4 are not consistent for the duration of the study because of the lack of front terraces during visits or due to human error in the form of forgetfulness as a result of distraction or lack of concentration. Elevation of the back terrace at Site 4 E relative to the marsh platform had an initial value of 24 cm on May 28th but was only 9.5 cm deep on July 8th, the terrace then increased in depth on March 4th, 2016 to a value of 34 cm (Fig. 25). Elevations of the front terrace at this location were measured on May 28th, 2015 to be 32 cm and 14 cm on March 4th, 2016. The initial marsh edge to station marker measurement was 18.61 m and eroded to a length of 18.02 m by the conclusion of the study. This resulted in a total erosion of 0.59 m from May 28th, 2015 to March 4th, 2016. Site 4 E Pin recorded the greatest amount of erosion during Epoch 1 with an erosion amount of 0.27 m. There was no measurement

52

taken on September 24th, 2015 because the pin could not be located as a result of high waters. This location underwent the lowest magnitude of erosion during the course of the study.
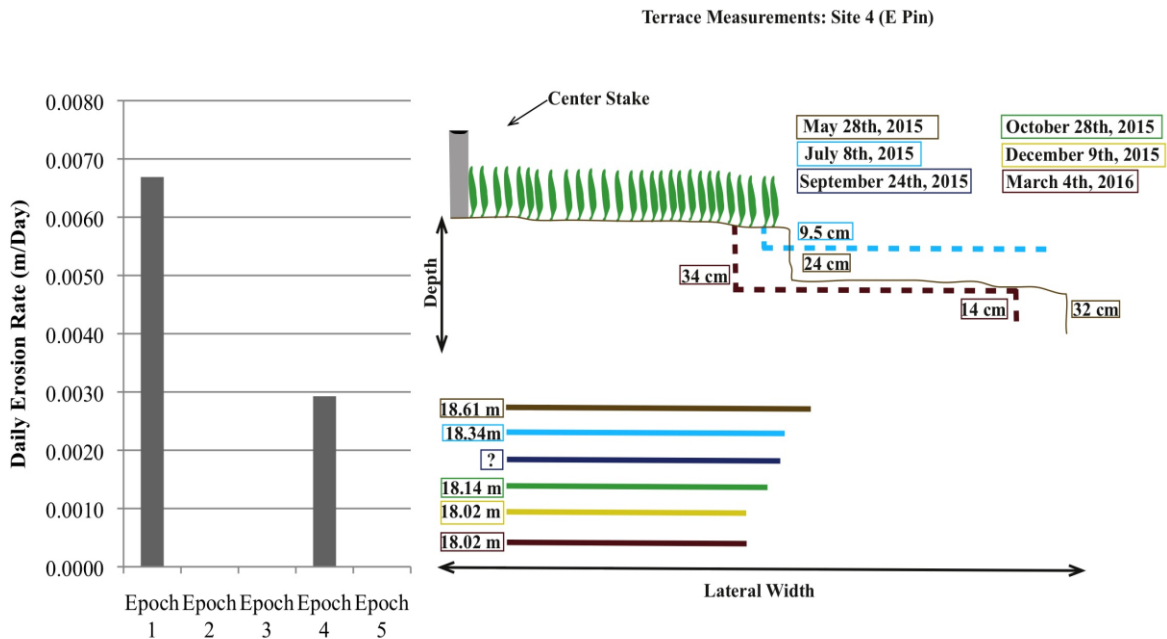
Figure 25. Left side of figure shows the calculated daily erosion rate for each epoch on the basis of Site 4 E erosion pin measurements. The right side is a cross sectional depiction of the marsh edge and terrace systems, at Site 4 E Pin. Site 4 E Pin only has daily erosion rate calculations for Epochs 1, 4, and 5 because the pin could not be located on September 24th, 2015 and therefore the erosion rates for Epochs 2 and 3 could not be calculated.

Site 4 E* Pin served as the replacement pin when the original Site 4 E Pin was not found as a result of high water on September 24th, 2015. Terrace depth measurements below the vegetated marsh platform and lateral extent measurements from the station marker to the marsh edge are shown in figure 26 This pin was placed approximately 0.5 m to the south, closer to the tip of an adjacent protruding headland, from the original pin Site 4 E Pin. All measurements were taken between September 24th, 2015 and March 4th, 2016. Back terrace measurements were taken on September 24th, 2015 at a depth of 37 cm and on March 4th, 2016 at a depth of 34 cm below

53

the vegetated marsh platform (Fig. 26). There is only one front terrace measurement that was made on March 4th, 2016 with a depth of 14 cm. Both the front and back terrace depths have similar values to those of the original Site 4 E pin. Lateral measurements from the station marker to the marsh edge at this site had an initial measurement of 18.87 m on September 24th, 2015 and eroded to 18.41 m by March 4th, 2016 resulting in removal of a total of 0.46 m. A maximum amount of erosion of 0.28 m occurred within Epoch 5, which extended from December 9th, 2015 to March 4th, 2016 (Fig. 26).
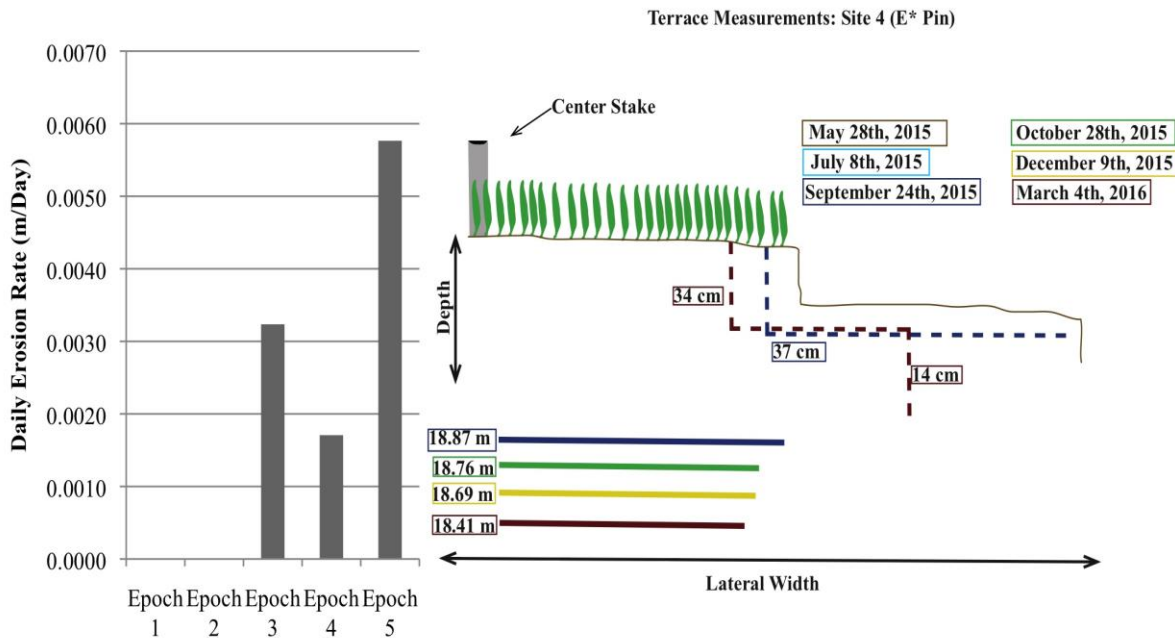
Figure 26. Left side of figure shows the calculated daily erosion rate for each epoch on the basis of Site 4 E* erosion pin measurements. The right side is a cross sectional depiction of the marsh edge and terrace systems, at Site 4 E* Pin. Site 4 E* Pin served as the replacement pin when the original Site 4 E Pin was not found as a result of high water on September 24th, 2015. As a result of this, daily erosion rates could only be calculated for Epochs 3-5.

Figure 27 shows terrace depth and lateral tape measurements at Site 4 W Pin. Back terrace measurements at this site are abundant and show a pattern that transitioned from a slight increase in terrace depth initially that decreased in depth by the end of the study. All back

terrace elevation measurements have small variations from 14 cm (March 4th, 2016) to 23 cm

(September 24th, 2016). Front terrace measurements were only taken on May 28th, 2015 with a

measured depth of 7 cm below the marsh platform and on March 4th, 2016 with a measured

depth of 48 cm (Fig. 27). There is little variation in front terrace depths at this location but back

terrace measurements during the corresponding site visit dates are extremely variable (Fig. 27).

The initial lateral extent of the platform from the station marker to the edge of the marsh was

14.6 m on May 28th, 2015. The total erosion over the duration of the study is 1.48 m.
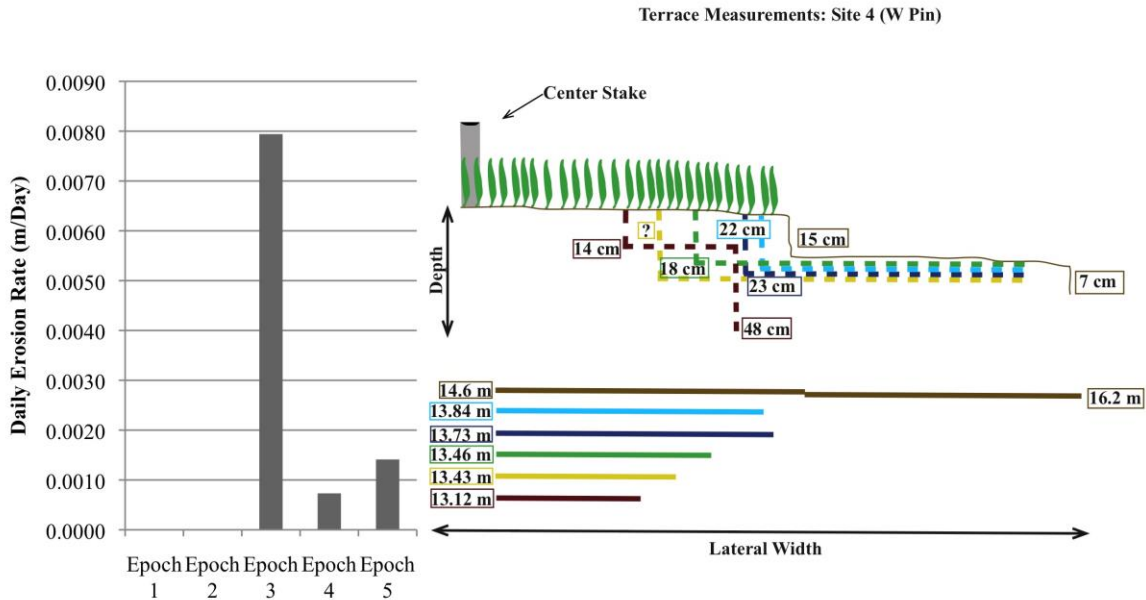
Figure 27. Left side of figure shows the calculated daily erosion rate for each epoch on the basis of Site W erosion pin measurements. The right side is a cross sectional depiction of the marsh edge and terrace systems, at Site 4 W Pin.

4.4.3 Photo Comparison and Marsh Edge Characteristics

Figure 28 is a timeline of photos that were taken during each site visit for the

duration of the study. These photos are the basis for evaluating the marsh edge geometries that

are discussed in the following section. During the initial site visit on May 28th, 2015 the western

segment of the marsh edge had a series of zeta-form clefts and necks with the bays acting as shell catchments. Similarly, to the east the bays and headlands were zeta-form shaped along the marsh edge. The marsh edge on July 8th, 2015 was extremely similar to the marsh edge that was observed on May 28th, 2015. However, it appeared as if vegetation had started to die off near the marsh edge. On September 24th, 2015, the edge was similar to what has been previously observed. Photos from October 28th, 2015 are missing due to file corruption.

By December 9th, 2016 *Spartina alterniflora* had died off along the marsh edge and as well as approximately 0.75-1.25 m into the marsh interior but was still characterized by zeta-form bays and headlands. During the final site visit, new *Spartina alterniflora* had begun to grow along the marsh edge and marsh interior – this is the only site where this occurred near the edge at this point in time. The shoreline to the west was characterized by a minimal amount of cleft and neck formations that transitioned into bays and headlands that were zeta-form in shape. At this point in time, zeta-form bays and headlands still continued to dominate the shoreline to the east. However, many of the bays had become more embayed resulting in necks that were

more exposed relative to previous observations.
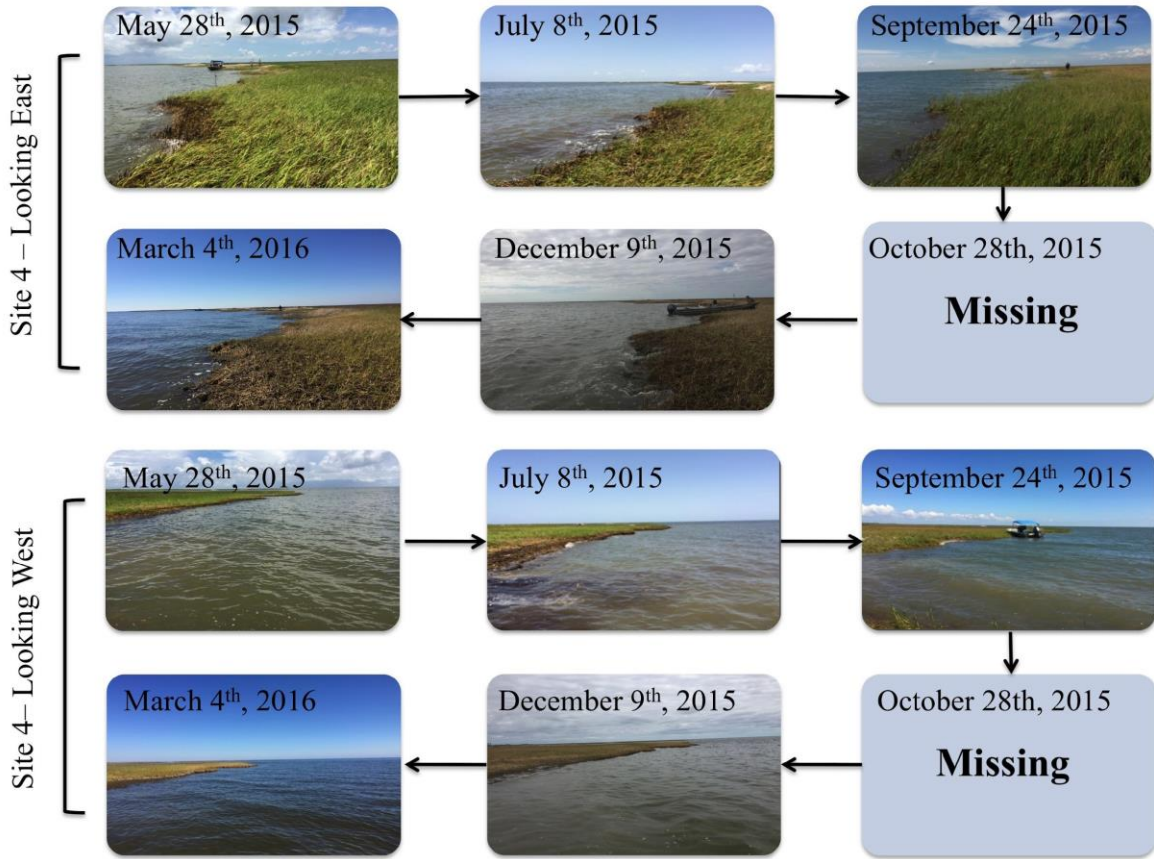
Figure 28. A timeline of photos that were taken during each site visit to Site 4 that were used to track marsh-edge characteristics. The photos in the upper-half of the figure are taken with the perspective along the marsh edge that is oriented to the east. Photos in the bottom-half of the figure represent the perspective along the marsh edge that is oriented westward. Photos from October 28th, 2015 are missing due to file corruptions.

Table 2. Erosion pin exposure and station marker measurements in m that were measured during each field visit for sites 1-4. Erosion that occurred between epochs is shown on the far right hand side of the table for sites 1-4. N/A on the table means that there was no data collected at a particular pin because the pin could not be located or the pin was not yet set. A value of [1]1+ indicates that the pin was fully removed and a new pin was put in place with an initial exposure length of 0.12m. A value of [2]1+ indicates that the pin was removed and was replaced with a new pin with an initial exposure length of 0.17m. Bolded numbers are the initial measurements that were taken when the first pin was put in place. An upper-case E as the superscript indicates that there is a possible error with the pin exposure measurement due to the pin being bent between measurements.

		5/28/15	7/8/15	9/24/15	10/28/15	12/9/15	3/4/16	Epoch 1	Epoch 2	Epoch 3	Epoch 4	Epoch 5	Totals
Site 1	Station Marker	0.6	0.61	0.59	0.58	0.55	0.55						
	NE Pin	0.16	0.36	1+	0.6	0.96	0.59	0.20	0.64	0.48	0.36	0.49	2.17
	SW Pin	0.2	0.36	1+	0.16	0.30	0.41	0.16	0.64	0.04	0.14	0.11	1.10
Site 2	Station Marker	0.65	0.62	0.67	0.66	0.60	0.57						
	NE Pin	0.13	0.40	1+	0.39	1+	0.51	0.27	0.60	0.27	0.61	0.39	2.14
	SW Pin	0.15	0.35	1+	0.35	0.36	0.57^E	0.20	0.65	0.23	0.013	0.21	1.3
Site 3	Station Marker	0.55	0.52	0.46	0.41	0.42	0.37						
	N Pin	0.15	0.30	1+	1+	0.29	0.49	0.15	0.70	0.88	0.12	0.28	2.13
	S Pin	0.16	0.43	1+	0.22	0.75	0.41	0.27	0.57	0.1	0.53	0.2	1.67
Site 4	Station Marker	0.37	0.67	0.63	0.64	0.62	0.64						
	E Pin	0.15	0.42	N/A	0.62	0.74	0.74	0.27	N/A	N/A	0.12	0	0.59
	E* Pin	N/A	N/A	0.12	0.23	0.30	0.79	N/A	N/A	0.11	0.07	0.49	0.67
	W Pin	N/A	N/A	0.12	0.39	0.42	0.54	N/A	N/A	0.27	0.03	0.12	0.42

4.5 Shell Berm Measurements

Two shell berms located near Site 4 were measured during the study and are labeled as the "East Shell Berm" and the "West Shell Berm." During the study, several measurements were taken at each berm in an attempt to document the growth of the berm and are provided in Table 3 and 4. However, it was not expected that the berm would transgress landward during the course of the study. The following results include information on the berm height and movement during the study.

4.5.1 East Shell Berm

This berm (see fig. 1) is the easternmost berm out of the two that were studied. Measurements and observations of the berm evolution will be discussed in the following text with reference to Table 3. During May 28th, 2015 two stakes were placed 15 m apart, with one labeled as the "land stake" on the landward side of the berm and a "sea stake" that fronted the berm on the seaward side. The height of the berm during this site visit was measured to be 0.66 m. During the following visit on July 8th, 2015, the height increased to 0.79 m. During Epoch 2 the height of the berm decreased to 0.63 m on September 24th, 2015. The most substantial amount of change at the berm occurred during Epoch 3 when the berm was smeared across the marsh platform. This resulted in a decrease in elevation of the berm to a height of 0.37 m and the landward stake was covered by the berm rather than being behind it. A subsequent site visit on December 9th, 2015 showed a slight decrease in height to 0.34 m. By March 4th, 2016 the berm had grown to 0.48 m in height.

In addition to a reduction in height of the berm when as it was smeared across the platform, the berm width changed as well. The initial berm width was measured to be 7.10 m on

59

May 28th, 2015, whereas the width decreased to 6.43 m on July 8th, 2015 and decreased once

again to 6.34 m on September 24th, 2015. After September 24th, the berm width was no longer

measured from the landward most to the seaward most area of the berm. Instead, berm migration

was measured along the same bearing of 142° from the landward stake to the landward most

extent of the berm. The first measurement recorded on October 28th, 2015 showed that the berm

had migrated 3.22 m landwards of the land sake. This measurement remained consistent during

Epoch 4 and the berm migrated landward slightly on March 4th, 2016 with a lateral measurement

of 3.25 m. The total measured landward migration of the East Shell Berm was approximately

11.5 m from May 28th, 2015 to March 4th, 2016. Throughout the study, the seaward stake height

(SS Height) also increased from an initial height of 0.7 m to 0.87 m as the final height. This

indicates that the stake had become more exposed and the surrounding material was eroded

away.

Table 3. Recorded measurements for the sea stake height (SS Height), land stake height (LS Height), height of the berm (Height of Berm), as described in the methods section, width of the berm (Berm Width), berm migration for all site visits after September 24th, 2015 (Berm Migration), and the total migration (Total Migration) in m for the East Shell Berm for the duration of the study.

East Berm	5/28/15	7/8/15	9/24/15	10/28/15	12/9/15	3/4/16
SS Height (h_{SS})	0.7	0.71	0.79	0.84	0.86	0.87
LS Height (h_{LS})	0.65	0.67	0.64	0.3	0.33	0.29
Height of Berm (H_B)	0.66	0.79	0.63	0.37	0.34	0.48
Berm Width (W_B)	7.1	6.43	6.34	N/A	N/A	N/A
Berm Migration (M_B)	N/A	N/A	N/A	3.22	0	0.03

4.5.2 West Shell Berm

This berm (see fig. 1) is the westernmost berm out of the two that were studied. Measurements and observations of the berm evolution will be discussed in the following text with reference to Table 3. During May 28th, 2015 two stakes were placed 15 m apart with one labeled as the "land stake" on the landward site of the berm and a "sea stake" that fronted the berm on the seaward side. On this date, the height of the berm was measured to be 0.5 m. The height during the next site visit was observed to be 0.59 m. On September 24th, 2015, the berm height was observed as 0.55 m. During Epoch 3 the most substantial mount of change at the berm occurred when the berm migrated landward and decreased in height. On October 28th, 2015, the landward stake was covered by the berm rather than being behind and the berm had been reduced to a height of 0.34 m. A subsequent visit on December 9th, 2015 the berm height was recorded as 0.44 m. By March 4th, 2016 the berm had slightly decreased to 0.37 m.

Similar to the East Shell Berm, the West Shell Berm also underwent a change in width and migrated landward during the study. During the initial site visit the berm width was measured to be 5.3 m on May 28th, 2015, whereas the width increased slightly to 6.1 m on July 8th, 2015. The measurement for berm width on September 24th, 2015 was not recorded and is a result of human error in the form of forgetfulness due to distraction and a lack of concentration. After September 24th, the berm width was no longer measured and berm migration was measured in its place along the same bearing of 125° from the landward stake to the landward most extent of the berm. On October 28th, 2015, the first of berm migration shows that the berm migrated 2.56 m landwards of the land sake. On December 9th, 2015, the berm migrated landward slightly

with a lateral measurement of 2.57 m and remained consistent during Epoch 5. The total

measured landward migration of the West Shell Berm was 12.27 m. While the land stake (LS

Height) decreased in height for much of the study as a result of the landward transgression of the

berm, the seaward stake height (SS Height) increased from an initial height of 0.65 m on May

28th, 2015 to 0.83 m on March 4th, 2016 as the material surrounding it was winnowed away with

the landward migration of the adjacent berm.

Table 4. Recorded measurements for the sea stake height (SS Height), land stake height (LS Height), of the berm (Height of Berm), as described in the methods section, width of the berm (Berm Width), berm migration for all site visits after September 24th, 2015 (Berm Migration), and the total migration (Total Migration) in m for the West Shell Berm for the duration of the study.

West Berm	5/28/15	7/8/15	9/24/15	10/28/15	12/9/15	3/4/16
SS Height (h_{SS})	0.65	0.65	0.71	0.84	0.84	0.83
LS Height (h_{LS})	0.66	0.64	0.65	0.40	0.30	0.37
Height of Berm (H_B)	0.50	0.56	0.55	0.34	0.44	0.37
Berm Width (W_B)	5.30	6.10	N/A	N/A	N/A	N/A
Berm Migration (M_B)	N/A	N/A	N/A	2.56	0.01	0
Total Migration						12.27

4.6 Meteorological & Wind Data Analyses

4.6.1 Meteorological Events

Surface analysis maps were analyzed for wind speed, direction, and dew point for

each epoch of the study to evaluate the frequency and type of meteorological events that

occurred. During the course of the study, a total of 32 cold fronts, 8 warm fronts, 1 occluded

front, and 12 stationary fronts passed over the study site (Table 2). Two tropical storms, Tropical

Storm Bill during Epoch 1 and Hurricane Joaquin during Epoch 3 resulted in a change of wind

speed and direction at the study sites. Epoch 2 spanned the beginning of the cold front season

when 5 cold fronts of different intensities occurred from July 8th to September 24th, 2015. As

cold front season began, warm fronts also began developing proximal to the study site as a result

of the location of cyclogenesis. The largest number of stationary fronts occurred during the

beginning of cold front season when cold air advection was weakest as a result of dominant

warm and moist air from the Gulf of Mexico battling a weak polar jet stream. Cold fronts

increased during Epochs 3 through 6 as cold air was funneled southward across the United States

through the enhanced polar jet stream.

Table 5. Meteorological event frequency during each epoch of the study. Each event was counted as a singular event and was totaled together for each epoch. Epoch 1 May 28th to July 8th, 2015; Epoch 2 July 8th to September 24th, 2015; Epoch 3 September 24th to October 28th, 2015; Epoch 4 October 28th to December 9th, 2015; Epoch 5 December 9th, 2015 to March 4th, 2016. TS influence is defined as a "tropical storm" resulted in a change of wind speed and direction at study sites.

	Epoch 1	Epoch 2	Epoch 3	Epoch 4	Epoch 5	Total
Cold Front	0	5	6	6	15	32
Warm Front	0	1	1	1	5	8
TS Influence	1	0	1	0	0	2
Occluded Front	0	0	1	0	0	1
Stationary Front	1	4	2	3	2	12

In addition to analyzing surface analysis maps for metrological events, wind data

from station WYCM6 – 8747437 at Bay Waveland Yacht Club was analyzed for speed and

direction. Before analyzing wind data, the impact of wind direction and wind speed on each

marsh edge the direction of wind had to be compared against the orientation of the shoreline.

This was done by defining the "Shoreline Azimuth," which was defined as the range of azimuth degrees where shoreline exists at each site (Table 6). By defining the "Shoreline Azimuth" at each site, the shoreline can be defined by a range of azimuth degrees of open shoreline that is exposed to wave action. Each shoreline has a differing "Shoreline Azimuth" based on its azimuth degree range of shoreline that is exposed to wave action. Due to this, most sites were analyzed to have differing maximum wind speed values across for each epoch although the data comes from the same gauge.

4.6.2 Maximum Wind Speeds: Sites 1 & 2

Maximum wind speeds for Site 1 NE & SW and Site 2 NE & SW existed during Epoch 2 with wind speeds of 20.50 m s^{-1}. Maximum average wind speeds at both of these sites occurred during Epoch 5 with an average wind speed of 4.07 m s^{-1} at Site 1 NE & SW and 4.23 m s^{-1} at Site 2 NE & SW. During Epoch 2, both sites also experienced the highest percentage of winds blowing obliquely to the shoreline with winds impacting the shoreline 53.44% of the duration of Epoch 2 at Site 1 NE & SW and 51.15% at Site 2 NE & SW.

4.6.3 Maximum Wind Speeds: Sites 3 & 4

Site 3 N & S experienced its highest wind speed of 20.50 m s^{-1} during Epoch 2 but experienced the highest percentage of winds during Epoch 4 where the wind was blowing onshore 81.24% of the duration of Epoch 4. During Epoch 3 Site 3 N & S had an average wind of 4.98 m s^{-1} which is the maximum average wind speed at this Site during the study. The highest maximum and average wind speeds at Site 4 E & E* occurred during Epoch 3 with a maximum wind speed of 17.60 m s^{-1} and a maximum average wind speed of 5.40 m s^{-1}. The maximum percentage of winds blowing obliquely to the shoreline was 35.11% during Epoch 5 at Site 4 E &

E*. At Site 4 W the maximum wind speed and average wind speed occurred during Epoch 3 with a maximum-recorded wind speed of 17.60 m s^{-1} and a maximum average wind speed of 3.81 m s^{-1}. The highest percentage of winds blowing obliquely to the shoreline occurred during Epoch 5 when winds impacted the shoreline 37.74% of the epoch.

Table 6. Wind data from station WYCM6 – 8747437 at Bay Waveland Yacht Club that is specific to the "Shoreline Azimuth" of each site during each epoch of the study. "Percentage" is the percentages of the total day count for the epoch that wind blew towards the ocean-facing shoreline. "Max Wind" is the maximum-recorded wind speed in m s^{-1} during a particular epoch for each site. "Avg Wind" is the average wind speed in m s^{-1} during a particular epoch for each site. The "Shoreline Azimuth" is marsh edge at each site where the platform meets open water. An asterisk (*) indicates a maximum value for all epochs of the study for a particular site. Site 4 E* was installed on September 24th, 2015 because Site 4 E pin could not be found as a result of high water. During the following site visit, Site 4 E pin was found and Site 4 E* pin became an additional pin for this site. Site 4 W was also not installed until September 24th, 2015 therefore data prior to Epoch 3 is not listed.

	Epoch 1 (40 days)				
	Site 1 NE & SW	Site 2 NE & SW	Site 3 N & S	Site 4 E & E*	Site 4 W
Percentage (%)	45.09	39.81	17.77	35.49	N/A
Max Wind (m s^{-1})	16.00	16.00	16.00	12.20	N/A
Avg Wind (m s^{-1})	2.42	2.43	2.55	4.47	N/A
Shoreline Azimuth (°)	219 to 26	242 to 39	328 to 154	87 to 182	131 to 230
	Epoch 2 (76 days)				
Percentage (%)	*53.44	*51.15	42.86	20.51	N/A
Max Wind (m s^{-1})	*20.42	*20.42	*20.42	13.20	N/A
Avg Wind (m s^{-1})	2.87	2.93	3.83	4.28	N/A
	Epoch 3 (34 days)				
Percentage (%)	38.85	44.01	71.30	28.02	21.29
Max Wind (m s^{-1})	10.90	10.90	17.60	*17.60	*17.60
Avg Wind (m s^{-1})	2.82	3.06	*4.98	*5.40	*3.81
	Epoch 4 (41 days)				

Percentage (%)	37.00	44.32	*81.24	33.97	21.37
Max Wind (m s^{-1})	12.20	14.50	14.50	12.80	11.40
Avg Wind (m s^{-1})	2.97	3.25	4.72	4.76	3.24
	Epoch 5 (85 days)				
Percentage (%)	41.66	39.85	54.43	*36.11	*37.54
Max Wind (m s^{-1})	13.30	13.30	12.90	8.93	13.40
Avg Wind (m s^{-1})	*4.07	*4.23	4.69	4.47	3.59

4.6.4 Wind Data Analysis: Cumulative

Figure 29 shows the wind climate data at Bay Waveland Yacht Club, Mississippi, approximately 25.75 km from the study site. A wind rose was generated that shows the wind frequency, direction, and magnitude between May 28th, 2015 and March 4th, 2016 (Fig. 29) and the same data for a longer duration of time from August 28th, 2008 to March 4th, 2016 (Fig.29). These data show that during the duration of the study there was a bimodal distribution of wind directions that were dominantly from the north and south-southeast. The majority of winds ranged between 2.23-4.74 m s^{-1} for approximately 38.2% of the duration of the study. The prevailing wind direction was from 157.5° but winds from the north contributed a higher percentage of high magnitude winds. The longer duration of wind climate analysis shown on the right-hand side of Figure 29 differs slightly from the wind rose for the duration of the study. The prevailing wind direction is from 135° with a slightly higher wind speed of 4.16 m s^{-1}. This wind rose also indicates that the distribution of winds is mostly focused from the southeast but has a greater frequency from the north, although not as great as the wind rose for the duration of the study. However, the highest winds for the long-term wind analysis come from the north to north-

northwest in comparison to the highest winds being from the southeast to east-southeast for the duration of the study.

4.6.5 Wind Data Analysis per Epoch

Magnitude, directional distribution, and frequency varied during each epoch. Epochs 1 and 2 range from May 28th to September 24th, 2015 and they share the same prevailing wind direction of 157.5° and similar average wind speeds of 3.49 m s^{-1} during Epoch 1 and 3.30 m s^{-1} during Epoch 2 (Fig. 30). During Epoch 1 the prevailing wind direction of 157.5° occurred 18.2% of the epoch. The dominant wind direction begins to dampen during Epoch 2 with the prevailing wind direction occurring only 8.9% of the epoch. However, the wind roses show a difference in the distribution of wind direction during the two epochs. The greatest frequency of wind during Epoch 1 is mostly unimodal and is distributed towards the south-southeast while winds during Epoch 2 occur in almost equal frequencies for all directions with the exception of winds ranging from east to southeast. Epoch 1 also recorded a greater percentage of higher winds with winds exceeding 6.71 m s^{-1} occurring 8.4% of the epoch with the majority of maximum wind speeds being recorded from the southeast (Fig. 30). During Epoch 2, the highest wind speed was recorded at a speed of 20.52 m s^{-1} and the majority of maximum winds from the east-southeast and southeast (Fig. 30).

As the season changes from summer to fall, the prevailing wind direction changes from the 157.5° to 360° and the average wind speed decreases as shown in wind roses for Epochs 3 through 5 (Fig. 30). Winds during Epoch 3 are unimodal in direction from the north for 16.5% of the epoch with some larger frequencies of winds from the northeast, southeast, and south-southeast. The average wind speed during Epoch 3 has increased to 4.38 m s^{-1} and winds

67

exceeding 6.71 m s^{-1} increased to 16.8% of the epoch (Fig. 30). The highest wind speeds were recorded from the east-southeast to south-southeast. During Epoch 4 the prevailing wind direction remains constant at 360° during 13.7% of the epoch but directional wind frequency is distributed differently than in Epoch 3 (Fig. 30). While the prevailing wind is from the north at 360°, the rose is almost characteristic of a multimodal distribution with a high frequency of winds blowing from the north to the south-southeast. During this epoch, the average wind speed increased to 4.52 m s^{-1} with wind speeds greater than 6.71 m s^{-1} occurring 18.8% of the epoch (Fig. 30). Maximum wind speeds do not match the prevailing wind direction and are focused out of the north-northeast and east-southeast (Fig. 30). Epoch 5 marks the latter part of winter from December 9th, 2015 to March 4th, 2016 and while the prevailing wind direction is still 360° for 11.8% of the epoch, the overall frequency directional distribution is bimodal as winds begin to shift to blowing from the south to southeast (Fig. 30). During Epoch 5, the average wind speed decreases to 4.29 m s^{-1} and winds exceeding 6.71 m s^{-1} decrease to occurring during 14.5% of the epoch (Fig. 30). Maximum wind speeds during this epoch occurred from the south to south-southeast.
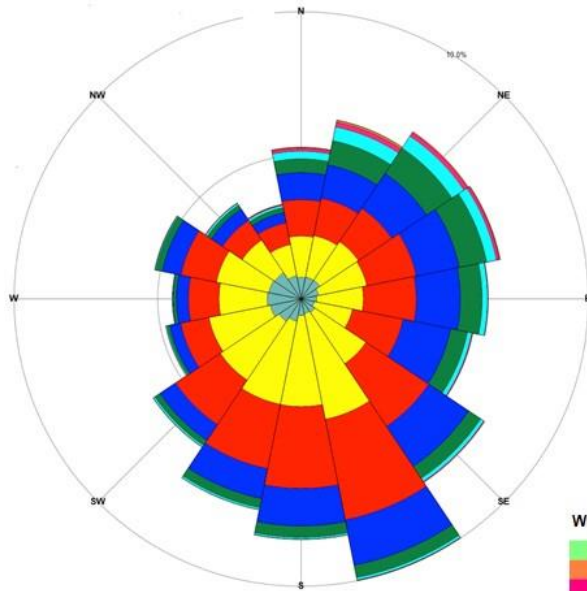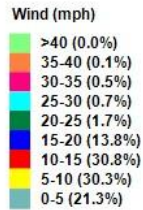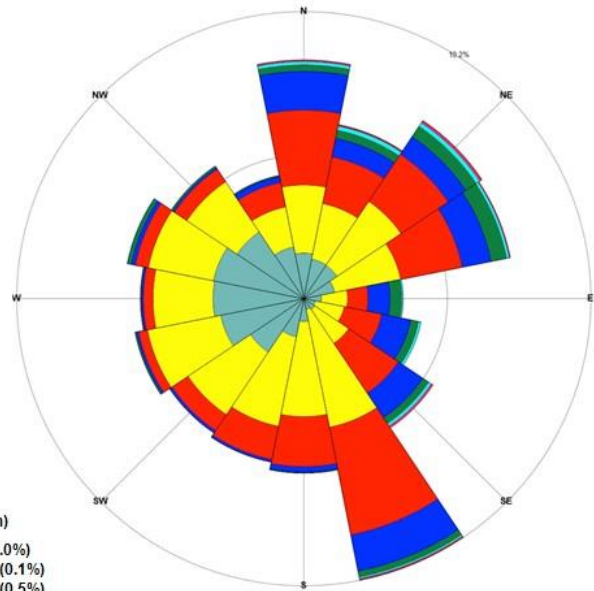
Figure 29. Cumulative wind rose on the left illustrates the magnitude, frequency, and wind direction for epochs 1 through 5 beginning on May 28th, 2015 and ending on March 4th, 2016. Cumulative wind rose on the right illustrates the magnitude, frequency, and wind direction for an extended duration of time beginning when data was available, on August 28th, 2008 and ending on March 4th, 2016. All data is from National Data Buoy Center's Bay Waveland Yacht Club, WYCM6 – 8747437, observing station. The length of each petal from the center around the rose is related to the frequency of time that the wind blows from that particular direction. The range of magnitude of winds in each bin is indicated in the legend.
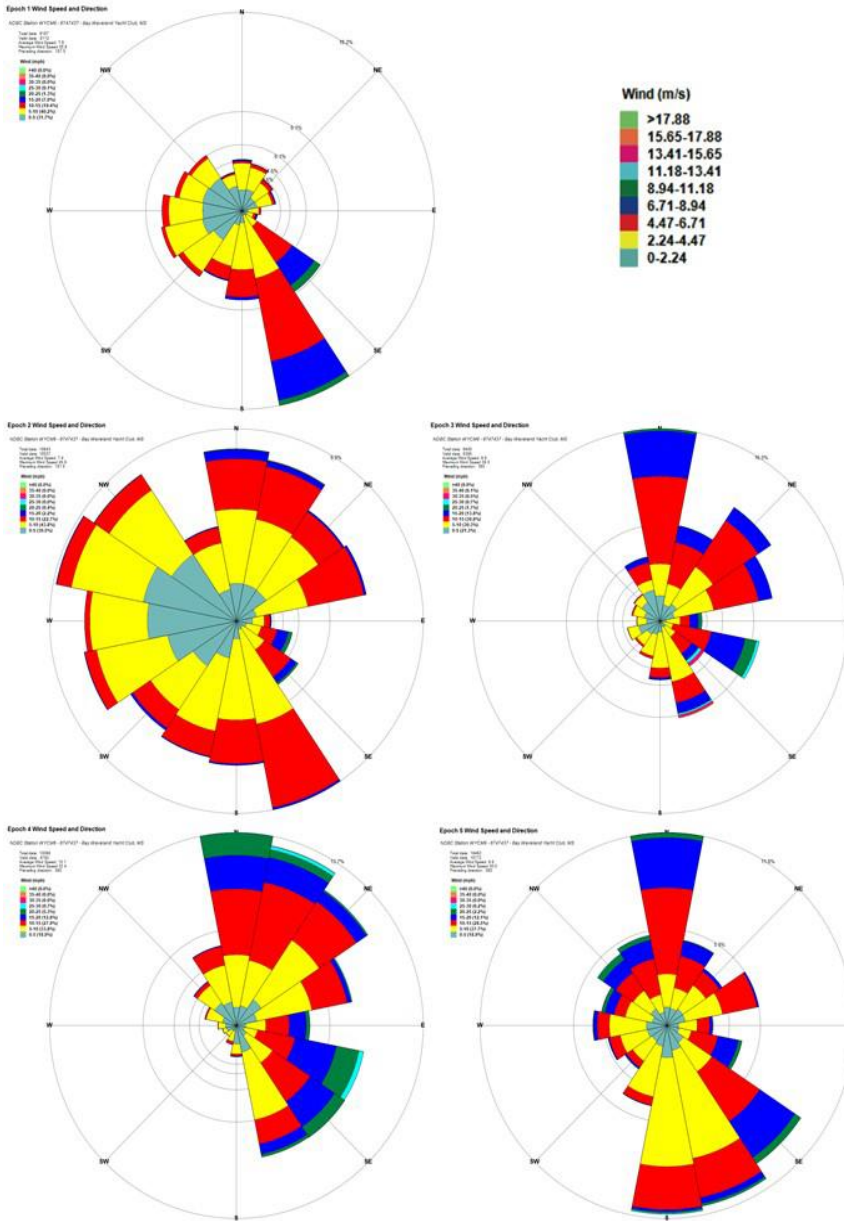
Figure 30. Wind roses showing the magnitude, frequency, and wind direction for epochs 1 through 5 beginning on May 28th, 2015 and ending on March 4th, 2015 (National Data Buoy Center's Bay Waveland Yacht Club, WYCM6 – 8747437 station). Epoch 1 is shown in the upper left corner and represents the wind climate from May 28th to July 8th, 2015. Epoch 2 is in the top-center and represents the wind climate from July 8th, 2015 to September 24th, 2015. Epoch 3 is shown in the upper right corner and has recorded data from September 24th to October 28th, 2015. Epoch 4 is shown in the lower left hand corner and represents the wind climate from October 28th to December 9th, 2015. Epoch 5 is shown in the lower right hand corner and represents the wind climate from December 9th, 2015 to March 4th, 2016. The length of each petal from the center around the rose is related to the frequency of time that the wind blows from that particular direction. The range of magnitude of winds in each bin is indicated in the legend.

70

4.7 Statistical Analysis

The purpose of this study is to compare the data that was collected with the mentioned methods spatially and temporally. In order to do this, the data needed to be checked for normality. This was done by creating a histogram in *RStudio* of total erosion from each erosion pin at each site against the frequency of recorded measurements of similar values. The resulting histogram indicated a non-normal distribution of the data was not evenly distributed. With the previous statement in mind, t-tests were run for each site to compare erosion pin measurements. With this test p-values and t-values were given for each site to determine if the null hypothesis was accepted or rejected with an alpha value of 0.05. It should be noted that a t-test could not be ran on Site 4 because there were more than 2 datasets to compare and a t-test allows a comparison of no more than 2 datasets at once. To resolve this issue, a box plot was created in *RStudio* and was interpreted for statistical significance across all pin measurements at Site 4. Further in depth intelligent analysis of the data for assumptions about its statistical relationship and significance could not be conducted because of the non-normality of the data.

Figure 31 shows the statistical analysis results for erosion measurements at each site. The alpha value of 0.05 accepts the null hypothesis and analysis proves that there are no p-values above 0.05 and therefore the null hypothesis is accepted. P-values could not be calculated for Site 4 because there were 3 datasets at the site with different observations. A box plot was used to display the distribution of the data at Site 4 and shows that each erosion pin data set is not statistically significant from one another. It should be noted that during the initial analysis of the data, none of the datasets were normally distributed. The results shown in figure 31 should

71

not be considered to be data without error. As a result of the low number of observations, intelligent analysis of assumptions is not recommended.

	t-value	p-value	n
Site 1 NE & SW	2.3924	0.06874	5
Site 2 NE & SW	1.3058	0.2313	8
Site 3 N & S	0.51529	0.6233	7
Site 4 E	N/A	N/A	4
Site 4 W	N/A	N/A	3
Site 4 E*	N/A	N/A	3
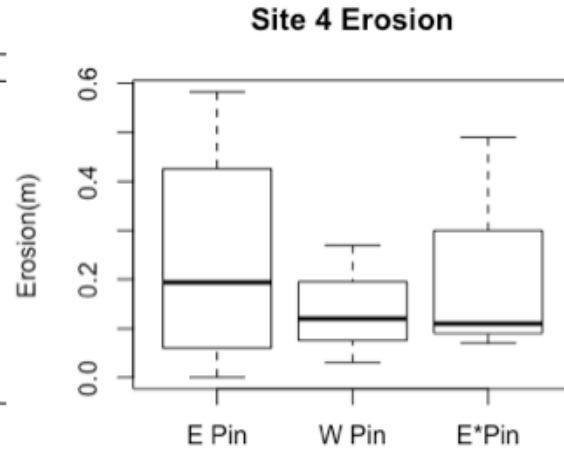
Figure 31. The statistical results for erosion pin measurements all sites with the correlative t-values, p-values, and number of observations is on the left. On the right is a box plot for Site 4 erosion pins. A t-test could not be ran on this site because there were more than 2 data sets, therefore there is no t-value or p-value for any dataset at Site 4.

72

CHAPTER 5. DISCUSSION

5.1 Historical Shoreline Erosion Rates

Marsh erosion rates are extremely varied across the Mississippi River delta plain. For example, rates of erosion for the Biloxi Marsh range between 2.90 m year^{-1} (Martinez et al., 2009) to 62.30 m year^{-1} (Trosclair, 2013) depending on meteorological event frequency, relative sea level rise, anthropogenic influence, and the time frame of the measurement when calculated, as it can skew erosion rates based on temporal differences. In order to compare marsh erosion rates of other locations to the study site an analysis of historical imagery was undertaken and serves as the basis of –long-term erosion rate calculations of the study site.

A comparison of imagery from between October 1989 and August 2015 revealed that each site of this study had different erosion rates during this interval of time (Fig. 32). Historical shoreline rates were calculated along transects with the same bearings as those used for erosion pin placement. The historical difference in daily rates of erosion is indicative of the fact that each shoreline is subject to different processes that drive erosion.

Figure 32. *Google Earth* images from October 24th, 1989 for each site. Polygons show the areas of each site that was examined for geomorphic changes using historical shoreline imagery. Numbers indicate features that are discussed in text. Numbers 1 through 3 correspond to Site 1, numbers 4 through 6 correspond to Site 2, numbers 7 and 8 correspond to Site 3, and numbers 9 and 10 correspond to Site 4.

5.1.1 Site 1

Site 1 has tidal channels to the northeast and southwest, and a bay. These shoreline features were visible during the duration of the research and are visible from *Google* imagery from October of 1989 to August of 2015 (Fig. 32, 1-3). Historically, tidal channels that lead into interior bay areas enhance erosion at this site. Tidal creeks provide an area of flow into the interior, causing erosion along the banks. With the exception of tidal creeks, this shoreline switches characteristics between that of an alternating headland and bay shoreline to that of a linear shoreline as an equilibrium is trying to be reached along the shore. The majority of erosion took place during the time period between January 28th, 1998 to January 19th of 2004 where the daily rate of erosion is calculated to be 4.0 cm day^{-1} for the NE Pin and 3.5 cm day^{-1} for the SW pin.

Historical Erosion: Site 1
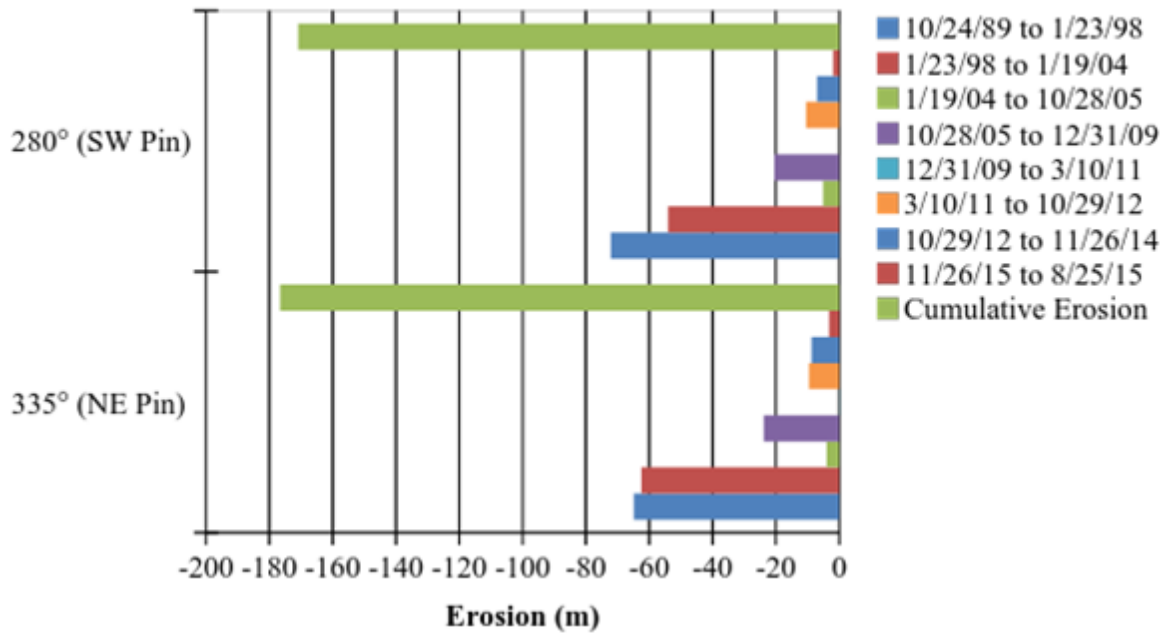
Figure 33. Historic erosion in m for Site 1 from October 24th, 1989 to August 25th 2015 along consistent bearings for each pin at the site.

5.1.2 Site 2

Three major shoreline features at Site 2 were observed during the duration of the study and on *Google* imagery. The features included tidal channels to the northeast (Fig. 32, 4), marsh ponds to the southwest (Fig. 32, 5), and what began as a shell pocket beaches within a zeta form shoreline bay (Fig. 32, 6). The largest daily rate of erosion that was calculated was for the period from 1/19/04 to 10/28/05was an average of 3.8 cm day^{-1} eroded from the shoreline for the NE Pin and a rate of 1.5 cm day^{-1} for the SW Pin. During this time period, 18 tropical cyclones entered the Gulf of Mexico and the eye of two storms approached within 120 km of the study sites. The largest storm was Hurricane Katrina, which was a category 4 hurricane as it passed through the Biloxi Marsh (Knabb et al., 2005). The presence of tidal creeks that lead to an interior bay prior to this time period allowed for surging waters to rush through the creeks and

into the bay, leading to failure of the tidal creeks and a transgression of the shoreline towards the interior bay.

Historical Erosion: Site 2
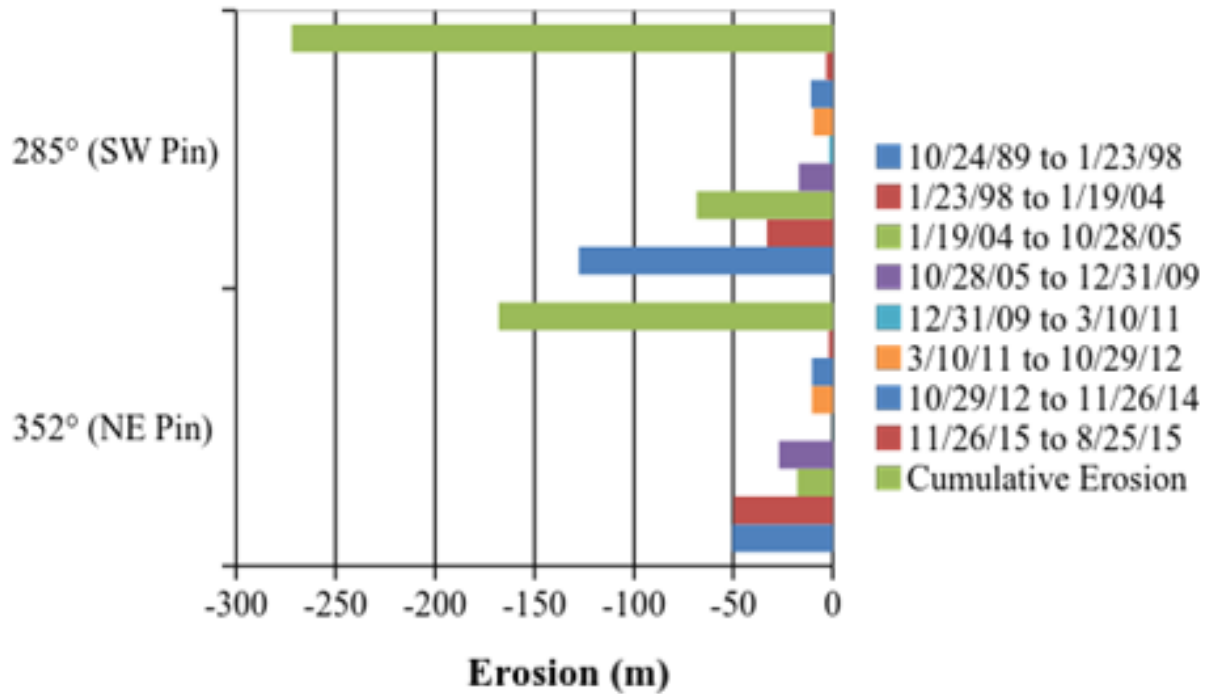
Figure 34. Historic erosion in m for Site 2 from October 24th, 1989 to August, 25th 2015 along consistent bearings for each pin at the site.

5.1.3 Site 3

There are two major shoreline features that were visible during the study and on *Google* imagery at Site 3 that influence geomorphologic changes (Fig. 32, 7-8). The shoreline that extended the length of the research site evolved through time from a headland-bay, to crenulate shaped bays, to neck and cleft, and then again to a headland-bay visually characterized shoreline. Historically, the tidal channel directly to the south of this location became less established and somewhat overgrown with intermittent periods where it appears to have a higher volume of water flowing through it. The mouth of this channel also became an established shell

beach by November 26th, 2014 to August 25th, 2015. The greatest amount of shoreline erosion that took place along the N Pin transect occurred from January 19th, 2004 to October 28th, 2005 where the daily erosion rate was calculated to be 4.3 cm day^{-1}. During this time period, the Biloxi Marsh was exposed to two active hurricane seasons. The 2004 hurricane season exposed the Biloxi Marsh to the impacts of Tropical Storm Matthew, which made landfall near Grand Isle, LA, and Hurricane Ivan, which made landfall twice, once to the east near Orange Beach, AL as a category 3 hurricane, and again to the west near Holly Beach, LA as a tropical depression. The 2005 hurricane season resulted in 5 hurricanes; the first of which was Hurricane Cindy that made landfall as a category 1 hurricane near Grand Isle, LA, the second storm of the season was Hurricane Dennis, which made landfall near Santa Rosa Island, FL as a cateorgy 3 hurricane, the third was Hurricane Katrina, which made landfall near Buras-Triumph, LA as a category 3 hurricane, followed by Hurricane Rita that made landfall near Holly Beach, LA as a category 3 hurricane, and finally the season in Louisiana ended with the landfall of Hurricane Humberto as a category 1 hurricane near High Island, TX (Roth, 2010). After analyzing the tracks of hurricanes during this time period, it is possible that Hurricane Katrina resulted in the largest amount of erosion at this site due to its strength as a category 3 hurricane while passing over the Biloxi marsh and the orientation of its path with respect to the shoreline. Hurricane Katrina's eye passed directly to the west of the site. Due to the shoreline orientation of this location and the position of Katrina, the shoreline was subjected to the full force of the northeastern quadrant. This time period alone lead to a shoreline loss of nearly 200 m along the N Pin transect. The S Pin transect experienced the greatest shoreline loss from March 10th, 2011 to October 29th, 2012

77

when a bay that is adjacent to the southern headland incised further as the adjacent headland

eroded.

Historical Erosion: Site 3
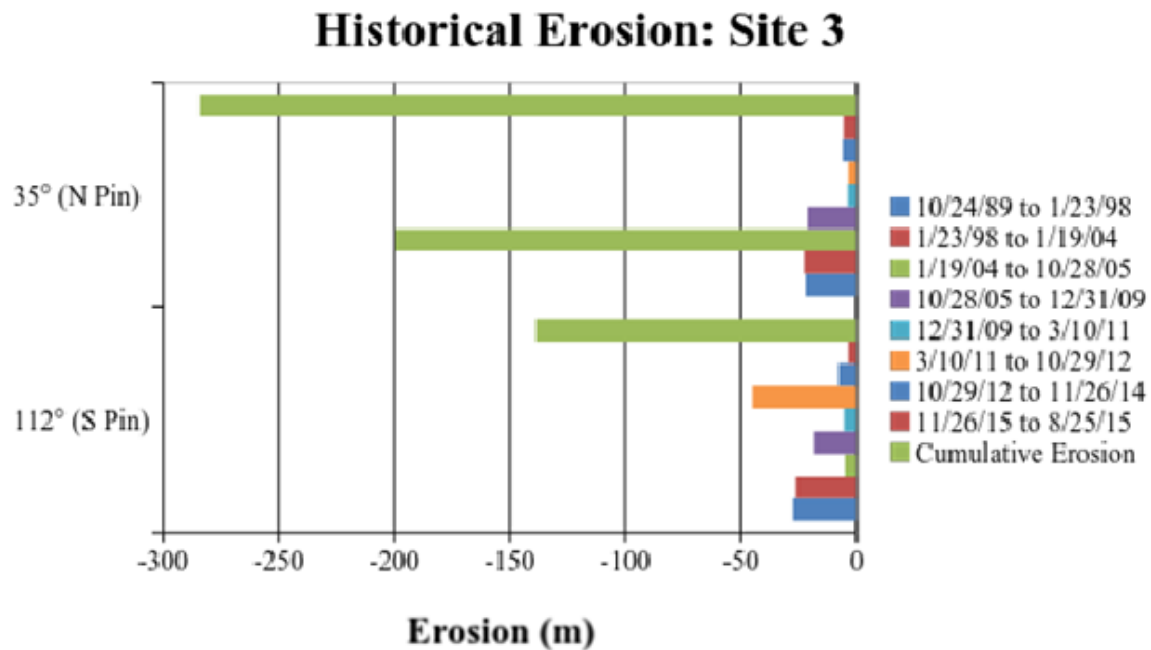

Figure 35. Historic erosion in m for Site 3 from October 24th, 1989 to August, 25th 2015 along consistent bearings for each pin at the site.

5.1.4 Site 4

The tidal channel to the east and adjacent shell berm features were observed

during the study and on *Google* imagery. These features influenced geomorphologic changes at

Site 4 (Fig.32, 9-10). Through time, the shoreline is dominated by transgressing shell berms that

change in abundance, shape, and size. It is characterized by a zeta form shape with the bays

acting as catchments for shell pocket beaches. Bays and headlands of the shoreline are enhanced

with incising bays and protruding headlands initially. However, during various periods of time

the bays and headlands are widened and become more shore-normal. When an event occurs that

forces the landward transgression and of shell berms, the berms are moved and the shoreline

becomes more zeta form in shape with a more oblique angle to the shoreline in the direction of

the dominate wave direction. Historically, the large channel to the east widens slightly at the mouth. From December 31st, 2009 to November 26th, 2014 it appears as if the western bank of the channel is zeta form in shape and has began catching shells in the bays. Advancing through time, the berms are moved landward and become a less dominant, almost non-existent, feature. The W Pin has a bias of a large amount of erosion due to the bearing of the transect being nearly parallel in its orientation to the shoreline that extends to a westward channel. During the time between January 23rd, 1998 to January 19th, 2004 the larger bay has incised and the transect is more perpendicular to the shoreline. The greatest daily rate of erosion that was calculated was for the period from 1/23/98 to 1/19/04 where an average of 1.6 cm day^{-1} eroded from the shoreline for the E Pin and a rate of 2.6 cm day^{-1} for the SW Pin (Fig. 36)
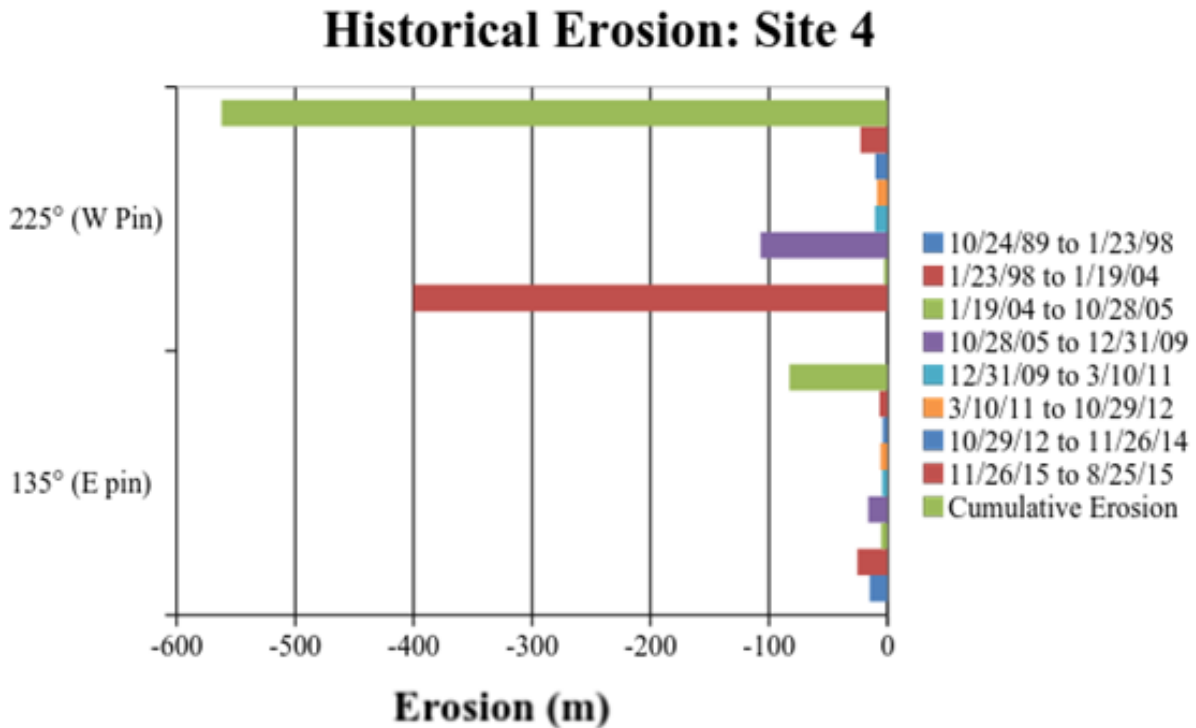

Figure 36. Historic erosion in m for Site 4 from October 24th, 1989 to August 25th, 2015 along consistent bearings for each pin at the site.

5.2 Station Marker Heights and Terrace Evolution

Station marker heights that were recorded during each site visit can be used as an indicator to tell if deposition or erosion occurred on the marsh platform between field visits. An increase in station marker height indicates that the removal of sediment occurred while a decrease in station marker height indicates deposition. Table 2 shows all station marker heights that were recorded during the study and Table 7 shows if there was an increase or decrease in station marker exposure height. Across all sites there was no discernible relationship between erosion, meteorological events and the amount of erosion or deposition that occurred.

Table 7. The difference in station marker height calculated for each site in m during each epoch by using the beginning measurement for the epoch and the ending measurement for the epoch. Negative values indicate a height reduction whereas positive numbers indicate an increase during the epoch.

Site Identification	Epoch 1	Epoch 2	Epoch 3	Epoch 4	Epoch 5
Site 1	**0.007**	-0.017	-0.010	-0.030	0
Site 2	**-0.028**	0.047	-0.009	-0.064	-0.026
Site 3	**-0.032**	-0.058	-0.048	0.012	-0.054
Site 4	**0.297**	-0.037	0.010	-0.020	0.02

Terrace depth evolution for the duration of the study is dependent on several factors varying between seasonality and stratigraphy. At sites 1 and 3 where stratigraphic data is available in the form of 1-m cores (Figs. 14, 15, 22, 23) the back terrace depth never exceeded the depth of sand lenses (Figs. 12, 13, 20, 21). However, the front terrace at all sites exceeded the depth of the sand lenses found in the stratigraphic column at some point during the study. At Site 1 the front terrace reached a depth of 1-m Near the NE pin and 95 cm Near the SW pin. These are the only front terrace measurements recorded for the duration of the study and cannot be used to determine a relationship between front terrace depth and stratigraphy. A Site 3 the front terrace depths varied more with the south pin recording a maximum depth of 90 cm near the south pin and 67 cm near the north pin.

Sites 2 and 4 do not have stratigraphic information because cores were not taken at these sites. However, during each site visit terrace depths were recorded and can be used with other measurements from to help describe a potential relationship between terrace depths across some sites (Fig. 37). Site 2 NE and SW have mostly opposing trends with Site 2 NE back terrace measurements decreasing in depth during Epoch 3 and then increasing in depth during Epochs 4 and 5 (Fig. 37). In contrast, Site 2 SW decreased in depth during each epoch (Fig. 37). This trend may be related to where the measurement was taken with regards to the proximity to necks and clefts. The measurement for Site 2 NE was taken near a neck while Site 2 SW was taken near a cleft during each site visit. The cleft remains somewhat protected from wave energy, whereas the neck is subjected to the full force of waves resulting in a greater forcing against the marsh edge and less wave transformation before exerting energy on the edge. This allows for wave depth to persist and be able to impact the bottom at greater depths. Site 3 N and S pins have a similar difference in their measurements with back terrace measurements near the north pin measured on a neck and measurements near the south pin measured in a cleft. Site 3 N back terrace measurements initially decreased in depth during Epochs 1 and 2, then increased in depth during Epochs 3 and 4, and decreased in depth once again during Epoch 5. The depth of terraces corresponds with shifts in seasonality from summer, when the terraces decreased in depth and then increased in depth during fall and decreased in depth again during the winter (Fig. 37). Seasonality per epoch will be described as follows: Epoch 1 represents summer months, Epoch 2 represents late summer to early fall, Epoch 3 represents fall months, Epoch 4 represents late fall to early winter, and Epoch 5 represents winter. Each epoch that is related with seasonality also corresponds with a shift of prevailing winds and directional distribution from 157.5° during

81

Epochs 1 and 2 to a prevailing direction of 360° during Epochs 3 and 4 and a bimodal

distribution during Epoch 5 from the north and southeast. While there may be a trend between

where the terrace depth measurement was taken with regards to proximity near necks and clefts,

it should be noted that terrace depth measurements might be erroneous based on the irregularity

of the bathymetry near the marsh edge. It should also be noted that at some sites measurements

were not consistently recorded during each site visit, thus explaining the lack of data for some

sites. More research is needed to determine the relationship between seasonality and terrace

evolution in the Biloxi Marsh.
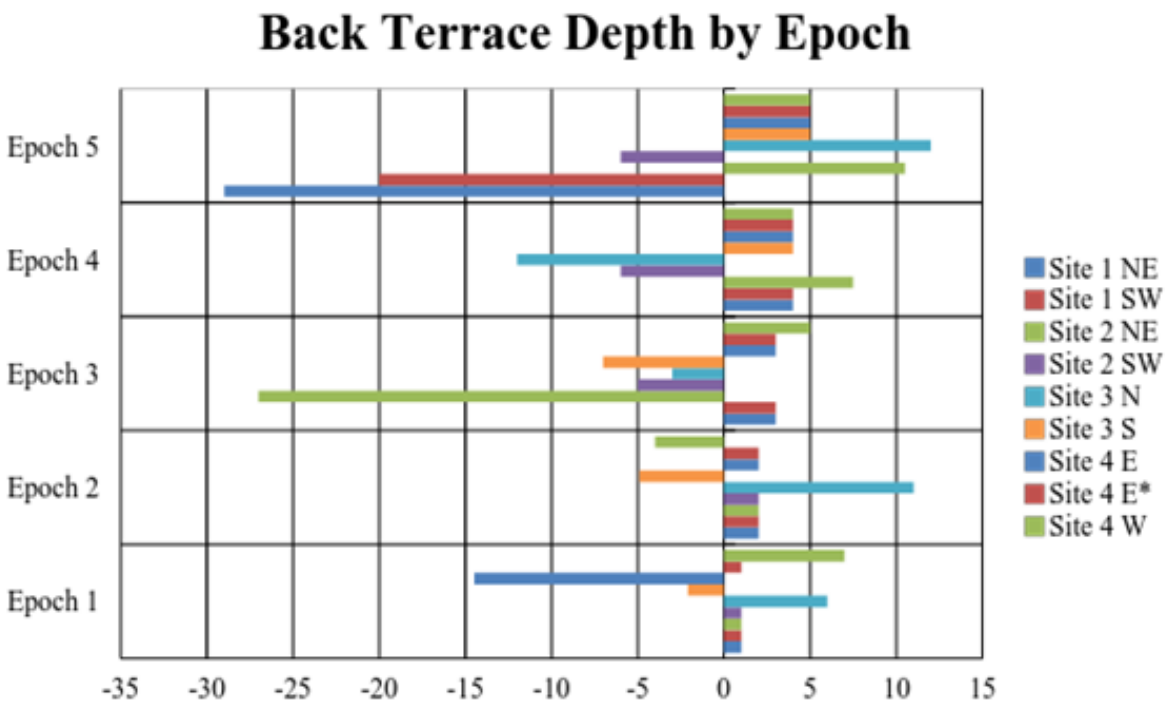
Figure 37. Back terrace depth measurements for each site for the duration of the study. Measurements were not taken consistently at some sites resulting in the lack of data across all epochs for all sites. A negative number indicates that the back terrace decreased in depth, in cm, and a positive number indicates that the back terrace increased in depth, in cm.

5.3 Marsh Edge Erosion

Marsh edge erosion at the research sites is the result of a variety of factors including stratigraphic variability, orientation of erosion pins with respect to the marsh edge, meteorological events, wave characteristics, and shoreline azimuth orientation with respect to open water. Each site variable amounts of total erosion were recorded, as well as the daily, time-averaged erosion rates across all epochs. Each of the factors suggested contribute to the erosion played a role in the observations of short and long-term erosion.

5.3.1 Marsh Edge Daily Erosion Rate Trends

5.3.1.1 Site 1

Daily erosion rates during each epoch at each site are shown in Table 2 and vary across all sites and epochs. At Site 1 NE the highest daily erosion rate of 1.41 cm day^{-1} (Fig. 12) during Epoch 3. During Epoch 3, at Site 1 NE, the wind climate changed due to the seasonality of increased cold fronts. Prevailing winds shifted from a dominant wind direction from157.5° to a unimodal directional distribution from 360° (Fig. 30). The maximum daily erosion rate of 0.84 cm day^{-1} at Site 1 SW during Epoch 2 is likely of pin exposure to the highest wind percent impact, which is defined as the percentage of time that wind blew onshore based on specific shoreline azimuth orientations for each site, and highest recorded wind speed for the entire study (Table 6).

5.3.1.2 Sites 2 & 3

At Site 2 NE the maximum daily erosion rate of 1.49 cm day^{-1} was recorded during Epoch 4 (Fig. 17). Site 2 SW pin erodes similarly to Site 1 SW pin in daily rates and the epoch during which the maximum daily erosion rate occurred. At Site 2 SW the maximum daily rate of 0.85 cm day^{-1} (Fig. 18) was recorded during Epoch 2 and is also likely a result of this marsh edge

experiencing the highest wind percent impact and maximum recorded wind speed for the entire study (Table 6). The maximum daily rate of erosion at Site 3 N occurred during Epoch 3 with a rate of 2.59 cm day^{-1} (Table 6). During this epoch, Site 3 N experienced the maximum average wind speed during the epoch of 4.98 m s^{-1} (Fig. 20). At Site 3 S the maximum daily erosion rate of 1.29 cm day^{-1} was recorded during Epoch 4 (Table 6). This may be related to the wind percent impact occurring during Epoch 4 at this site (Table 6).

5.3.1.3 Site 4

Maximum daily erosion rates at Site 4 were the lowest recorded out of all sites. The maximum daily erosion rate of 0.67 cm day^{-1} at Site 4 E was recorded during Epoch 1 (Fig. 25). This is likely a result of the dominant winds from 157.5° during Epoch 1 (Fig. 30) that lead to increased wave action at Site 4. Site 4 E* had a maximum daily erosion rate of 0.58 cm day^{-1} during Epoch 5 (Fig. 26), which corresponds with the beginning of the change in wave climate as a result of changing seasons from prevailing winds from 360° to a bimodal distribution with strong secondary prevailing winds from 180° (Fig. 30). Site 4 W recorded a maximum daily erosion rate of 0.79 cm day^{-1} during Epoch 3 (Fig. 27). This maximum corresponds to the epoch during which the maximum wind speed of 17.60 m s^{-1} was recorded and the maximum average wind speed of 3.81 m s^{-1} as well (Table 6).

5.3.1.4 Sites 1-4 Relationship Between Erosion and Wind Data

While Site 1 SW, Site 2 SW, Site 3 S, and Site 4 W have maximum daily erosion rates during epochs in which the pin was exposed to the maximum wind impact percent and/or occurred during the same epoch as when the maximum wind speed was recorded (Table 6), Site 1 NE, Site 2 NE, Site 3 N, Site 4 E, and Site 4 E* had no apparent relationship between wind

data that is shown in Table 6 and daily erosion rates. These sites instead recorded daily

maximum erosion rates during epochs when the directional distribution of winds changed. There

is no direct relationship between daily erosion rates across sites to one variable that is interpreted

through analysis of wind data.

5.3.2 Erosion and Stratigraphy

Overall erosion totals at sites where cores were taken, Sites 1 and 3, are shown in

Table 2 show. These results show that Site 1 NE and Site 3 N both show higher erosion totals in

comparison to Site 1 SW and Site 3 S. Site 1 NE underwent a total erosion of 2.17 m, whereas

Site 1 SW underwent only 1.09 m of erosion. The stratigraphy from cores that were taken from

Site 1 NE (Fig. 14) and Site 1 SW (Fig. 15) reveals obvious differences in the strata between

each site. Site 1 SW is comparatively more sand-rich than Site 1 NE; moreover, lenses of sand

are thicker than those at Site 1 NE (Figs. 14, 15). Total erosion at Site 3 N was recorded to be

2.13 m and Site 3 S recorded 1.67 m of total erosion (Table 2). Similar to Site 1, cores from Site

3 N and S indicate a sedimentary composition difference between sedimentary composition. Site

3 S has an abundant amount of sand (~20%) that was found within the core and has the highest

percentage of sand throughout the 1-m core in comparison to all other cores (Fig. 23), whereas

Site 3 N has the lowest percentage of sand (~5%) (Fig. 22). This suggests that there is a

relationship between the amount of sand found in the stratigraphic layers at each pin and the total

erosion amount. Cores with a higher percentage of sand were sites with lower total erosion

amounts for the study. On the basis of the erosion rates and stratigraphic variability at each site it

appears that the physical characteristics of soil play a role in determining erodibility (Grabowski

et al., 2011). With more abundant sand lenses interbedded between clay, the sediment is more resistant to erosion (Grabowski et al., 2011).

5.3.3 Marsh Edge Evolution and Characteristics

5.3.3.1 Wind Impact Days and Total Erosion

During data analysis, an interesting trend was found between wind percent impact days, which is defined as the percentage of time that wind blew onshore based on specific shoreline azimuth orientations for each site, and total erosion (Table 6). This trend did not exist across all pins and sites. N/NE pins (Fig. 38, left) and pins that are labeled as S/SW (Fig. 38, right) have dissimilar relationships. For example, Site 1 SW, Site 2 SW, and Site 3 S (Fig. 38, right) showed a better positive linear relationship, R^2 values of 0.72825 or higher, after the data was separated from all other data while Site 1 NE, Site 2 NE, and Site 3 N had a weaker negative linear relationship, R^2 value of 0.51411, (Fig. 38, left).

5.3.3.2 Placement of Pins and Marsh Edge Erosion

Upon further inspection of these opposing trends, it was recognized that the placement of pins relative to features along the marsh edge is a controlling factor in the total erosion that was recorded. For example, inspection of close-up photos that were taken of each pin during each site visit suggests that the placement of pins that by happenstance were labeled as N/NE were placed on necks in the majority of the study, whereas S/SW pins were placed within clefts. The mentioned necks and clefts were small-scale features along the marsh edge with the total measured distance from neck to cleft was measured as less than a meter. While the results of this study suggest that there is a connection between marsh edge shape and erosion, future work

86

should be conducted to measure the overall sinuosity of the marsh edge and its relationship to erosion.
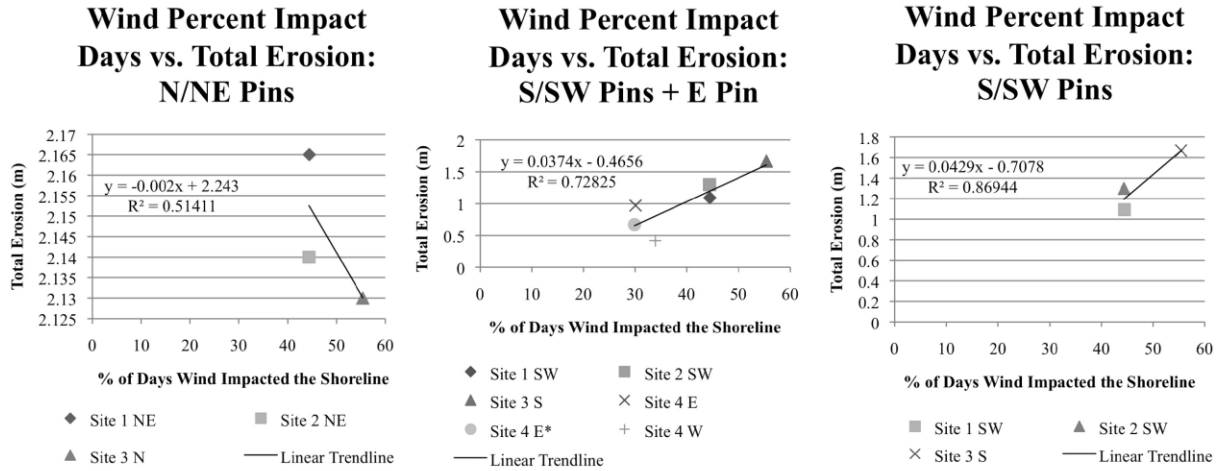
Figure 38. Wind percent impact days versus the total erosion in meters at each site across all epochs. Wind percent impact days is defined as the percentage of time that wind blew onshore based on specific shoreline azimuth orientations for each site. The graph on the left-hand side of the figure represents wind percent impact days versus total erosion for Site 1 NE pin, Site 2 NE pin, and Site 3 N pin. The graph in the center of the figure represents wind percent impact days versus total erosion for Site 1 SW pin, Site 2 SW pin, Site 3 S pin, Site 4 E pin, Site 4 E* pin, and Site 4 W pin. The graph on the right-hand side of the figure represents wind percent impact days versus total erosion for Site 1 SW pin, Site 2 SW pin, and Site 3 S pin.

It is evident that placement of pins along the marsh edge is a driving factor in determining how much erosion occurs. At Site 4 the initial pin (Site 4 E) was placed on the farther within the interior of a bay. This pin was the only pin that was not replaced during the study. In comparison, when Site 4 E* pin was installed on September 24th, 2015 because it was believed that the initial pin was removed, it was placed slightly farther seaward on a neck at a distance of approximately 0.5 m from the initial pin. This pin placement explains why the initial pin (Site 4 E) recorded its highest daily erosion rate of 0.67 cm day^{-1} during Epoch 1, in contrast Site 4 E* recorded its highest daily erosion during Epoch 5 (Figs. 25-27). The proximity of pins to large-scale headlands is also controlling how erosion occurs at the study sites. For example,

Site 1 NE pin recorded the highest amount of erosion that occurred for the duration of the study with an amount of 2.17 m eroding on the basis of pin measurements (Table 2).

5.3.3. Seasonality and Marsh Edge Evolution

During the study, the shape of the marsh edge changed seasonally (Figs. 16, 19, 24, 28). Seasonality per epoch will be described as follows: Epoch 1 represents summer months, Epoch 2 represents late summer to early fall, Epoch 3 represents fall months, Epoch 4 represents late fall to early winter, and Epoch 5 represents winter. During the transition from the summer to the beginning of cold front season during Epoch 2, the marsh edge at sites 1 and 2 began to evolve from laterally incised cleft and neck formations with some shoreline linearity to closer spaced, less horizontally pronounced and more abundant cleft and neck formations by the peak of cold front season (Figs. 16, 19). Laterally pronounced and broader cleft and neck formations during summer months are likely a result of the lack of continuous significant meteorological events occurring during the epoch resulting in the generation of consistent wind, thus wave climate, with few long-lasting disturbances from the north. Throughout the duration of the study, average wind speed increased, with the exception of a slight decrease during Epoch 3, during each epoch, (Table 2). As the sites begin to experience a higher wind speeds during Epochs 3-5 as a result of more frequent cold fronts, wind-driven, lower amplitude, waves begin to impact the marsh edge with as pre-and post-frontal wind durations decreased between each front. At Site 3 the presence of cleft and neck formations along the marsh edge may be a factor of wind dominance and the unimodal or bimodal distribution of winds. Southeasterly winds dominate the summer months and cleft and neck formations were pronounced during that time period. During the fall months wind direction had a multimodal distribution with prevailing winds from the southeast and cleft

and neck formations incised during this time frame (Fig. 28). As seasons transitioned into early winter a bimodal distribution with prevailing winds from the north became dominant and the shoreline became more linear in shape towards the north with cleft and neck formations to the south. Transitioning into later winter the bimodal distribution began to shift from prevailing north winds to predominant south winds with an almost equal distribution and the shoreline became more linear. Seasonally across all sites, *Spartina alterniflora* along the marsh edge began to die off during fall months and continued to brown from the marsh edge towards the interior of the marsh from late fall into winter.

5.4 Shell Berm Movement

During Epoch 3 the shell berm transgressed by approximately 11.15 m at the East Shell Berm and by 12.27 m at the West Shell Berm (Fig. 39). The chief driver of this event was wind-driven waves and water elevation. On October 24th, 2015, an extra-tropical cyclone developed over the northwestern Gulf of Mexico and it quickly evolved into a fully developed extratropical cyclone. As the front approached strong winds, from the south to southeast within the warm sector associated with the passage of the warm front, resulted in a gale warning from National Weather Service (NWS-KLIX,2015). The warning included the study area and warned of winds in excess of 17.88 to 24.59 m s^{-1} and wave heights of 0.91 to 1.22 m with some waves of 1.83 m (NWS-KLIX, 2015)**.** During this event, a maximum wind speed of 17.60 m s^{-1} occurred, on the basis of shoreline azimuth orientations of 88° to 208° at the East Shell Berm and 99° to 176° at the West Shell Berm. It is reasonable to expect that the strong south-southeast to southeasterly winds created large waves, which coupled with water set up most likely contributed to transgression of the berm. Waves along the berm would have likely contributed to

89

entrainment of shells and with landward propagation translation of the berm landward. This

cyclone created the second highest winds recorded during the study and most likely resulted in

the movement of each berm leaving behind unvegetated mud platforms. It can be argued that

during this epoch several other meteorological events occurred, however this event is the only

one that resulted in strong winds directly against each shell berm and was correlated with a gale

warning.
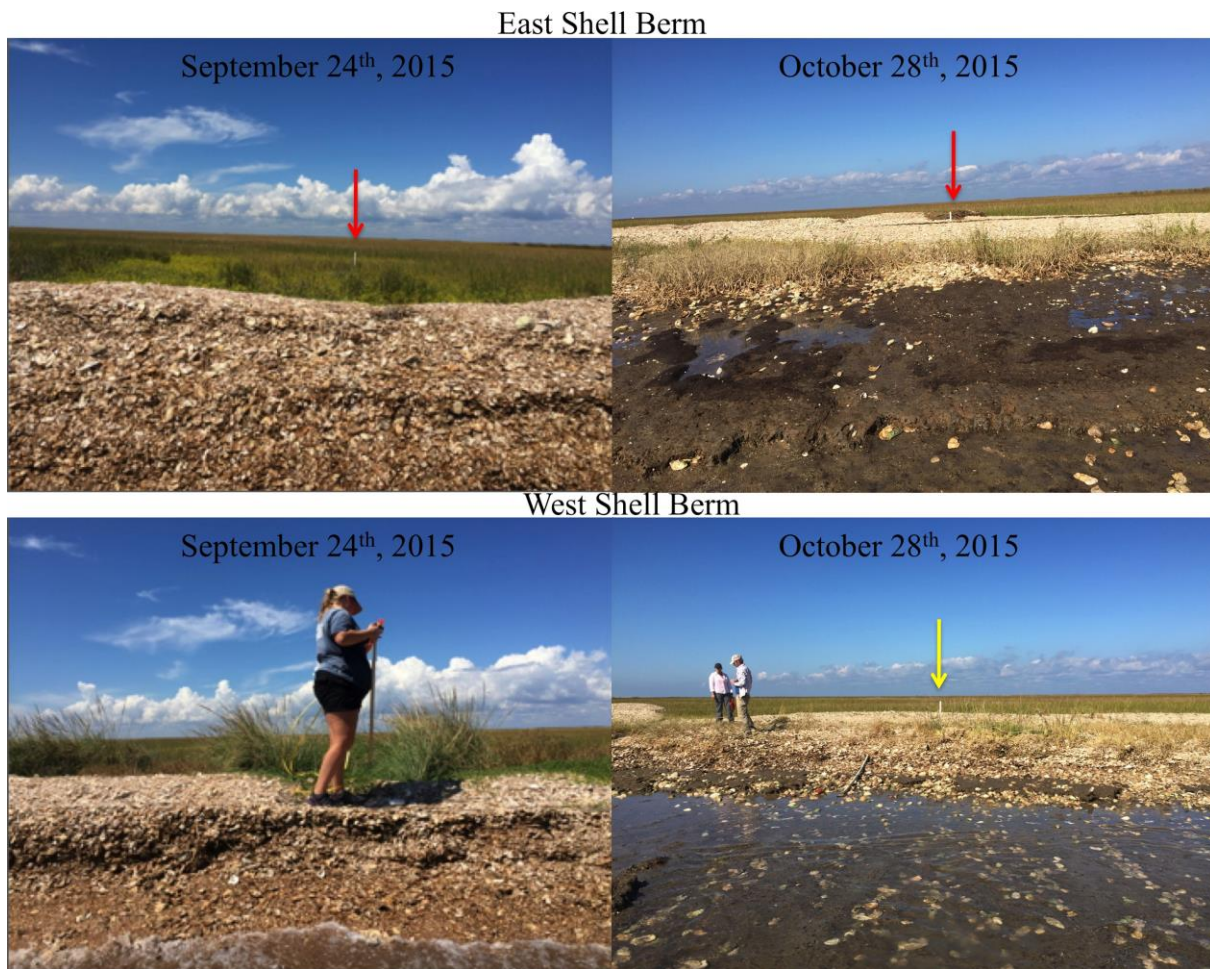
Figure 39. The two upper pictures provide a side-by-side comparison of the East Shell Berm and the red arrow indicates the position of the land stake at this site on September 24th, 2015 and October 28th, 2015. The two lower pictures are of the West Shell Berm and the yellow arrow indicates the position of the land stake at this site on October 28th, 2015. The land stake was not visible from the sea stake on September 24th, 2015 because of vegetation.

5.5 Meteorological Influence

Meteorological forcing is the main component that drives wave climate on the marsh edge and wave forcing is an important factor in determining erosion. This is because waves are related to wind direction and speed as these generate waves and determine their direction. Wind direction is important because it drives the wave direction over a body of water meaning that it determines the distance over which the wave will travel. However, many of the sites in this study do not show a direct correlation between daily erosion rates and the number of meteorological events that occur, maximum wind speed, average wind speed, or prevailing wind direction. Instead sites show different relationships to different meteorological factors and events. For example, the highest frequency of cold fronts during an epoch occurred during Epoch 5 and there were 3 times as many cold fronts during Epoch 5 in comparison to any other epoch. However, only Site 4 E* recorded its maximum daily erosion rate across all epochs and this maximum daily erosion was influenced by warm fronts associated with extra-tropical cyclones as winds due to post-front winds from a cold front would not impact the marsh edge based on the orientation of azimuth degrees. Therefore, there is not a direct correlation between the frequency of cold fronts and daily erosion rates at any of the sites. Rather, it seems as if there is a relationship between meteorological events that differ between sites.

While the majority of sites did not have a direct correlation between maximum wind speed and erosion for each epoch, Site 1 SW and Site 4 W both have a strong positive linear relationship between the maximum wind speed and erosion for each epoch (Fig. 40). While this relationship is evidents based on the results of this study, further research with more sites and a longer study duration will need to be conducted to test the validity of the relationship. Further

analysis of meteorological data through surface analysis maps, wind data, NWS warnings, and radar loops shows that the highest wind speeds were achieved through a variety of meteorological events. During Epoch 1, the maximum wind speed of 16.60 m s^{-1} from 7° occurred on June 24th, 2015 as a result of a strong outflow boundary with an independent line of thunderstorms that also prompted a marine warning for the Mississippi Sound. The maximum wind speed of 20.50 m s^{-1} from 21° during Epoch 2 was the result of a strong outflow boundary associated with a strong line of storms as well on August 9th, 2015. This storm also prompted a marine warning from the NWS. During Epoch 3 the maximum wind speed of 17.60 m s^{-1} on October 26th, 2015 was achieved as a result of the passage of a warm front that was associated with an extratropical cyclone that developed in the northwest Gulf of Mexico. During Epoch 4, post-cold front winds from the northeast were enhanced by the development of a strong low-pressure system over the Gulf of Mexico that resulted in a maximum wind speed during this epoch of 14.50 m s^{-1} from 29° on November 8th, 2015. The development of another extratropical cyclone in the northwest Gulf of Mexico from an area of disturbance in tandem with a stationary front resulted in the maximum recorded wind speed of 13.40 m s^{-1} from 160° within the warm sector of the system on February 23rd, 2016. With this being said, it is clear that maximum wind speeds that have a positive linear relationship with Site 1 SW and Site 4 W were not the result of strong post-cold front winds. Instead, the strongest wind speeds in three instances were the result of the non-traditional development of an extra-tropical cyclone in the northwest Gulf of Mexico and in two instances were associated with the warm sector of the cyclone.

Max Wind Speed vs. Erosion per Epoch: Site 1 SW

Erosion (m) vs. Max Wind Speed (m/s)

- ■ Epoch 1
- ▲ Epoch 2
- ✕ Epoch 3
- ✳ Epoch 4
- ● Epoch 5
- — Linear Trendline

$y = 0.0586x - 0.6366$
$R^2 = 0.85914$

Max Wind Speed vs. Erosion per Epoch: Site 4 W

Erosion (m) vs. Max Wind Speed (m/s)

- ■ Epoch 3
- ▲ Epoch 4
- ✕ Epoch 5
- — Linear Trendline

$y = 0.0382x - 0.4006$
$R^2 = 0.99656$
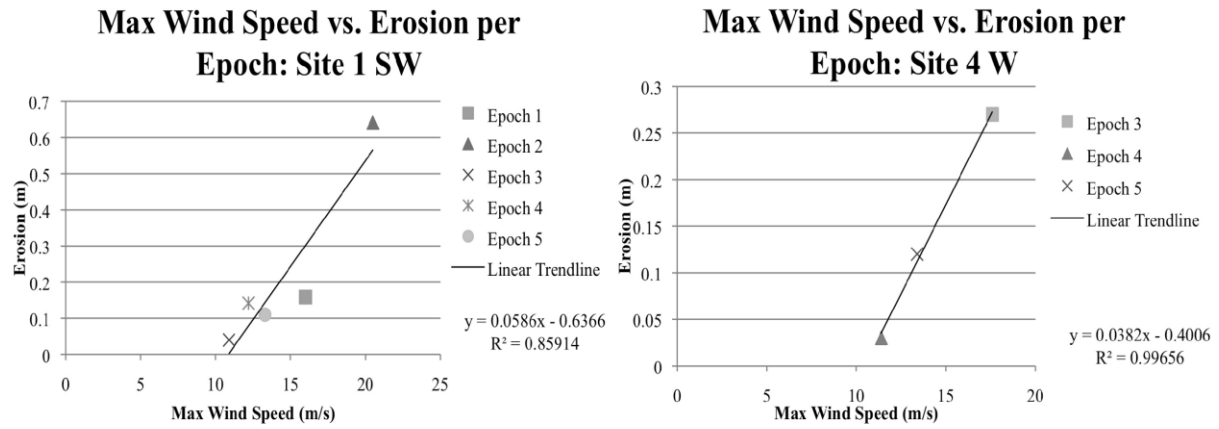
Figure 40. Maximum wind speed recorded in miles per hour during each epoch against erosion on the basis of pin exposure measurements for each epoch for Site 1 SW on the left and Site 4 W on the right.

CHAPTER 6. CONCLUSIONS

The Biloxi Marsh is exposed to meteorological forces ranging from large-scale, mid-latitude cyclones to smaller scale storms. These conditions are the dominant control in creating wind-driven waves that impact the marsh edge. By understanding how the marsh edge is impacted by differing meteorological events and seasonality, a better understanding of marsh edge erosion can be achieved. It is important to understand how the marsh edge is eroding because without these marshes, the full force of storm waves would occur on the Mississippi and eastern Louisiana coastlines.

This study examined the connection between wind speeds, stratigraphic composition, marsh edge morphology, and marsh edge erosion at 4 sites in the Biloxi Marsh. The primary hypothesis was that waves produced by winds will force a change of the marsh edge morphology based on the characteristics of the winds (e.g. velocity, direction, and duration) and if these characteristics can be used to approximate the style of marsh edge modification. A secondary hypothesis of this study was that shell berm movement at this location was a function of water level controls and an acting meteorological force.

During the 9-month study, 2.165 m of erosion recorded by erosion pin exposure measurements, 5.03 m of erosion recorded from tape measurements, and a maximum, average erosion rate of 2.59 cm day^{-1} was recorded. Meteorological conditions created by a strong low-pressure system near the site resulted in high waves that resulted in the transgression of shell berms. While the documentation of these events is significant, there were no distinct correlations across all sites between wind speeds and erosion. In addition to this, Sites 1 SW, 1 NE, 2 SW, 2NE, and 3 S all had a positive relationship between total erosion and wind percent impact days,

which is defined as the percentage of time that wind blew onshore based on specific shoreline azimuth orientations for each site. Some sites also had a positive correlation between maximum wind speeds and erosion during the study (Sites 1 SW and 4 W).

However, it is apparent that at these sites in the Biloxi Marsh wind data alone is not enough to determine erosion rates. Instead, it seems that stratigraphic variability seems to on the base of wind frequency, speed, and direction data to contribute toward erosional susceptibility. Sites where there was more sand present in the stratigraphic column did not erode as much or as quickly as those that had less sand. In addition to stratigraphic variability, the proximity to clefts and necks also seems to contribute to erosional susceptibility. The closer the pin was to the tip of a protruding neck, the faster the erosion. However, this was only true if the pin was placed on the portion of the neck that was also exposed to wave energy – if it was on the opposing side of energetic wave action, the pin was thus sheltered. Seasonality changes the dominant direction from which winds come from and will change where and how erosion is occurring at each site. For example, during the summer months, the majority of the sites were dominated by larger laterally incised clefts with necks that protruded farther into the ocean. During the winter, these features were minimized and a series of terraces developed at sites. Thus, pins that were once sheltered by laterally incised clefts became more exposed to energetic wave activity than during summer months. Therefore, there are a variety of factors such as stratigraphy, proximity to necks, seasonality, and meteorological forcing that influence and control local marsh edge erosion.

In contrast, there is a distinct connection between shell berm movement and high wind speeds oriented towards the shoreline. It was documented in this study that both the East and

95

West Shell Berms transgressed by 10 or more meters as the result of one event. This is an important result in that the high winds that created waves high enough and energetic enough to move the berm were the result of a warm front. The southerly to southeasterly winds were produced by a warm front as a result of an extratropical cyclone that developed in the northwest Gulf of Mexico, an often forgotten place where cyclogenesis can occur within the United States. This warm front resulted in the issuance of a gale warning (NWS-KLIX, 2015) that warned of winds in excess of 17.88 to 24.59 m s^{-1} and wave heights of 0.91 to 1.22 m with some waves of 1.83 m (NWS-KLIX, 2015**).** This event alone suggests that the traditional perception that cold fronts results in high rates of erosion and geomorphologic changes within marshes should not be considered in absence of exploring other meteorological events as well.

While the results presented in this study advance stratigraphic, geomorphological, and meteorological events as they relate to marsh edge erosion and shell berm transgression, there is still much to be explored before definite conclusions can be made as to how much erosion occurs as a result of these factors. The goal of this research was to see if meteorological events and the winds that they produced correlated to marsh edge erosion. This research provides evidence that a relationship may exist between wind speed and marsh edge erosion, with a stronger relationship between wind speed and shell berm transgression. However, a concise relationship cannot be confirmed due to the duration of this study and the few number of sites.

Future studies should be made in a location where constant monitoring of small-scale marsh edge erosion can be made over a prolonged period of time. In addition to this, multiple study sites should be monitored at the same time with differing shoreline orientations relative to open water in order to properly assess how meteorological events influence the marsh. An

increase in the temporal and spatial resolution of the data can allow future researchers to study how specific and finer scale meteorological events influence marsh edge erosion and geomorphology. Future studies should also include a scientific wave and wind recording station that is specific to the site in order to verify meteorological events and the conditions that were produced at the marsh edge. In order to capture a more defined variation in erosion as a result of meteorological forcing and the associated winds, further and more comprehensive research is required by the scientific community.

References

Ahrens, C. D. (2011). *Essentials of meteorology: an invitation to the atmosphere*. Cengage Learning.

Anderson, M. E., McKee Smith, J., & McKay, S. K. (2011). *Wave dissipation by vegetation*. USACE.

Allen, J. R. L. (1984). Experiments on the settling, overturning and entrainment of bivalve shells and related models. *Sedimentology*, *31*(2), 227-250.

Barras, J. A. (2006). Land area changes in coastal Louisiana after the 2005 hurricanes. *A Presentation to the Coastal Wetlands Planning, Protection and Restoration Act Task Force on*, *18*, 2006-1274.

Baumann, R. H. (1980). Mechanisms of maintaining marsh elevation in a subsiding environment.

Barbier, E. B., Georgiou, I. Y., Enchelmeyer, B., & Reed, D. J. (2013). The value of wetlands in protecting southeast Louisiana from hurricane storm surges. *PloS one*, *8*(3), e58715.

Bendoni, M., Mel, R., Solari, L., Lanzoni, S., Francalanci, S., & Oumeraci, H. (2016). Insights into lateral marsh retreat mechanism through localized field measurements. *Water Resources Research*, *52*(2), 1446-1464.

Bianchette, T. A., Liu, K. B., Qiang, Y., & Lam, N. S. N. (2015). Wetland Accretion Rates Along Coastal Louisiana: Spatial and Temporal Variability in Light of Hurricane Isaac's Impacts. *Water*, *8*(1), 1.

Boesch, D. F., Josselyn, M. N., Mehta, A. J., Morris, J. T., Nuttle, W. K., Simenstad, C. A., & Swift, D. J. (1994). Scientific assessment of coastal wetland loss, restoration and management in Louisiana. *Journal of Coastal Research*, i-103.

Boutwell, L., & Westra, J. (2015). The Economic Value of Wetlands as Storm Buffers. In *2015 Annual Meeting, January 31-February 3, 2015, Atlanta, Georgia* (No. 196854). Southern Agricultural Economics Association.

Cahoon, D. R., Reed, D. J., Day Jr, J. W., Steyer, G. D., Boumans, R. M., Lynch, J. C., ... & Latif, N. (1995). The influence of Hurricane Andrew on sediment distribution in Louisiana coastal marshes. *Journal of Coastal Research*, 280-294.

Conservation, L. C. W., Force, R. T., Conservation, W., & Authority, R. (1998). Coast 2050: Toward a sustainable coastal Louisiana. *Louisiana Department of Natural Resources, Baton Rouge, Louisiana*.

Costanza, R., Pérez-Maqueo, O., Martinez, M. L., Sutton, P., Anderson, S. J., & Mulder, K. (2008). The value of coastal wetlands for hurricane protection. *AMBIO: A Journal of the Human Environment*, *37*(4), 241-248.

Couvillion, B. R., Barras, J. A., Steyer, G. D., Sleavin, W., Fischer, M., Beck, H., ... & Heckman, D. (2011). *Land area change in coastal Louisiana (1932 to 2010)* (pp. 1-12). US Department of the Interior, US Geological Survey.

Currin, C., Davis, J., Baron, L. C., Malhotra, A., & Fonseca, M. (2015). Shoreline Change in the New River Estuary, North Carolina: Rates and Consequences. *Journal of Coastal Research*, *31*(5), 1069-1077.

Day, J. W., Britsch, L. D., Hawes, S. R., Shaffer, G. P., Reed, D. J., & Cahoon, D. (2000). Pattern and process of land loss in the Mississippi Delta: a spatial and temporal analysis of wetland habitat change. *Estuaries*, *23*(4), 425-438.

Dingler, J. R., Reiss, T. E., & Plant, N. G. (1993). Erosional patterns of the Isles Dernieres, Louisiana, in relation to meteorological influences. *Journal of Coastal Research*, 112-125.

Ellison, M. (2011). Subsurface controls on mainland marsh shoreline response during barrier island transgressive submergence.

Fagherazzi, S., Palermo, C., Rulli, M. C., Carniello, L., & Defina, A. (2007). Wind waves in shallow microtidal basins and the dynamic equilibrium of tidal flats. *Journal of Geophysical Research: Earth Surface*, *112*(F2).

Fagherazzi, S., & Wiberg, P. L. (2009). Importance of wind conditions, fetch, and water levels on wave- generated shear stresses in shallow intertidal basins. *Journal of Geophysical Research: Earth Surface*, *114*(F3).

Fagherazzi, S., Kirwan, M. L., Mudd, S. M., Guntenspergen, G. R., Temmerman, S., D'Alpaos, A., ... & Clough, J. (2012). Numerical models of salt marsh evolution: Ecological, geomorphic, and climatic factors. *Reviews of Geophysics*, *50*(1).

Feagin, R. A., Lozada-Bernard, S. M., Ravens, T. M., Möller, I., Yeager, K. M., & Baird, A. H. (2009). Does vegetation prevent wave erosion of salt marsh edges?. *Proceedings of the National Academy of Sciences*, *106*(25), 10109-10113.

Fisk, H. N. (1944). *Geological investigation of the alluvial valley of the lower Mississippi River* (p. 78). War Department, Corps of Engineers.

FitzGerald, D., Kulp, M. A., & Penland, S. (2003). Tidal prism changes within Barataria Bay and its effects on sedimentation patterns and barrier shoreline stability.

Frazier, D. E. (1967). Recent deltaic deposits of the Mississippi River: their development and chronology.

Georgiou, I. Y., FitzGerald, D. M., & Stone, G. W. (2005). The impact of physical processes along the Louisiana coast. *Journal of Coastal Research*, 72-89.

Grabowski, R. C., Droppo, I. G., & Wharton, G. (2011). Erodibility of cohesive sediment: the importance of sediment properties. *Earth-Science Reviews*, *105*(3), 101-120.

Gulf Coast Ecosystem Recovery Task Force (2011) Gulf of Mexico Regional Ecosystem Restoration Strategy. Gulf Coast Ecosystem Recovery Task Force, Washington, D.C., December 2011.

Hardy, J. W., & Hsu, S. A. (1997). A Climatology of Winter Cyclogenesis Intensity in the Northwest Gulf of Mexico. *Natl Weather Dig*, 22, 3-7.

Howes, N. C., FitzGerald, D. M., Hughes, Z. J., Georgiou, I. Y., Kulp, M. A., Miner, M. D., ... & Barras, J. A. (2010). Hurricane-induced failure of low salinity wetlands. *Proceedings of the National Academy of Sciences*, *107*(32), 14014-14019.

Iowa Environmental Mesonet (IEM) :: RADAR & NWS Warnings. (n.d.). Retrieved May 17, 2016, from https://mesonet.agron.iastate.edu/GIS/apps/rview/warnings.phtml?autopilot=0

Karimpour, A., Chen, Q., & Twilley, R. R. (2015). A Field Study of How Wind Waves and Currents May Contribute to the Deterioration of Saltmarsh Fringe. *Estuaries and Coasts*, 1-16.

Kirwan, M. L., & Murray, A. B. (2007). A coupled geomorphic and ecological model of tidal marsh evolution. *Proceedings of the National Academy of Sciences*, *104*(15), 6118-6122.

Knabb, R. D., Rhome, J. R., & Brown, D. P. (2005). *Tropical cyclone report: Hurricane katrina, 23-30 august 2005*. National Hurricane Center.

Kulp, M. (2005). Sand-rich lithosomes of the Holocene Mississippi River delta plain.

Leonard, L. A., & Reed, D. J. (2002). Hydrodynamics and sediment transport through tidal marsh canopies. *Journal of Coastal Research*, *36*(2), 459-469.

Lightbody, A. F., & Nepf, H. M. (2006). Prediction of velocity profiles and longitudinal dispersion in salt marsh vegetation. *Limnology and Oceanography*, *51*(1), 218-228.

Lopez, J. A. (2009). The multiple lines of defense strategy to sustain coastal Louisiana. *Journal of Coastal Research*, 186-197.

Louisiana, Coastal Protection and Restoration Authority (CPRA) (2012). Louisiana's Comprehensive Master Plan for a Sustainable Coast.

Martinez, L., O'Brien, S., Bethel, M., Penland, S., & Kulp, M. (2009). Louisiana Barrier Island Comprehensive Monitoring Program (BICM) Volume 2: Shoreline Changes and Barrier Island Land Loss 1800's-2005.

McKee, K. L., & Cherry, J. A. (2009). Hurricane Katrina sediment slowed elevation loss in subsiding brackish marshes of the Mississippi River delta. *Wetlands*, *29*(1), 2-15.

Moeller, C. C., Huh, O. K., Roberts, H. H., Gumley, L. E., & Menzel, W. P. (1993). Response of Louisiana coastal environments to a cold front passage. *Journal of Coastal Research*, 434-447.

Möller, I., & Spencer, T. (2002). Wave dissipation over macro-tidal saltmarshes: Effects of marsh edge typology and vegetation change. *Journal of Coastal Research*, *36*(1), 506-521.

Möller, I. (2006). Quantifying saltmarsh vegetation and its effect on wave height dissipation: Results from a UK East coast saltmarsh. *Estuarine, Coastal and Shelf Science*, *69*(3), 337-351.

Mudd, S. M. (2011). The life and death of salt marshes in response to anthropogenic disturbance of sediment supply. *Geology*, *39*(5), 511-512.

National Data Buoy Center (NDBC). Station WYCM6 - 8747437 - Bay Waveland Yacht Club, MS. (n.d.). Retrieved May 16, 2016, from http://www.ndbc.noaa.gov/station_page.php?station=wycm6

National Weather Service New Orleans/Baton Rouge (NWS-LIX), Radar & NWS Warnings. (October 26, 2015). Retrieved May 02, 2016, from https://mesonet.agron.iastate.edu/vtec/2015-O-NEW-KLIX-GL-W-0003.html#2015-O-NEW-KLIX-GL-W-0003/USCOMP-N0Q-201510251805

Nyman, J. A., Crozier, C. R., & DeLaune, R. D. (1995). Roles and patterns of hurricane sedimentation in an estuarine marsh landscape. *Estuarine, Coastal and Shelf Science*, *40*(6), 665-679.

Penland, S., Boyd, R., & Suter, J. R. (1988). Transgressive depositional systems of the Mississippi delta plain: a model for barrier shoreline and shelf sand development. *Journal of Sedimentary Research*, *58*(6), 932-949.

Penland, S., Beall, A. D., & Britsch III, L. D. (2002). Geologic classification of coastal land loss between 1932 and 1990 in the Mississippi River Delta Plain, southeastern Louisiana.

Pepper, D. A., & Stone, G. W. (2004). Hydrodynamic and sedimentary responses to two contrasting winter storms on the inner shelf of the northern Gulf of Mexico. *Marine Geology*, *210*(1), 43-62.

Piazza, B. P., Banks, P. D., & La Peyre, M. K. (2005). The potential for created oyster shell reefs as a sustainable shoreline protection strategy in Louisiana. *Restoration Ecology*, *13*(3), 499-506.

Reed, D. J. (1989). Patterns of sediment deposition in subsiding coastal salt marshes, Terrebonne Bay, Louisiana: the role of winter storms. *Estuaries*, *12*(4), 222-227.

Roberts, H. H. (1997). Dynamic changes of the Holocene Mississippi River delta plain: the delta cycle. *Journal of Coastal Research*, 605-627.

Rogers, B. E., Kulp, M. A., & Miner, M. D. (2009). Late Holocene chronology, origin, and evolution of the St. Bernard Shoals, northern Gulf of Mexico, USA. *Geo-Marine Letters*, *29*(6), 379-394.

Rodriguez, A. B., Fodrie, F. J., Ridge, J. T., Lindquist, N. L., Theuerkauf, E. J., Coleman, S. E., ... & Kenworthy, M. D. (2014). Oyster reefs can outpace sea-level rise. *Nature climate change*, *4*(6), 493-497.

Roth, D. (2010). *Louisiana hurricane history*. National Weather Service.

Sasser, C., Visser J., Mouton, E., Linscombe, J., & Hartley, S. (2014). Vegetation types in coastal Louisiana in 2013. *US Geological Survey Scientific Invesitagations Map, 3290(1).*

Saravanan, R., & Chang, P. (2000). Interaction between tropical Atlantic variability and El Nino-southern oscillation. *Journal of Climate*, *13*(13), 2177-2194.

Schuerch, M., Vafeidis, A., Slawig, T., & Temmerman, S. (2013). Modeling the influence of changing storm patterns on the ability of a salt marsh to keep pace with sea level rise. *Journal of Geophysical Research: Earth Surface*, *118*(1), 84-96.

Schwimmer, R. A. (2001). Rates and processes of marsh shoreline erosion in Rehoboth Bay, Delaware, USA. *Journal of Coastal Research*, 672-683.

Stedman, S. M., & Dahl, T. E. (2008). *Status and trends of wetlands in the coastal watersheds of the eastern United States, 1998 to 2004*. National Oceanic and Atmospheric Administration, National Marine Fisheries Service.

Temmerman, S., Bouma, T. J., Van de Koppel, J., Van der Wal, D., De Vries, M. B., & Herman, P. M. J. (2007). Vegetation causes channel erosion in a tidal landscape. *Geology*, *35*(7), 631-634.

Tonelli, M., Fagherazzi, S., & Petti, M. (2010). Modeling wave impact on salt marsh boundaries. *Journal of Geophysical Research: Oceans (1978–2012)*, *115*(C9).

Tornqvist, T. E., Kidder, T. R., Autin, W. J., & van der Borg, K. (1996). A revised chronology for Mississippi River subdeltas. *Science*, *273*(5282), 1693.

Trosclair, K. J. (2013). Wave transformation at a saltmarsh edge and resulting marsh edge erosion: observations and modeling.

Turner, R. E., Baustian, J. J., Swenson, E. M., & Spicer, J. S. (2006). Wetland sedimentation from hurricanes Katrina and Rita. *Science*, *314*(5798), 449-452.

Tweel, A. W., & Turner, R. E. (2014). Contribution of tropical cyclones to the sediment budget for coastal wetlands in Louisiana, USA. *Landscape ecology*, *29*(6), 1083-1094.

Wamsley, T., Atkinson, J., Cialone, M.A., Grzegorzewski, A.S., Dresback, K., Kolar, R., & Westerink, J. (2007, November). Influence of wetland degradation on surge. In

Proceeding of 10th International Workshop on Wave Hindcasting and Forecasting and Coastal Hazard Symposium (pp. 11-16).

Wamsley, T. V., Cialone, M. A., Smith, J. M., Atkinson, J. H., & Rosati, J. D. (2010). The potential of wetlands in reducing storm surge. *Ocean Engineering*, *37*(1), 59-68.

Watzke, D. A. (2004). *Short-term evolution of a marsh island system and the importance of cold front forcing, Terrebonne Bay, Louisiana* (Doctoral dissertation, Faculty of the Louisiana State University and Agricultural and Mechanical College in partial Fulfillment of the requirements for the degree of Master of Science in The Department of Oceanography and Coastal Sciences By Dana Ann Watzke BS, University of New Orleans).

Weather Prediction Center (WPC), Surface Analysis Archive. (n.d.) Retrieved April 22, 2016, from http://www.wpc.ncep.noaa.gov/archives/web_pages/sfc/sfc_archive.php

Weill, P., Mouazé, D., Tessier, B., & Brun- Cottan, J. C. (2010). Hydrodynamic behaviour of coarse bioclastic sand from shelly cheniers. *Earth Surface Processes and Landforms*, *35*(14), 1642-1654.

White, W. A., & Tremblay, T. A. (1995). Submergence of wetlands as a result of human-induced subsidence and faulting along the upper Texas Gulf Coast. *Journal of Coastal Research*, 788-807.

Williams, S. J. (1995). *Louisiana Coastal Wetlands: A Resource at Risk*. US Department of the Interior, US Geological Survey.

Wilson, C. A., & Allison, M. A. (2008). An equilibrium profile model for retreating marsh shorelines in southeast Louisiana. *Estuarine, Coastal and Shelf Science*, *80*(4), 483-494.

Zhang, C. (2012). *Effect of Hurricane Forward Speed and Approach Angle on Coastal Storm Surge* (Doctoral dissertation, Faculty of the Louisiana State University and Agricultural and Mechanical College In partial fulfillment of the requirements for the degree of Master of Science in The Department of Oceanography and Coastal Sciences by Chenguang Zhang BS, Nanjing University).

Vita

The author was born and raised in Excelsior Springs, Missouri where her passion for earth sciences blossomed. She earned her Bachelor's degree in Geosciences with a concentration in professional meteorology at Mississippi State University during May of 2014. The following August she entered the Earth and Environmental Sciences department at the University of New Orleans to pursue a Master's of Science with a concentration in coastal geomorphology under the advisement of Dr. Mark Kulp. She is currently working at the Foundation for Louisiana as a Coastal Program Manager Fellow where she is working with others to execute a resilience framework in Plaquemines parish that will be implemented in other coastal parishes as well.